Identification of novel components involved in selective and unselective autophagic pathways

Dissertation

for the award of the degree
“Doctor rerum naturalium“

of the Georg-August-University Goettingen

submitted by

Evelyn Cornelia Welter

from Ottweiler

Goettingen 2011

Supervisor:
Prof. Dr. Michael Thumm
Department of Biochemistry II
Center for Biochemistry and Molecular Cell Biology
Georg-August University, Goettingen

Member of the Thesis Committee (First Reviewer):
Prof. Dr. Peter Rehling
Department of Biochemistry II
Center for Biochemistry and Molecular Cell Biology
Georg-August University, Goettingen

Member of the Thesis Committee (Second Reviewer):
Prof. Dr. Gerhard Braus
Deptartment of Molecular Microbiology and Genetics
Institute for Microbiology and Genetics
Georg August University Goettingen

Member of the Thesis Committee:
Prof. Dr. Ralf Ficner
Department of Molecular Structural Biology
Goettingen Center for Molecular Biosciences
Georg August University Goettingen

Date of oral exam: 16.05.11

Affidavit:

I herewith declare, that this thesis has been written independently and with no other sources and aids than quoted.

I. Contents

I. Contents ..... **i**
II. List of figures ..... **iv**
III. List of tables ..... **v**
IV. Abbreviations ..... **vi**

1. Summary **1**

2. Introduction **3**

2.1 The model organism *Saccharomyces cerevisiae* **3**

2.2 Autophagy **4**
2.2.1 Macroautophagy 4
2.2.1.1 The Atg1 kinase and its regulators 5
2.2.1.2 The two PtdIns 3 –kinase complexes 6
2.2.1.3 The pre-autophagosomal structure 7
2.2.1.4 The two conjugation systems 7
2.2.1.5 Atg9 cycling 9
2.2.2 Microautophagy 9
2.2.3 Chaperone-mediated autophagy 9
2.2.4 Selective autophagy 10
2.2.4.1 The Cytoplasm to Vacuolar Trafficking pathway 10
2.2.4.2 Pexophagy 10
2.2.4.3 Ribophagy 11
2.2.4.4 Piecemeal Microautophagy of the Nucleus 11
2.2.4.5 Mitophagy 12
2.2.5 Membrane fusion events in autophagy 13
2.2.5.1 The AAA^+ ATPase Cdc48 13
2.2.5.1.1 Cdc48 and autophagosome biogenesis 14

2.3 The ESCRT machinery **15**
2.3.1 ESCRT and autophagy 16

2.4 Aim of the study **17**

3. Material and Methods **18**

3.1 Material **18**
3.1.1 *Saccharomyces cerevisiae* strains 18
3.1.2 *Escherichia coli* 24
3.1.3 Plasmids 25
3.1.4 Oligonucleotides 25
3.1.5 Media 28
3.1.6 Antibodies 31
3.1.7 Kits 32
3.1.8 Chemicals 32
3.1.9 Consumables and equipment 34

3.2 Cell biological methods.....36
3.2.1 Cultivation of *S. cerevisiae* 36
3.2.2 Storage of *S. cerevisiae*.....36
3.2.3 Cultivation of *E. coli*.....36
3.2.4 Storage of *E. coli* 36
3.2.5 Mating of haploid yeast cells 36
3.2.6 Mating type switch 37
3.2.7 Mating type determination.....37
3.2.8 Sporulation of yeast cells 37
3.2.9 Separation of haploid tetrads.....38
3.2.10 Microscopy.....38
3.2.10.1 Test for the accumulation of autophagic bodies inside the vacuole 38
3.2.10.2 Fluorescence microscopy 38
3.2.10.2.1 Staining of the nucleus using Hoechst 33324.....39
3.2.10.2.2 Staining of endosome and vacuole using FM4-64.....39
3.2.11 Synthetic genetic array.....39
3.2.11.1 Generation of the query strain 40
3.2.11.2 SGA - screen.....41

3.3 Molecular biological methods 43
3.3.1 Isolation of chromosomal DNA 43
3.3.2 Transformation of DNA.....43
3.3.3 Transformation of plasmid-DNA 44
3.3.4 Preparation of electrocompetent *E. coli*.....44
3.3.5 Plasmid transformation in *E. coli* 44
3.3.6 Isolation of plasmid DNA from *E. coli*.....44
3.3.7 Restriction of DNA.....45
3.3.8 DNA agarose gel electrophoresis 45
3.3.9 DNA gel extraction.....45
3.3.10 Ligation of DNA fragments 46
3.3.11 Polymerase chain reaction (PCR).....46
3.3.12 Sequencing of DNA.....46
3.3.13 Construction of knock out strains.....47
3.3.14 Chromosomal C-terminal fusion with a GFP-taq.....47
3.3.15 Plasmid construction.....48

3.4 Protein biochemical methods 50
3.4.1 Alkaline lysis.....50
3.4.2 Cell lysis for the detection of Atg8-PE.....50
3.4.3 SDS-PAGE.....51
3.4.4 Western Blot.....52
3.4.5 Measurement of autophagy dependent degradation of GFP-fused proteins.....53
3.4.5.1 Macroautophagy 53
3.4.5.2 PMN 53
3.4.5.3 Mitophagy.....53
3.4.6 Pull down of GST-Shp1.....54
3.4.6.1 Purification of recombinant GST-Shp1 54
3.4.6.2 Coupling of GST-fusion protein to sepharose.....54
3.4.6.3 Native cell extracts.....54
3.4.6.4 GST-Pull down 55

4. Results.....56

4.1 Synthetic Genetic Array.....56

4.2 Detection of nonselective bulk autophagy using Pgk1-GFP.....59

4.3 Cdc48 and its cofactor Shp1 are needed for functional autophagy.....62
4.3.1 Shp1 is the exclusive cofactor of Cdc48 needed for autophagy.....62
4.3.2 Shp1 is needed for autophagy but not for the Cvt pathway and CPY maturation 65
4.3.3 No accumulation of autophagic bodies occurs in *shp1*Δ cells.....66
4.3.4 The formation of the PAS occurs normal in *shp1*Δ cells.....67
4.3.5 Lipidation of Atg8 occurs normal in *shp1*Δ cells.....69
4.3.6 Pull down experiments of recombinant GST-Shp1.....69

4.4 Mitophagy in *S. cerevisiae*.....71
4.4.1 Chromosomal integration of Om45-GFP.....71
4.4.2 The pre-autophagosomal structure localises to mitochondria.....72
4.4.3 Construction of mito-GFP.....73
4.4.4 Different methods to induce mitophagy.....74
4.4.5 Mitophagy is increased in *yme1*Δ cells.....80
4.4.6 Part of the ESCRT machinery is required for mitophagy.....81
4.4.7 Doa4 is involved in mitophagy but not in unselective autophagy.....83

4.5 Piecemeal microautophagy of the nucleus.....85
4.5.1 Screen for selective PMN cargos.....85
4.5.2 Microscopic analysis of nucleolar GFP fusion proteins.....86
4.5.3 Nucleus-vacuole junctions localise at the nucleolus.....88
4.5.4 The PAS localises at the nucleolar part of the nucleus.....90

5. Discussion.....91

5.1 Synthetic Genetic Array (SGA).....91

5.2 Establishment of a novel assay to easily measure unselective autophagy using Pgk1-GFP.....95

5.3 A complex of Ccd48, Shp1 and Atg8 is needed for autophagosome biogenesis in yeast.....98
5.3.1 Shp1 is the exclusive cofactor of Cdc48 needed for autophagy.....98
5.3.2 Shp1 interacts with Atg8.....100

5.4 Insights into mitophagy in *S. cerevisiae*.....103
5.4.1 Differentiation between mitophagy of superfluous or damaged mitochondria.105
5.4.2 Mitophagy is increased in *yme1*Δ cells.....109
5.4.3 Part of the ESCRT machinery is required for mitophagy.....110
5.4.4 Ubiquitination affects mitophagy in *S. cerevisiae*.....111

5.5 The nucleolus might represent a specific cargo for PMN.....114

6. Literature.....117

II. List of figures

Figure 1: Cell cycle of *Saccharomyces cerevisiae* 3
Figure 2: Scheme of autophagy 4
Figure 3: The regulatory TOR kinase complex for autophagy induction 6
Figure 4: The two Phosphatidylinositol 3-kinase complexes in *S. cerevisiae* 7
Figure 5: The two conjugation systems 8
Figure 6: Model of piecemeal microautophagy of the nucleus (PMN) 12
Figure 7: Model of Cdc48-Shp1 complex 14
Figure 8: The ESCRT machinery of MVB sorting pathway 16
Figure 9: Scheme of mating type determination 37
Figure 10: Preparation of the query strain 41
Figure 11: Synthetic genetic array methodology 42
Figure 12: Scheme for construction of a knockout strain 47
Figure 13: Scheme for the construction of chromosomal Om45-GFP 48
Figure 14: Scheme of western blot equipment 52
Figure 15: Mating and sporulation for query strain generation was controlled by microscopy 56
Figure 16: SGA plates 57
Figure 17: Monitoring unselective autophagy using Pgk1-GFP 60
Figure 18: Fluorescence microscopy of cells expressing Pgk1-GFP 61
Figure 19: Ubx1 but no other UBX domain protein is required for autophagy 62
Figure 20: Ufd proteins are not required for autophagy 63
Figure 21: Otu1 and Der1 are not required for autophagy 64
Figure 22: Macroautophagy is not affected in *doa4*Δ cells 64
Figure 23: Shp1 is required for autophagy but not for the Cvt-pathway 65
Figure 24: The maturation of Ape1 and CPY occurs normal in *shp1*Δ cells 66
Figure 25: No vacuolar accumulation of autophagic bodies in *shp1*Δ cells 67
Figure 26: The formation of the PAS occurs normal in *shp1*Δ cells 68
Figure 27: The lipidation of Atg8 occurs normally in *shp1*Δ cells 69
Figure 28: Pull down experiments with recombinant GST-Shp1 70
Figure 29: Monitoring mitophagy by western blot using Om45-GFP 72
Figure 30: Localisation of the PAS at mitochondria 72
Figure 31: Fluorescence microscopy and western blot analysis of cells expressing mito-GFP 73
Figure 32: Incubation for 3 days in lactate medium induces mitophagy 75
Figure 33: Rapamycin induces mitophagy 75
Figure 34: Mitophagy is induced by oxidative stress (H_2O_2) 77
Figure 35: Paraquat induces mitophagy 79
Figure 36: Quantification of mitophagy in *yme1*Δ 80
Figure 37: Part of the ESCRT machinery is required for mitophagy 82
Figure 38: Doa4 is needed for mitophagy 84
Figure 39: Western Blot analysis for the identification of specific PMN cargos 86
Figure 40: Microscopic analysis of strains expressing nucleolar GFP fusion proteins 87
Figure 41: PMN structures in Nog1-GFP 87
Figure 42: Nucleus-vacuole junctions localise adjacent the nucleolus 89
Figure 43: The pre-autophagosomal structure localises partially at the nucleolus 90

III. List of tables

Table 1: Strains of BY4741 background used in this study 18
Table 2: Strains of BY4742 background used in this study 19
Table 3: Strains of WCG background used in this study 19
Table 4: RFP-fusion strains used in this study 20
Table 5: GFP-fusion strains used in this study 20
Table 6: Strains used for SGA 24
Table 7: Strains for mating type determination 24
Table 8: *Escherichia coli* strains used in this study 24
Table 9: Plasmids used in this study 25
Table 10: Oligonucleotides used in this study 25
Table 11: Anibodies used in this study 31
Table 12: Kits used in this study 32
Table 13: Chemicals used in this study 32
Table 14: Consumables and equipment used in this study 34
Table 15: Standard Tri Dye 1 kb 45
Table 16: Contents of SDS-PAGE 51
Table 17: Precision Plus Protein All Blue Standard 51
Table 18: Strains occurring as synthetic lethal in SGA 57
Table 19: Summary of tested ESCRT mutants 83

IV. Abbreviations

Abbreviation	
%	Per cent
Σ	Sum
(v/v)	(Volume/volume)
(w/o)	Without
(w/v)	(Weight/volume)
°C	Degree in celcius
AAA^+ ATPase	ATPases associated with various cellular activities
AB	Autophagic body
amp	Ampicillin
Ams1	α-mannosidase
AP	Autophagosome
Ape1	Aminopeptidase1
APS	Ammonium persulfate
arg	Arginine
atg	Autophagy related gene
bp	Base pairs
BSA	Bovine serum albumine
can	Canavanine
clonNAT	Nourseotricine
CM	Complete minimal medium
CM	Chloramphenicol
CPY	Carboxypeptidase Y (Pcr1)
Cvt	Cytosolic to vacuolar
DMA	Deletion mutant array
DMSO	Dimethylsulfoxide
DNA	Deoxyribonucleic acid
dNTP	Deoxynucleosidetriphosphate (dATP, dGTP, dCTP, dTTP)
DO	Dropout mix
E. coli	*Escherichia coli*
e.g.	For example
ECL	Enhanced chemiluminescence
EDTA	Ethylenediamintetraacedic acid
ERAD	Endoplasmic reticulum associated protein degradation
ESCRT	Endosomal sorting complex required for transport
EtOH	Ethanole
fig.	Figure
g	Gramm
g	Gravity
G418	Kanamycin
GFP	Green fluorescent protein
GST	Glutathione S-transferase
h	Hour
H. polymorpha	*Hansenula polymorpha*
H_2O	Dihydrogen monoxide (water)
H_2O_2	Hydorgen peroxide
his	Histidine

Abbreviation	
-his	Without histidine
-his/arg/lys	Without histidine/arginine and lysine
HOPS	Homotypic fusion and vacuole protein sorting
ILV	Intralumenal vesicles
IPTG	Isopropyl-α-D-Thiogalactopyranoside
KAN	Kanamycin
kb	Kilo bases
kDa	Kilo dalton
kg	Kilo gramm
l	Liter
leu	Leucine
-leu/arg/lys	Without leucine/arginine and lysine
lyp	Thialysine
lys	Lysine
M	Molar
mA	Milli ampere
-met	Without methionine
min	Minutes
mito	Mitochondrial
ml	Milli liter
mM	Milli molar
MV	Minimal medium
MVB	Multi vesicular body
n	Number of independent experiments
NADPH	Nicotinamidadenindinukleotidphosphat
NAT	Nourseotricine (clonNAT)
NEB	New england biolabs
nm	Nano meter
NSF	N-ethylmaleimide-sensitive factor
NV junction	Nuclear vacuolar junction
O_2^-	Superoxide anion
OD	Optical indensity
ORF	Open reading frame
OSBP	Oxysterol-binding protein
p	Plasmid
paraquat	N, N'-dimethyl-4,4'-bipyridinium dichloride
P. pastoris	*Pichia pastoris*
PAGE	Poly acryl amide gel electrophoresis
PAS	Pre-autophagosomal structure
PBS	Phosphate buffered saline
PCR	Polymerase chain reaction
PE	Phosphatidylethanolamine
pH	Negative logarithm of H+ concentration
PMN	Piecemeal microautophagy of the nucleus
PMSF	Phenylmethylsulfonylfluoride
PVDF	Polyvinylidene Fluoride
RFP	Red fluorescent protein
RNA	Ribonucleic acid
ROS	Reactive oxygen species
rpm	Rounds per minute

Abbreviation	
RT	Room temperature
s	Seconds
S.cerevisiae	*Saccharomyces cerevisiae*
SD	Synthetic minimal medium
SD-N	Synthetic minimal medium lacking nitrogen (SD (-N))
SDS	Sodium dodecyl sulfate
sec	Secretory pathway
SEM	Standard error of the mean
SGA	Synthetic genetic analysis
SNAP	Synaptomal-associated protein
SNARE	Soluble NSF attachment receptor
SOC	Super optimal broth containing glucose
ß-ME	Beta mercaptoethanole
tab.	Table
TAE	Tris-acetate-EDTA-buffer
Taq	Thermus aquaticus
TBST	Tris buffered saline with Tween
TCA	Trichloroacatic acid
TEMED	N,N,N´,N´-Tetramethylethylenediamine
TOR	Target of rapamycin
U	Units
ura	Uracile
-ura	Without uracile
UV	Ultraviolet
V	Volt
YPD	Yeast Peptone Dextrose
YPL	Yeast Peptone Lactate
V_{max}	Maximum speed
Vps	Vacuolar protein sorting
WT	Wild type
YPD	Yeast extract peptone dextrose
YPL	Yeast extract peptone lactate
µg	Micro gramm
µl	Micro liter
µM	Micro molar

1. Summary

Autophagy is a ubiquitous protein degradation pathway in eukaryotic cells. As response upon nutrient starvation, cytosolic material and also whole organelles are engulfed by a double membrane-layered vesicle, the autophagosome. The formation of the autophagosome starts at the pre-autophagosomal structure (PAS). The completed autophagosome is then targeted to the vacuole. After fusion with the vacuole, a single membrane-layered vesicle, the autophagic body, is released into the vacuole. After lysis of the membrane, the contents of the autophagic body are degraded and the contained macromolecules are recycled. The aim of this study was the identification of cooperating or redundant genes to different autophagic genes, to uncover molecular details of autophagosome formation and to allow mechanistic insights into different selective variants of autophagy.

For the identification of autophagy related cooperating or redundant genes, the Synthetic Genetic Array analysis (SGA) was used. This is a powerful high-throughput technique to identify synthetic lethal double deletions, probably reflecting the same essential function of the respective gene products. For this purpose, the query strains *atg8*Δ*, atg15*Δ*, atg18*Δ *and atg21*Δ were generated in this study and crossed to the entire deletion library available for *S. cerevisiae.* Unfortunately, the procedure resulted in only false positive matches.

In addition to the common marker protein GFP-Atg8, this study introduces the marker protein Pgk1-GFP to detect unselective autophagy by western blot and microscopy. Compared to the autophagic substrate GFP-Atg8, the use of this cytosolic protein allows the unbiased detection of unselective bulk autophagy.

The molecular details of the biogenesis of autophagosomes are poorly understood. Our group identified the AAA^+ ATPase Cdc48 and its cofactor Ubx1 (Shp1) as novel components needed for autophagosome biogenesis. In accordance with former experiments in the laboratory, this study presents Shp1 as the exclusive cofactor of Cdc48 needed for autophagy. *SHP1* deleted cells show no accumulation of autophagosomes in the vacuole, while the formation of the PAS or the lipidation of Atg8, which both are important steps during autophagosome formation, are not impaired in *shp1*Δ cells. Furthermore, a suggested interaction of Shp1 and Atg8 was proven by recombinant pull down experiments using GST-Shp1 and some truncated versions. In mammals, the homologues of Cdc48 and Shp1, p97 and p47, are involved in the ubiquitin-dependent mitotic Golgi reassembly. In contrast, the complex of Cdc48 and Shp1 in yeast, requires the ubiquitin-like Atg8 for its function in

autophagy. This gives for the first time a rationale for the use of Atg8 during unselective autophagy and explains why the delipidation of Atg8-PE by Atg4 is necessary for efficient autophagy.

Mitochondria are the sites of ATP production in aerobic cells. As a consequence, they are at the same time a major source for reactive oxygen species (ROS), which damage mitochondria and other organelles. Thus, a quality control for mitochondria is essential for cellular survival. Mitophagy, the selective autophagic degradation of mitochondria, might fulfil such a role, but is still poorly understood in yeast. In this study, the construction of a marker protein and its use in degradation assay experiments by western blot allow the quantitative measurement of mitophagy. In contrast to a commonly used chromosomal Om45-GFP fusion, the novel marker protein can be expressed vom a plasmid, avoiding time consuming chromosomal integration. Different conditions to induce mitophagy were established. These different conditions allow the differentiation between mitophagy of superfluous or damaged mitochondria. Hereby, proteins of the ESCRT machinery, not required for unselective bulk autophagy, were found to be needed for mitophagy. In humans, Parkin ubiquitinates mitochondrial substrates to induce mitophagy. In this study, the ubiquitin isopeptidase Doa4 is shown to be required for mitophagy, indicating for the first time a mitophagy-related role of ubiquitin in yeast.

Another selective variant of autophagy is PMN, the piecemeal microautophagy of the nucleus. A specific cargo-recognition in PMN is indispensable to preserve the integrity of the nucleus. Therefore, the still unknown nuclear cargo was a focus of interest. The results of this study point to a specific cargo-recognition of nucleolar proteins in PMN. Strains expressing different nucleolar GFP fusion proteins were investigated, some showed PMN-like structures in microscopy. Furthermore, nucleus-vacuole junctions, the contact sites between the nucleus and the vacuolar membrane, are shown to localise near the nucleolus.

2. Introduction

2.1 The model organism *Saccharomyces cerevisiae*

Saccharomyces cerevisiae is a budding yeast and belongs to the family of the Saccharomycetae. It is one of the best-studied eukaryotic model organisms in molecular and cell biology, comparable to the procaryotic counterpart *Escherichia coli*.

The cells have a size of about 5 – 10 µm and can either be haploid or diploid. In both forms the cells can undergo a mitotic division by forming a bud. Furthermore, upon nutrient limitation a diploid cell, which results out of the mating between two haploid cells (a and α), also undergoes meiotic division by sporulation. This leads to the formation of an ascus containing four haploid spores, two of each mating type (Mat a and α) (Figure 1).

The genome of *S. cerevisiae* is completely sequenced and has 16 chromosomes consisting of about 13 000 000 bp coding for about 5800 genes (Mewes, 1997).

As most of the proteins are highly conserved, information can often be transferred to higher eukaryotic cells, therefore *S. cerevisiae* is one of the major model organisms in cell- and developmental biology.

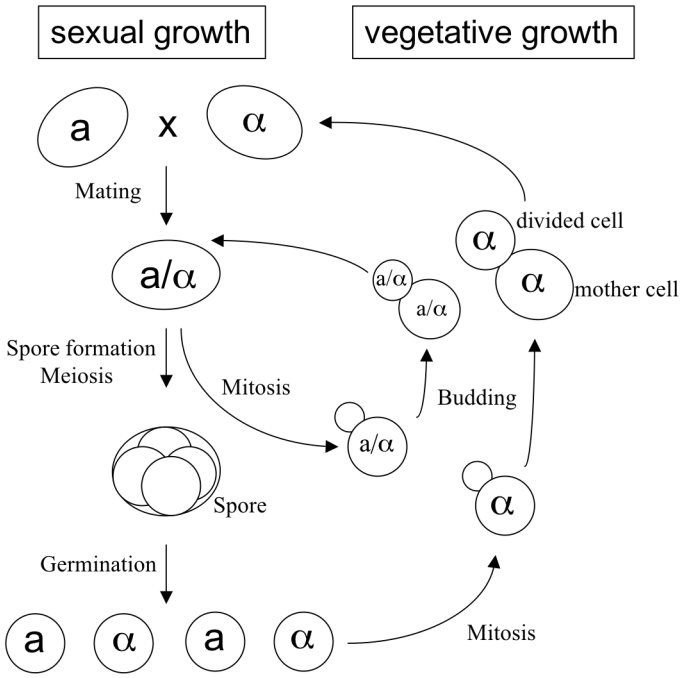

Figure 1: Cell cycle of *Saccharomyces cerevisiae*
((Herskowitz, 1988); modified)

2.2 Autophagy

All eukaryotic cells share a major intracellular degradative pathway. This pathway, called autophagy, delivers cytoplasm, including whole organelles, to the vacuole for their degradation. Therefore, autophagy plays an important role in the recycling of cellular building blocks (Figure 2). In contrast to the selective ubiquitin dependent degradation of short-lived proteins via the proteasome, autophagy is a starvation induced, unselective or selective, degradation process of long-lived proteins and can be divided into different subtypes: macroautophagy, microautophagy and chaperone mediated autophagy.

Proteins involved in autophagy are termed Autophagy related proteins (Atg) (Klionsky, 2003). In the last decades 34 Atg proteins were identified (Suzuki; Farre, 2009; Kanki, 2009b; Okamoto, 2009).

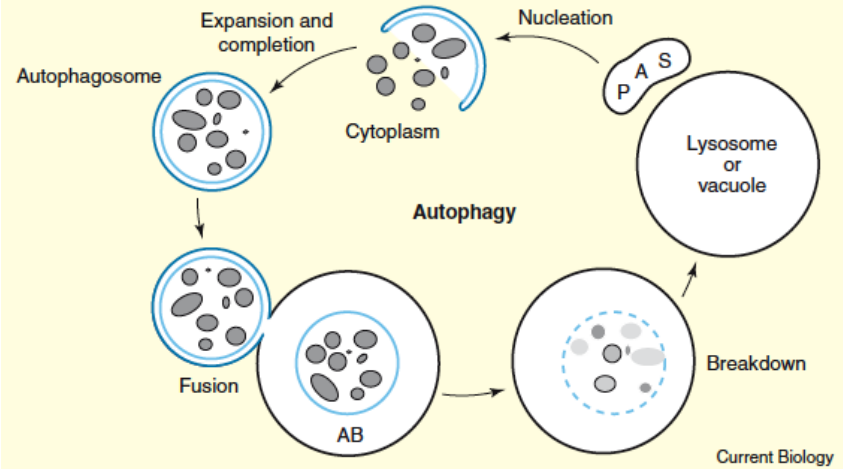

Figure 2: Scheme of autophagy

A double-membrane-layered vesicle, the autophagosome, sequesters cytoplasm, fuses with the lysosome or vacuole and a single-membrane autophagic body (AB) is released into the lysosome/vacuole where it is lysed and the cargo is degraded for the recycling of the resulting macromolecules (Klionsky, 2005).

2.2.1 Macroautophagy

Macroautophagy is a starvation-induced process resulting in the formation of double membrane-layered vesicles, of 300 – 900 nm in diameter. These vesicles, called autophagosomes, are formed out of a phagophore at the pre-autophagosomal structure (PAS) and engulf unselectively cytosolic material and also whole organelles by expansion of the phagophore (Takeshige, 1992; Ishihara, 2001).

The outer membrane of the autophagosome fuses with the vacuole and a still single membrane-layered vesicle, called autophagic body, is released into the vacuole (Baba, 1994).

This fusion event of the autophagosome and the vacuole requires the homotypic vacuolar fusion machinery (Ishihara, 2001). The membrane of the autophagic body is lysed inside the vacuole and the cytoplasm-derived materials are degraded by vacuolar hydrolases. Up to now, the only identified enzyme, involved in the intravacuolar lysis, is the putative lipase Atg15, which is transported to the vacuole via the multi vesicular body (MVB) pathway (Epple, 2001; Epple, 2003). Macroautophagy, further named unselective autophagy, is up regulated under longer periods (several hours) of nutrient starvation as an adaptive response to recycle amino acids for survival. This bulk degradation of cytosolic material needs a set of Atg proteins, which belong to parts of different subcomplexes.

2.2.1.1 The Atg1 kinase and its regulators

The target of rapamycin (TOR) kinase is a negative regulator of autophagy and responds specifically to rapamycin or nitrogen starvation via an unknown upstream sensor (Figure 3). It controls the phosphorylation state of Atg13, one of the core Atg proteins. Under nutrient rich conditions the TOR kinase is active. Atg13 is highly phosphorylated in a TOR-dependent manner and therefore has low affinity to Atg1. Under nitrogen starvation the TOR kinase is inactivated and Atg13 is rapidly dephosphorylated. Therefore Atg13 associates with Atg1 as a result of a higher affinity. This interaction of Atg13 and Atg1 somehow regulates and enhances the serine/ threonine kinase activity of Atg1, which is essential for autophagy.
Further proteins interact with the Atg1-Atg13 complex, such as Vac8, Atg11 or Atg17. Atg11, needed for both Cvt pathway and pexophagy but not for unselective autophagy, appears to function as an adaptor or scaffold protein and allows the selective cargo recognition (Kim, 2001). Vac8 and Atg11 are also phosphorylated but independently of the Atg1-Atg13 complex. The role of their phosphorylation is unknown (Scott, 2000). Atg17 is essential for autophagy and not for the Cvt pathway, by somehow regulating the size of the forming vesicles (Kabeya, 2005). The kinase activity of Atg1 is not essential for the recruitment of all Atg proteins to the pre-autophagosomal structure (PAS). *ATG1* deleted cells show an accumulation of e.g. Atg8, while Atg2 is absent from the PAS (Yorimitsu and Klionsky, 2005; Nakatogawa, 2009). The Atg1 kinase regulators Atg17, Atg29 and Atg31 function in the initial step of autophagosome formation, they are autophagy specific genes and from a ternary complex. This complex associates with the Atg1-Atg13 complex in response to nutrient starvation and is important for the activation of Atg1. This association has an essential function in the organisation of the PAS by recruitment of other core Atg

proteins to the PAS, suggesting a function in autophagosome formation (Kawamata, 2008; Nakatogawa, 2009).

An alternative activation of Atg1 in an Atg13-independent manner under respiratory growth conditions is suggested, but still unclear (Okamoto, 2009).

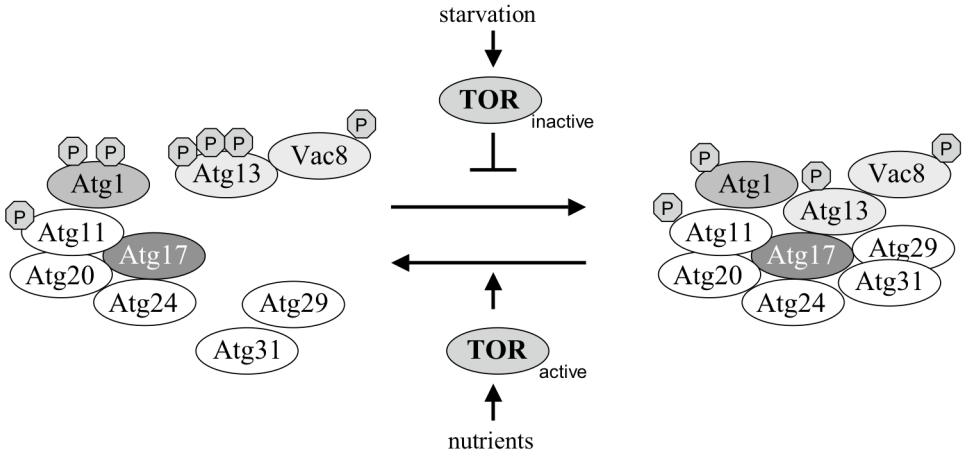

Figure 3: The regulatory TOR kinase complex for autophagy induction
((Yorimitsu and Klionsky, 2005; Nakatogawa, 2009); modified)

2.2.1.2 The two PtdIns 3 –kinase complexes

Phosphatidylinositol 3-phosphate is essential for autophagy. Vps34 is the only identified PtdIns 3-kinase in yeast and part of at least two different PtdIns 3-kinase complexes. Complex I consists, additionally to Vps34, of Vps15, Atg6 (Vps30) and Atg14, while complex II in contrast, includes Vps38 instead of Atg14 (Figure 4 (A) and (B)).

Complex I plays an important role in autophagy and the Cytoplasm to vacuolar trafficking (Cvt) pathway, therefore the deletion of *ATG14* causes a block in autophagy and the Cvt pathway. The deletion of *VPS38*, the essential factor of complex II, leads to a block in the multivesicular body (MVB) pathway and the sorting of carboxypeptidase Y (CPY) (Kihara, 2001; Yorimitsu and Klionsky, 2005). Early data have indicated, that the PtdIns 3-kinase complex I is essential for the recruitment of Atg8-PE and the Atg12-Atg5-Atg16 conjugate (see 2.1.4) to the pre-autophagosomal structure (Suzuki, 2001; Yorimitsu and Klionsky, 2005; Klionsky, 2007; Nakatogawa, 2007; Nakatogawa, 2009; Inoue and Klionsky, 2010).

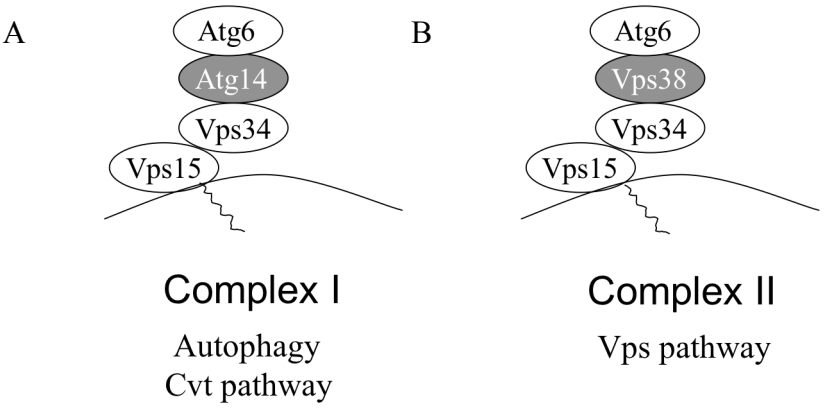

Figure 4: The two Phosphatidylinositol 3-kinase complexes in *S. cerevisiae*
Both complexes contain Vps15, Vps34 and Atg6 (Vps30), (A) Complex I required for autophagy and the Cvt pathway contains Atg14. (B) Complex II containing Vps38 is involved in Vps/MVB pathway ((Yorimitsu and Klionsky, 2005); modified)

2.2.1.3 The pre-autophagosomal structure

The biogenesis of the double membrane-layered autophagosomes starts with the formation of the so-called phagophore (isolation membrane) at the pre-autophagosomal structure (PAS). The PAS, observed in close proximity to the vacuole, is considered to be the place where autophagosome formation starts and where the autophagic core proteins colocalise. Atg18 is recruited to the PAS in a PtdIns 3-kinase complex I-dependent manner. Mediated by the crosstalk between the different systems, during the initiation of autophagy, Atg8 is transported to the PAS in a most likely PtdIns 3-kinase dependent manner, even in the absence of Atg1 (Guan, 2001; Suzuki, 2001; Strømhaug, 2004; Suzuki, 2007).

2.2.1.4 The two conjugation systems

The two ubiquitin-like conjugation systems are widely conserved in eukaryotic cells and play an essential role for autophagy. In the Atg12-Atg5 conjugation system Atg12 and Atg5 are coupled via an isopeptide bond between a C-terminal glycine of Atg12 and a central lysine of Atg5. Atg12 therefore is activated by the E1-like protein Atg7 that functions like a ubiquitin-activating enzyme. Hence, Atg12 is conjugated through the activity of Atg10 (an E2-like ubiquitin conjugation enzyme) to Atg5. The Atg12-Atg5 conjugate binds to Atg16. Atg16 itself can form a homo-oligomer and therefore mediates the formation of a higher multimeric Atg12-Atg5-Atg16 complex. (Figure 5 (A)). This complex has an E3-like function in the second ubiquitin-like conjugation system, the Atg8-phosphatidylethanolamine (Atg8-PE)

conjugation system (Figure 5 (B)). In the first step, an arginine at the extreme C-terminus of Atg8 is cleaved off via the cysteine protease Atg4. Thereby, the glycine residue, essential for subsequent reactions, is exposed. Furthermore, Atg8 is activated by the E1-like Atg7 and transferred to the E2-like Atg3, supported by the Atg12-Atg5-Atg16 complex. Atg3 induces an amide-bound between the C-terminal glycine of Atg8 and an aminogroup of PE, thereby coupling Atg8-PE to the outer and inner membrane of the autophagosome. In contrast to the conjugation of Atg12 to Atg5, the lipidation of Atg8 is reversible. After the formation of the autophagosome, the part of Atg8 at the outer membrane is cleaved off via the cysteine protease Atg4. In contrast, Atg8-PE, bound to the inner surface of the autophagosome, is delivered to the vacuole and degraded. Therefore, GFP-Atg8 is a useful marker protein for the detection of autophagy in degradation assay experiments. Furthermore, GFP-Atg8 has been shown to concentrate at the PAS. Therefore GFP-Atg8 can also be used as marker protein for the visualisation of the PAS in microscopic experiments (Ichimura, 2000; Kirisako, 2000; Ohsumi and Mizushima, 2004; Yorimitsu and Klionsky, 2005; Inoue and Klionsky, 2010).

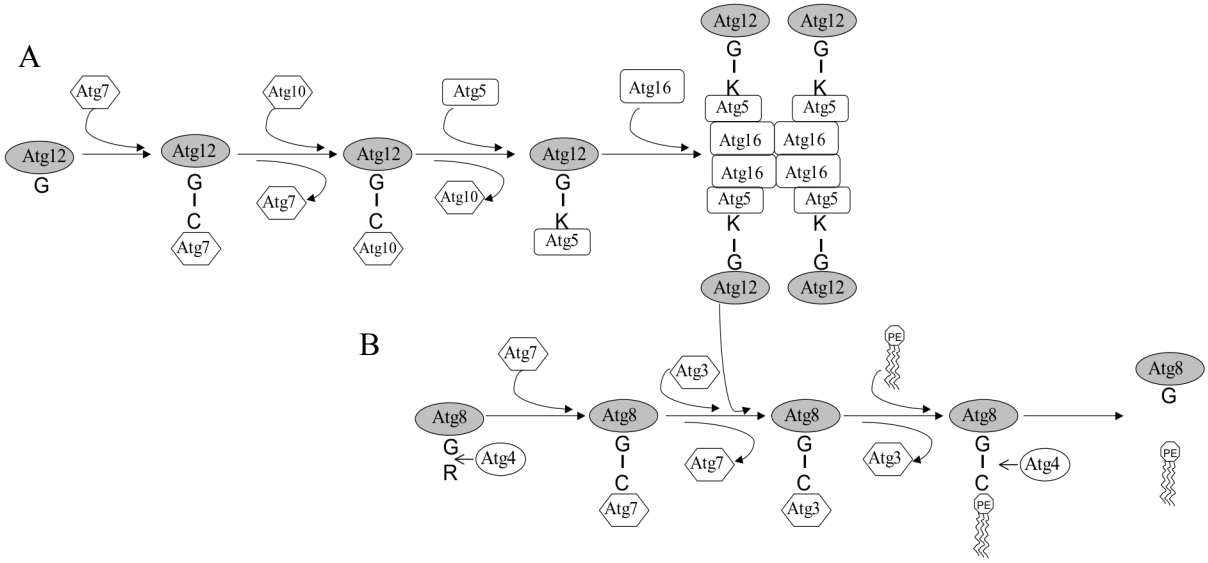

Figure 5: The two conjugation systems

(A) The Atg12-Atg5 conjugation system and (B) the Atg8-PE conjugation system ((Nakatogawa, 2009); modified)

2.2.1.5 Atg9 cycling

Atg9 is an integral membrane protein, which is recruited to the PAS during assembly. It also localises at a peripheral pool and cycling between both sites has been proposed. A localisation of the peripheral pool at mitochondria, the ER or the Golgi is still under discussion (Ishihara, 2001; Reggiori, 2005; Longatti and Tooze, 2009). Atg9 is thought to mediate the delivery of membranes of unknown origin for the formation of the autophagosome. This suggested lipid flow might be regulated via the Atg1-Atg13 complex and the PtdIns 3-kinase complex I, including a role of Atg2 and Atg18. Atg9 does not affect the formation of the Atg12-Atg5-Atg16 complex or Atg8-PE, but is required for their proper localisation at the PAS. The anterograde transport of Atg9 to the PAS has been shown to depend on Atg11, Atg23 and Atg27, whereas Atg1-Atg13 and Atg2-Atg18 are required for the retrograde transport back to the peripheral sites. Due to the cycling of Atg9 to the PAS, also GFP-Atg9 is a useful marker for the visualisation of the PAS in microscopy (Suzuki, 2001; Wang, 2001; Reggiori, 2004a; Reggiori, 2005; Inoue and Klionsky, 2010).

2.2.2 Microautophagy

During microautophagy, cytosolic components or organelles are directly engulfed by an invagination of the vacuolar membrane (Farre, 2009). This process topologically reminds to invagination occurring during multivesicular body formation at the endosome (see chapter 2.3), but the mechanism is still unclear. Examples for selective microautophagic processes are pexophagy (see 2.2.4.2) or PMN, the piecemeal microautophagy of the nucleus (see 2.2.4.4).

2.2.3 Chaperone-mediated autophagy

The third subtype is chaperone-mediated autophagy, which has only been discovered in mammalian cells but not in *S. cerevisiae* and whose dysregulation is associated with Parkinson's disease (PD) (Yang, 2009). Cytosolic proteins, containing a particular pentapeptide consensus motif (KFERQ), are degraded after the lysosomal import (Cuervo, 2010).

2.2.4 Selective autophagy

2.2.4.1 The Cytoplasm to Vacuolar Trafficking pathway

The Cytoplasm to Vacuolar Trafficking (Cvt) pathway selectively transports two specific cargos to the vacuole: pro-aminopeptidase I (prApe1) and α-mannosidase (Ams1). The Cvt pathway requires most of the Atg components and is therefore regarded as a selective autophagic process, which is only active under nutrient rich conditions (Klionsky, 1992; Harding, 1996).

The pro-form of aminopeptidase I (prApe1) is synthesised in the cytosol, where it assembles into the so-called Ape1-complex, an oligomeric structure. The specific receptor protein Atg19 binds to this complex, forming the Cvt-complex, which is recruited at the PAS to a double membrane-layered vesicle, the Cvt vesicle, dependent on Atg11, a protein specific for selective variants of autophagy (Kim, 2001). The Cvt vesicles, which are actually smaller than autophagosomes (140 – 160 nm in diameter) (Baba, 1997), fuse with the vacuole and a single membrane vesicle is released in the vacuolar lumen, where it is lysed and the prApe1 is matured to mApe1 (Klionsky, 1992; Scott, 1997).

2.2.4.2 Pexophagy

Pexophagy is the selective autophagic degradation of peroxisomes. Most of the current knowledge of pexophagy resulted from experiments in *P. pastoris* and *H. polymorpha.* Studies in *H. polymorpha* has shown, that the shift of methanol-grown cells to glucose medium initiates the selective degradation of superfluous peroxisomes in form of macropexophagy, while in *P. pastoris* the same conditions initiate micropexophagy and, however, ethanol induces macropexophagy in both yeasts (Veenhuis, 1983; Tuttle and Dunn, 1995; Sakai, 2006).

S. cerevisiae has been shown to adapt the amount of peroxisomes in response to different nutrient sources. This means, that cells, grown on oleic acid as sole carbon source, induce peroxisome biogenesis and a shift to glucose rich or nitrogen limited medium results in the degradation of peroxisomes via pexophagy. Most proteins required for unselective autophagy are also necessary for both micro- and macropexophagy. However, pexophagy requires additional pexophagy-specific proteins (Hutchins, 1999; Farré, 2008).

2.2.4.3 Ribophagy

Ribophagy is the selective degradation of assembled 40S and 60S ribosomal subunits by autophagy. Interestingly, the ubiquitin protease Ubp3 and its cofactor Bre5 were shown to be needed, indicating the removal of ubiquitin from an unknown substrate. Ubp3 is believed to deubiquitinate Atg19 and is therefore somehow involved in the Cvt pathway (Baxter, 2005), but ribophagy is dependent on the autophagic core machinery and is not affected in *atg19*Δ cells (Kraft, 2008).

2.2.4.4 Piecemeal Microautophagy of the Nucleus

Piecemeal microautophagy of the nucleus (PMN) selectively degrades portions of the nucleus at inter-organelle membrane contact sites, which are called the nucleus-vacuole (NV) junctions (Figure 6 (I)). These nucleus-vacuole junctions are formed by direct interaction of Vac8 and Nvj1 (Pan, 2000). Furthermore, Osh1, a member of the Osh family in yeast, is targeted to the nucleus-vacuole (NV) junctions through physical interaction with Nvj1. Due to the interaction with NV junctions, Osh1 exhibits a substrate for PMN and is therefore a common marker protein (Millen, 2009). PMN is a selective process and has been shown to depend on the autophagic core proteins (Krick, 2008b). As Atg17, a macroautophagy-specific protein, and Atg11, only required for selective autophagic processes, are involved in PMN, this process is a novel variant of selective autophagy (Roberts, 2003; Krick, 2008b).

Induced by starvation, invagination of the vacuolar membrane sequesters a portion of the nucleus (Figure 6 (II)). After fission of a nuclear membrane derived vesicle (III), a PMN vesicle is released into the vacuole (IV), where it is degraded by vacuolar hydrolases (V) (Krick, 2008b). Up to now, chromosomal DNA and nuclear pore complexes has been shown to be excluded from NV junctions (Pan, 2000; Roberts, 2003), but a specific nuclear cargo is still missing and is a major focus of investigation.

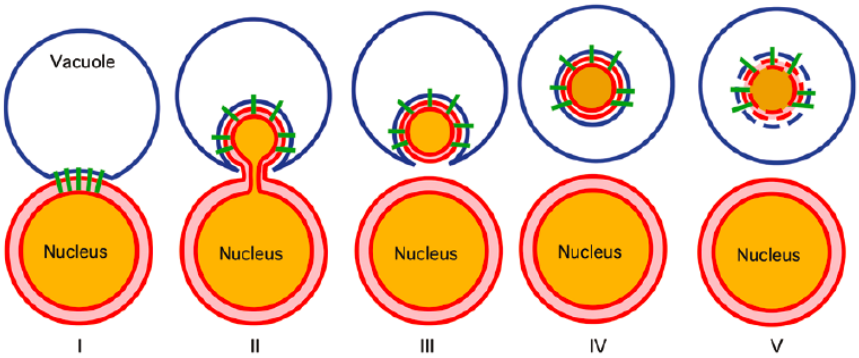

Figure 6: Model of piecemeal microautophagy of the nucleus (PMN)
The process of piecemeal microautophagy of the nucleus (PMN) starts with I) the formation of nuclear vacuolar junctions (green), II) then a part of the nucleus is engulfed by vacuolar extentions and III) the nucleus undergoes a fission event. IV) Afterwards a PMN vesicle is released into the vacuole and V) is degraded by vacuolar hydrolases (Krick, 2009).

2.2.4.5 Mitophagy

Mitochondria play a significant role in a lot of important metabolic processes, ranging from energy production to cell death. As a consequence, they are at the same time the major source of cellular reactive oxygen species (ROS), which cause oxidative damage to, for instance, mitochondrial DNA. Therefore a quality control of mitochondria is very important to maintain cellular homeostasis (Nieminen, 2003; Keeble and Gilmore, 2007). In addition to the oxidant defence system (Jamieson, 1998), the selective degradation of mitochondria via autophagy termed mitophagy might fulfil this indispensable role.

Until the last years, mitophagy got more into the focus of research, probably caused by its involvement in many neurodegenerative diseases in humans, like Alzheimer's and Parkinson's disease (PD) (Wallace, 2005; Goldman, 2010; Weber and Reichert, 2010). The ubiquitin ligase Parkin and the mitochondrial kinase PINK1 have been shown to fulfil a crucial role in preventing PD by labelling dysfunctional mitochondria for autophagic degradation (Narendra, 2008).

In *S. cerevisiae*, recent studies have identified Atg32, a receptor protein exclusively needed for mitophagy. Interaction of Atg32 with Atg8 and a nitrogen starvation induced interaction of Atg8 with Atg11 have been shown. *ATG32* deleted cells are no longer able to degrade mitochondria by selective autophagy (Kanki and Klionsky, 2008; Kanki, 2009c; Okamoto, 2009). The exact molecular mechanism of cargo recognition remains unclear.

2.2.5 Membrane fusion events in autophagy

For release of the autophagic body into the vacuole the double membrane-layered autophagosome fuses with the vacuole. Therefore the outer membrane of the autophagosome fuses with the vacuolar membrane. This fusion is mediated by the typical homotypic fusion machinery, including the SNARE proteins Vam3, Vam7, Vti1 and Ykt6, Sec17, Sec18 and Sec19, the Rab protein Ypt7 and members of the class C Vps/HOPS complex and furthermore Ccz1 and Mon1 (Darsow, 1997; Sato, 1998; Fischer von Mollard and Stevens, 1999; Wang, 2003). Even though Sec18 and Vti1 are essential for the fusion of the autophagosome with the vacuole, they are not essential for autophagosome formation, meaning the elongation or sealing of the phagophore (Ishihara, 2001). At today's state of research, the secretory membrane flow from the ER to the Golgi seems to be not directly required for autophagosome formation and there is no evidence for a role of SNAREs in the elongation or sealing of the autophagosomes or Cvt vesicles. Atg proteins might fulfil these essential functions, but the mechanism of autophagosome biogenesis remains unclear (Ishihara, 2001; Reggiori, 2004b; Longatti and Tooze, 2009).

2.2.5.1 The AAA^+ ATPase Cdc48

Cdc48 (the homologue of p97 in mammals) belongs to the family of AAA^+ ATPases (ATPases associated with various cellular activities) and is a highly conserved protein which is involved in many different cellular processes, including fusion of homotypic membranes, ubiquitin-proteasome-dependent protein degradation, regulation of apoptosis, endoplasmic reticulum (ER)-associated degradation (ERAD) and nuclear envelope reassembly (Latterich, 1995; Ye, 2001; Braun, 2002; Jarosch, 2002; Braun and Zischka, 2008). In all these processes a segregase activity of Cdc48/p97 is believed to be the underlying molecular mechanism. The required energy to extract substrate proteins from protein complexes or lipid membranes is provided by ATP hydrolysis (Braun, 2002; Schuberth and Buchberger, 2008).

To direct the multiple functions of Cdc48/p97, different cofactors mediate its activity to different cellular pathways. For instance, Cdc48/p97, interacting with the heterodimeric substrate-recruiting cofactor Ufd1/Npl4, affects the degradation of ubiquitinated protein substrates out the ER (Meyer, 2000). Other known cofactors are the members of the UBX protein family (e.g.Ubx1/Shp1), whose UBX domain is a general Cdc48/p97-binding module (Schuberth and Buchberger, 2008). Seven UBX proteins are known for yeast. Three of these UBX proteins, including Ubx1 (Shp1), possess an amino-terminal UBA domain, which binds

ubiquitinated proteins *in vivo* (Schuberth, 2004). p47 (the homologue to yeast Shp1) is needed for mitotic Golgi reassembly in mammals, by mediating the binding of p97 to a Golgi t-SNARE via an ubiquitinated putative fusion regulator and furthermore regulating the ATPase activity of p97 (Meyer, 1998; Meyer, 2005).

2.2.5.1.1 Cdc48 and autophagosome biogenesis

Beside the unknown origin of the autophagic membrane, also the process of autophagosome biogenesis has not been elucidated so far. A recent study has identified the AAA^+ ATPase Cdc48 and its cofactor Shp1/Ubx1 as essential factors for autophagosome biogenesis (Krick, 2010) (Figure 7).

In contrast to p97 (the human Cdc48 homologue) and its cofactor p47 (to human homologue of Ubx1/Shp1), which mediate Golgi reassembly by extraction of an unknown fusion regulator from a protein complex, the Cdc48/Shp1 complex does not require ubiquitination or the proteasome system for its autophagic function. Atg8 is crucial for control of autophagosomal size/elongation (Nakatogawa, 2007; Xie, 2008a), therefore it has been suggested that the ubiquitin-like Atg8 may replace ubiquitin. This model has been supported by an interaction between Shp1 and the ubiquitin-like protein Atg8. Data of this study contributed to the resulting publication (Krick, 2010).

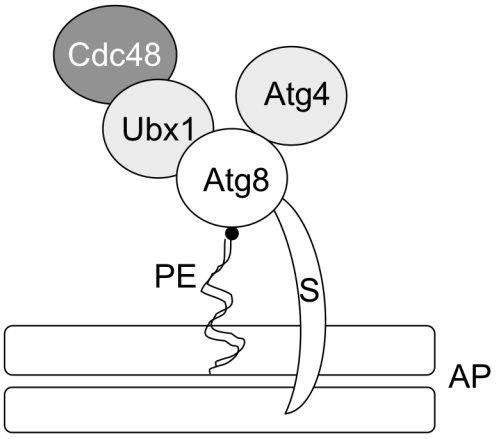

Figure 7: Model of Cdc48-Shp1 complex

The AAA^+ ATPase Cdc48 and its cofactor Shp1/Ubx1 form a complex needed for autophagosome biogenesis. Shp1 furthermore interacts with the ubiquitin-like protein Atg8, which is anchored via phosphatidylethanolamine (PE) into one layer of the double membrane of the autophagosome (AP). This PE conjugation is cleaved off by the cysteine protease Atg4, which is also needed for the previous lipidation of Atg8. Up to now, an involvement of a SNARE-like protein (S) is unclear.

2.3 The ESCRT machinery

Membrane-bound proteins are actively sorted to different places in the cell through defined processes. Some proteins are recycled back to the plasma membrane or Golgi and others are sorted to the vacuole. Topologic problems of degrading transmembrane proteins in the lumen of the vacuole are solved by the multivesicular body (MVB) pathway, which is mediated by the Vps class E proteins. Monoubiquitin serves as a signal to direct proteins into the MVB pathway. Parts of the endosomal membrane bud into the lumen and form intralumenal vesicles (ILVs). Late endosomes containing these ILVs are termed multivesicular bodies (MVBs). Deletion of one of the Vps class E proteins leads to the formation of an abnormal multicisternal endosome, which lacks internal vesicles and is referred to as class E compartment. The majority of these class E Vps proteins are members of the endosomal sorting complexes required for transport (ESCRT) (Figure 8). These protein complexes are recruited from the cytoplasm to the endosomal membrane, where they function in the sorting of transmembrane proteins into the MVB pathway or in the formation of MVB vesicles. The ESCRT machinery consists of the five subunits: ESCRT-0, ESCRT-I, ESCRT-II, ESCRT-III and the AAA^+ ATPase Vps4 (Babst, 2005; Raiborg and Stenmark, 2009). ESCRT-0 consists of Vps27 and Hse1, which both possess ubiquitin interaction motifs (UIMs). These two ubiquitin-binding proteins form a complex, which is recruited to the endosome, mediated by the FYVE domain of Vps27 (Burd and Emr, 1998; Misra and Hurley, 1999). Furthermore Vps27 recruits ESCRT-I, consisting of Vps23, Vps28, Vps37 and Mvb12 (Katzmann, 2001; Katzmann, 2003). This complex also binds to monoubiquitinated proteins, as well as ESCRT-II consisting of Vps22, Vps25 and Vps36. Then, the cargo proteins are deubiquitinated by Doa4 and packed into the MVB vesicles by ESCRT-III, which consists of Vps20, Vps32, Vps2 and Vps24 (Amerik, 2000; Babst, 2002). After membrane scission ESCRT-III is disassembled by Vps4 (Babst, 1997). Interestingly, no SNAREs are needed for this membrane scission event (Hurley and Hanson, 2010).

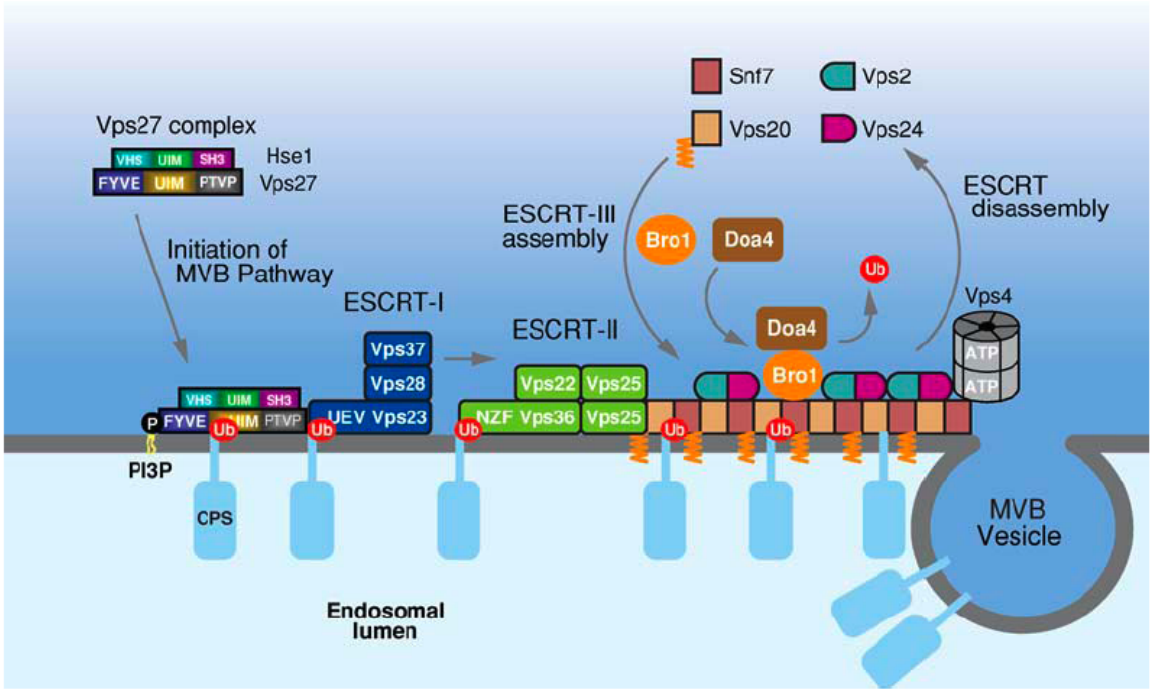

Figure 8: The ESCRT machinery of MVB sorting pathway
(Hurley and Emr, 2006)

2.3.1 ESCRT and autophagy

Several reports have analysed the fusion between early and late MVB endosomes with autophagosomes and the resulting generation of amphisomes in mammalian cells, indicating a multistep process (Eskelinen, 2005). Furthermore, in mammalian cells the depletion of ESCRT subunits (e.g. Vps24 (ESCRT-III)) results in an inhibition of the autophagic degradation (Filimonenko, 2007). However, little is known about the potential of MVBs, and the consequence of depleting ESCRT subunits, in autophagic degradation (Fader and Colombo, 2009). Several studies have suggested different roles of the ESCRT machinery. One publication speculates that the inactivation of the ESCRT machinery might prevent the closure of the phagophore, or that the ESCRT machinery might be required for amphisome and autolysosome formation or for lysosome biogenesis (Rusten and Stenmark, 2009). Several reports furthermore discuss the involvement of vacuolar proteins sorting in biogenesis of the vacuolar membrane. In yeast, it is also discussed that Vps class E mutants might impair the fidelity of the vacuolar membrane by defects in vacuolar protein sorting. But the exact influence is still unknown (Piper, 1995; Rieder, 1996; Babst, 1997; Bryant and Stevens, 1998). Nevertheless, in yeast, depletion of one of the Vps class E components, does not lead to a block in autophagy. For instance, the deletion of *VPS4*, *VPS23*, *VPS27* and *VPS28* did

not effect the maturation of prApe1 under growing or starvation conditions, or the degradation of GFP-Atg8 under starvation conditions (Reggiori, 2004b; Bremer, 2009). Some deletions lead to a reduced degradation of autophagic material, probably in an indirect way by the impaired vacuolar protein sorting activity and the resulting abnormal vacuolar membrane composition.

2.4 Aim of the study

Autophagy is a well-studied process in eukaryotic cells and is involved in numerous diseases, such as neurodegenerative. In yeast, 34 Autophagy related genes (Atg) have already been identified, but molecular details of the molecular mechanism of autophagy still remain unknown.

I. For the identification of autophagy related cooperating or redundant genes, the Synthetic Genetic Array analysis (SGA) should be used. SGA is a powerful high-throughput technique to identify synthetic lethal double deletions, probably reflecting that the gene products impinge on the same essential function. For this purpose, different query strains deleted in autophagic genes should be generated and crossed to the entire deletion library available for *S. cerevisiae.*

II. Different methods to measure selectively bulk autophagy are available, but require a lot of experience, specific deletion strains or are expensive. An aim of this study was to establish a standard method to measure bulk autophagy, using Pgk1-GFP as a marker protein.

III. Until now, the fusion events required for autophagosome biogenesis are poorly understood. No essential SNAREs or autophagy-specific Rab effectors have been identified, therefore a special autophagy fusion machinery might be required. Based on previous results our laboratory, the role of Cdc48 and its adaptor Shp1 in autophagosome formation should be analysed.

IV. In yeast, mitophagy, the selective degradation of mitochondria, is currently not well understood, therefore to monitor mitophagy and to differentiate between the degradation of superfluous or damaged mitochondria in yeast, a specific marker protein for a mitophagy assay and novel methods to induce mitophagy should be established.

V. A specific cargo-recognition in PMN, the piecemeal microautophagy of the nucleus, is indispensable to preserve the integrity of the nucleus. No selective nuclear cargo has been identified so far, therefore the degradation of different nuclear GFP fusion proteins should be analysed.

3. Material and Methods

3.1 Material

3.1.1 *Saccharomyces cerevisiae* strains

Table 1: Strains of BY4741 background used in this study

Strain	Genotype	Source
BY 4741	MATa *his3Δ1 leu2Δ0 met15Δ0 ura3Δ0*	Euroscarf
Y04547	BY4741 MATa *atg1Δ*::KAN	Euroscarf
Y02098	BY4741 MATa *pep4Δ*::KAN	Euroscarf
Y05700	BY4741 MATa *atg18Δ*::KAN	Euroscarf
Y02152	BY4741 MATa *atg21Δ*::KAN	Euroscarf
Y00253	BY4741 MATa *vac8Δ*::KAN	Euroscarf
Y05876	BY4741 MATa *ygr223cΔ*::KAN	Euroscarf
Y03104	BY4741 MATa *atg8Δ*::KAN	Euroscarf
Y05492	BY4741 MATa *vps4Δ*::KAN	Euroscarf
Y05381	BY4741 MATa *vps27Δ*::KAN	Euroscarf
Y02763	BY4741 MATa *vps28Δ*::KAN	Euroscarf
Y01580	BY4741 MATa *vps32Δ*::KAN	Euroscarf
Y05269	BY4741 MATa *vps38Δ*::KAN	Euroscarf
Y03084	BY4741 MATa *shp1Δ*::KAN	Euroscarf
Y05789	BY4741 MATa *atg15Δ*::KAN	Euroscarf
Y07090	BY4741 MATa *atg7Δ*::KAN	Euroscarf
Y05382	BY4741 MATa *atg3Δ*::KAN	Euroscarf
Y05325	BY4741 MATa *vps36Δ*::KAN	Euroscarf
Y04004	BY4741 MATa *doa4Δ*::KAN	Euroscarf
Y06148	BY4741 MATa *ubp3Δ*::KAN	Euroscarf
Y06078	BY4741 MATa *bre5Δ*::KAN	Euroscarf
Y02889	BY4741 MATa *nvj1Δ*::KAN	Euroscarf
Y01989	BY4741 MATa *atg4Δ*::KAN	Euroscarf
Y05113	BY4741 MATa *uth1Δ*::KAN	Euroscarf
Y03682	BY4741 MATa *vac1Δ*::KAN	Euroscarf
Y05798	BY4741 MATa *aup1Δ*::KAN	Euroscarf
Y02305	BY4741 MATa *atg32Δ*::KAN	Euroscarf
Y00560	BY4741 MATa *ubx2Δ*::KAN	Euroscarf
Y03788	BY4741 MATa *ubx3Δ*::KAN	Euroscarf
Y06200	BY4741 MATa *ubx4Δ*::KAN	Euroscarf
Y03689	BY4741 MATa *ubx5Δ*::KAN	Euroscarf
Y03888	BY4741 MATa *ufd2Δ*::KAN	Euroscarf
Y05063	BY4741 MATa *ufd3Δ*::KAN	Euroscarf
Y04859	BY4741 MATa *ufd4Δ*::KAN	Euroscarf
Y03341	BY4741 MATa *der1Δ*::KAN	Euroscarf
Y05665	BY4741 MATa *otu1Δ*::KAN	Euroscarf

Strain	Genotype	Source
WT Om45-GFP	BY4741 MATa Om45-GFP::HIS3MX6	This study
atg1Δ Om45-GFP	BY4741 MATa *atg1Δ::*KAN Om45-GFP::HIS3MX6	This study
pep4Δ Om45-GFP	BY4741 MATa *pep4Δ*::KAN Om45-GFP::HIS3MX6	This study
uth1Δ Om45-GFP	BY4741 MATa *uth1Δ*::KAN Om45-GFP::HIS3MX6	This study
atg32Δ Om45-GFP	BY4741 MATa *atg32Δ*::KAN Om45-GFP::HIS3MX6	This study

Table 2: Strains of BY4742 background used in this study

Strain	Genotype	Source
BY4742	Mat α *his3Δ1; leu2Δ0; lys2Δ0; ura3Δ0*	Euroscarf
Y11580	BY4742 MATα *vps32Δ*::KAN	Euroscarf
Y12098	BY4742 MATα *pep4Δ*::KAN	Euroscarf
Y12152	BY4742 MATα *atg21Δ*::KAN	Euroscarf
Y12580	BY4742 MATα *vps25Δ*::KAN	Euroscarf
Y12763	BY4742 MATα *vps28Δ*::KAN	Euroscarf
Y13084	BY4742 MATα *shp1Δ*::KAN	Euroscarf
Y13104	BY4742 MATα *atg8Δ*::KAN	Euroscarf
Y13416	BY4742 MATα *vps23Δ*::KAN	Euroscarf
Y14004	BY4742 MATα *doa4Δ*::KAN	Euroscarf
Y14890	BY4742 MATα *vps24Δ*::KAN	Euroscarf
Y15381	BY4742 MATα *vps27Δ*::KAN	Euroscarf
Y15492	BY4742 MATα *vps4Δ*::KAN	Euroscarf
Y15700	BY4742 MATα *atg18Δ*::KAN	Euroscarf
Y15876	BY4742 MATα *ygr223cΔ*::KAN	Euroscarf
Y16078	BY4742 MATα *bre5Δ*::KAN	Euroscarf
Y16148	BY4742 MATα *ubp3Δ*::KAN	Euroscarf

Table 3: Strains of WCG background used in this study

Strain	Genotype	Source
WCG4	WCG4a MATα *his3-11,15 leu2-3,112 ura3*	W. Heinemeyer, Stuttgart
WCG4	WCG4a MATa *his3-11,15 ura3 leu2-3,112*	W. Heinemeyer, Stuttgart
*atg21*Δ	WCG4a MATα *mai1*Δ*::*KAN	(Barth, 2002)

Strain	Genotype	Source
*atg27*Δ	WCG4a MAT a *atg27*Δ*::*HIS3	(Bremer, 2009)
doa4Δ	WCG4a MATα *doa4Δ*::NAT	This study
shp1Δ	WCG4a MATα *shp1Δ*::NAT	This study
YCV10	WCG4a MATα *atg4Δatg8Δ*	C. Voss
YKMW33	WCG4a MATα *vps34Δ*::KAN	K. Meiling-Wesse
YMTA	WCG4a MATa *pep4Δ*::HIS	M. Thumm
YUE92	WCG4a MATα *vps23Δ*::KAN	U. Epple
YUE94	WCG4a MATα *vps28Δ*::KAN	U. Epple
YYW08	WCG4a MATα *nvj1Δ*::HIS	(Krick, 2008b)

Table 4: RFP-fusion strains used in this study

Strain	Genotype	Source
Sik1-RFP	S288c MATa *ura3 leu2 his3* Sik1-RFP::kanMX6	Falvo
Sik1-RFP *atg1Δ*	S288c MATa *ura3 leu2 his3* Sik1-RFP::kanMX6 *atg1Δ*::NAT	This study
Sik1-RFP *vac8Δ*	S288c MATa *ura3 leu2 his3* Sik1-RFP::kanMX6 *vac8Δ*::NAT	This study

Table 5: GFP-fusion strains used in this study

Strain	Genotype	Source
Pgk1-GFP *atg1Δ*	Attc201388 Mata *ura3 leu2 his3* Pgk1-GFP::HIS3MX6 *atg1Δ*::NAT	This study
Sik1-GFP *atg1Δ*	Attc201388 Mata *ura3 leu2 his3* Sik1-GFP::HIS3MX6 *atg1Δ*::NAT	This study
Cic1-GFP *atg1Δ*	Attc201388 Mata *ura3 leu2 his3* Cic1-GFP::HIS3MX6 *atg1Δ*::NAT	This study
YDR227W	Attc201388 Mat a *ura3 leu2 his3* Sir4-GFP::HIS3MX6	Invitrogen
YFL008W	Attc201388 Mat a *ura3 leu2 his3* Smc1-GFP::HIS3MX6	Invitrogen
YJL109C	Attc201388 Mat a *ura3 leu2 his3* Utp10-GFP::HIS3MX6	Invitrogen
YKL182W	Attc201388 Mat a *ura3 leu2 his3* Fas1-GFP::HIS3MX6	Invitrogen
YMR219W	Attc201388 Mat a *ura3 leu2 his3* Esc1-GFP::HIS3MX6	Invitrogen
YPL231W	Attc201388 Mat a *ura3 leu2 his3* Fas2-GFP::HIS3MX6	Invitrogen
YBL045C	Attc201388 Mat a *ura3 leu2 his3* Cor1-GFP::HIS3MX6	Invitrogen

Strain	Genotype	Source
YBL058W	Attc201388 Mat a *ura3 leu2 his3* Shp1-GFP::HIS3MX6	Invitrogen
YBR009C	Attc201388 Mat a *ura3 leu2 his3* Hhf1-GFP::HIS3MX6	Invitrogen
YBR283C	Attc201388 Mat a *ura3 leu2 his3* Ssh1-GFP::HIS3MX6	Invitrogen
YCR012W	Attc201388 Mat a *ura3 leu2 his3* Pgk1-GFP::HIS3MX6	Invitrogen
YCR084C	Attc201388 Mat a *ura3 leu2 his3* Tup1-GFP::HIS3MX6	Invitrogen
YDL089W	Attc201388 Mat a *ura3 leu2 his3* YDL089W -GFP::HIS3MX6	Invitrogen
YDL126C	Attc201388 Mat a *ura3 leu2 his3* Cdc48-GFP::HIS3MX6	Invitrogen
YDL185W	Attc201388 Mat a *ura3 leu2 his3* Vma1/Tfp1-GFP::HIS3MX6	Invitrogen
YDL213C	Attc201388 Mat a *ura3 leu2 his3* Nop6-GFP::HIS3MX6	Invitrogen
YDR091C	Attc201388 Mat a *ura3 leu2 his3* Rli1-GFP::HIS3MX6	Invitrogen
YDR120C	Attc201388 Mat a *ura3 leu2 his3* Trm1-GFP::HIS3MX6	Invitrogen
YDR170C	Attc201388 Mat a *ura3 leu2 his3* Sec7-GFP::HIS3MX6	Invitrogen
YDR233C	Attc201388 Mat a *ura3 leu2 his3* Rtn1-GFP::HIS3MX6	Invitrogen
YDR298C	Attc201388 Mata ura3 leu2 his3 Atp5-GFP::HIS3MX6	Invitrogen
YDR320C	Attc201388 Mat a *ura3 leu2 his3* Aux1/Swa2-GFP::HIS3MX6	Invitrogen
YDR328C	Attc201388 Mat a *ura3 leu2 his3* Skp1-GFP::HIS3MX6	Invitrogen
YDR398W	Attc201388 Mat a *ura3 leu2 his3* Utp5-GFP::HIS3MX6	Invitrogen
YDR448W	Attc201388 Mat a *ura3 leu2 his3* Ada2-GFP::HIS3MX6	Invitrogen
YDR525W-A	Attc201388 Mat a *ura3 leu2 his3* Sna2-GFP::HIS3MX6	Invitrogen
YEL013W	Attc201388 Mat a *ura3 leu2 his3* vac8-GFP::HIS3MX6	Invitrogen
YEL024W	Attc201388 Mat a *ura3 leu2 his3* Rip1-GFP::HIS3MX6	Invitrogen
YFR050C	Attc201388 Mat a *ura3 leu2 his3* Pre4-GFP::HIS3MX6	Invitrogen
YFR052W	Attc201388 Mat a *ura3 leu2 his3* Rpn12-GFP::HIS3MX6	Invitrogen
YGL038C	Attc201388 Mat a *ura3 leu2 his3* Och1-GFP::HIS3MX6	Invitrogen
YGL073W	Attc201388 Mat a *ura3 leu2 his3* Hsf1-GFP::HIS3MX6	Invitrogen

Strain	Genotype	Source
YGL078C	Attc201388 Mat a *ura3 leu2 his3* Dbp3-GFP::HIS3MX6	Invitrogen
YGL122C	Attc201388 Mat a *ura3 leu2 his3* Nab2-GFP::HIS3MX6	Invitrogen
YGL153W	Attc201388 Mat a *ura3 leu2 his3* Pex4-GFP::HIS3MX6	Invitrogen
YGL172W	Attc201388 Mat a *ura3 leu2 his3* Nup49-GFP::HIS3MX6	Invitrogen
YGL187C	Attc201388 Mat a *ura3 leu2 his3* Cox4-GFP::HIS3MX6	Invitrogen
YGL194C	Attc201388 Mat a *ura3 leu2 his3* Hos2-GFP::HIS3MX6	Invitrogen
YGR095C	Attc201388 Mat a *ura3 leu2 his3* Rrp46-GFP::HIS3MX6	Invitrogen
YGR112W	Attc201388 Mat a *ura3 leu2 his3* Shy1-GFP::HIS3MX6	Invitrogen
YGR140W	Attc201388 Mat a *ura3 leu2 his3* ndc10/cbf2-GFP::HIS3MX6	Invitrogen
YGR159C	Attc201388 Mat a *ura3 leu2 his3* Nsr1-GFP::HIS3MX6	Invitrogen
YGR202C	Attc201388 Mat a *ura3 leu2 his3* Pct1-GFP::HIS3MX6	Invitrogen
YGR252W	Attc201388 Mat a *ura3 leu2 his3* Gcn5-GFP::HIS3MX6	Invitrogen
YHL020C	Attc201388 Mat a *ura3 leu2 his3* Opi1-GFP::HIS3MX6	Invitrogen
YHR052W	Attc201388 Mat a *ura3 leu2 his3* Cic1-GFP::HIS3MX6	Invitrogen
YHR195W	Attc201388 Mat a *ura3 leu2 his3* Nvj1-GFP::HIS3MX6	Invitrogen
YIL026C	Attc201388 Mat a *ura3 leu2 his3* Irr1-GFP::HIS3MX6	Invitrogen
YIL048W	Attc201388 Mat a *ura3 leu2 his3* Neo1-GFP::HIS3MX6	Invitrogen
YIL090W	Attc201388 Mat a *ura3 leu2 his3* Ice2-GFP::HIS3MX6	Invitrogen
YIL136W	Attc201388 Mat a *ura3 leu2 his3* Om45-GFP::HIS3MX6	Invitrogen
YJL001W	Attc201388 Mat a *ura3 leu2 his3* Pre3-GFP::HIS3MX6	Invitrogen
YJL173C	Attc201388 Mat a *ura3 leu2 his3* Rfa3-GFP::HIS3MX6	Invitrogen
YJR060W	Attc201388 Mat a *ura3 leu2 his3* Cbf1-GFP::HIS3MX6	Invitrogen
YKL049C	Attc201388 Mat a *ura3 leu2 his3* Cse4-GFP::HIS3MX6	Invitrogen
YKR092C	Attc201388 Mat a *ura3 leu2 his3* Srp40-GFP::HIS3MX6	Invitrogen
YKR095W	Attc201388 Mat a *ura3 leu2 his3* Mlp1-GFP::HIS3MX6	Invitrogen

Strain	Genotype	Source
YLR002C	Attc201388 Mat a *ura3 leu2 his3* Noc3-GFP::HIS3MX6	Invitrogen
YLR196W	Attc201388 Mat a *ura3 leu2 his3* Pwp1-GFP::HIS3MX6	Invitrogen
YLR197W	Attc201388 Mat a *ura3 leu2 his3* Sik1-GFP::HIS3MX6	Invitrogen
YLR347C	Attc201388 Mat a *ura3 leu2 his3* Kap95-GFP::HIS3MX6	Invitrogen
YML034W	Attc201388 Mat a *ura3 leu2 his3* Src1-GFP::HIS3MX6	Invitrogen
YML075C	Attc201388 Mat a *ura3 leu2 his3* Hmg1-GFP::HIS3MX6	Invitrogen
YMR243C	Attc201388 Mat a *ura3 leu2 his3* Zrc1-GFP::HIS3MX6	Invitrogen
YMR284W	Attc201388 Mat a *ura3 leu2 his3* Yku70-GFP::HIS3MX6	Invitrogen
YNL030W	Attc201388 Mat a *ura3 leu2 his3* Hhf2-GFP::HIS3MX6	Invitrogen
YNL037C	Attc201388 Mat a *ura3 leu2 his3* Idh1-GFP::HIS3MX6	Invitrogen
YNL037c	Attc201388 Mat a *ura3 leu2 his3* Idh1-GFP::HIS3MX6	Invitrogen
YNL330C	Attc201388 Mat a *ura3 leu2 his3* Rpd3-GFP::HIS3MX6	Invitrogen
YOL006C	Attc201388 Mat a *ura3 leu2 his3* TOP1-GFP::HIS3MX6	Invitrogen
YOL010W	Attc201388 Mat a *ura3 leu2 his3* Rcl1-GFP::HIS3MX6	Invitrogen
YOL072W	Attc201388 Mat a *ura3 leu2 his3* Thp1-GFP::HIS3MX6	Invitrogen
YOL144W	Attc201388 Mat a *ura3 leu2 his3* Nop8-GFP::HIS3MX6	Invitrogen
YOR230W	Attc201388 Mat a *ura3 leu2 his3* Wtm1-GFP::HIS3MX6	Invitrogen
YOR254C	Attc201388 Mat a *ura3 leu2 his3* Sec63-GFP::HIS3MX6	Invitrogen
YOR270C	Attc201388 Mat a *ura3 leu2 his3* Vph1-GFP::HIS3MX6	Invitrogen
YOR293W	Attc201388 Mat a *ura3 leu2 his3* Rps10a -GFP::HIS3MX6	Invitrogen
YOR310C	Attc201388 Mat a *ura3 leu2 his3* Nop5/Nop58-GFP::HIS3MX6	Invitrogen
YPL018W	Attc201388 Mat a *ura3 leu2 his3* Ctf19-GFP::HIS3MX6	Invitrogen
YPL128C	Attc201388 Mat a *ura3 leu2 his3* Tbf1-GFP::HIS3MX6	Invitrogen
YPL139C	Attc201388 Mat a *ura3 leu2 his3* Ume1-GFP::HIS3MX6	Invitrogen
YPL212C	Attc201388 Mat a *ura3 leu2 his3* Pus1-GFP::HIS3MX6	Invitrogen

Strain	Genotype	Source
YPR028W	Attc201388 Mat a *ura3 leu2 his3* Yop1-GFP::HIS3MX6	Invitrogen

Table 6: Strains used for SGA

Strain	Genotype	Source
Y8205	MAT α *can1*Δ::STE2pr-his5 *lyp1*Δ::STE3pr-LEU2 *ura3Δ0 leu2Δ0 his3Δ1 met15*Δ	Boone lab
BY4741 deletion library	MAT a $x_{(DMA)}$Δ::KAN *his3Δ1 leu2Δ0 met15Δ0 ura3Δ0*	Euroscarf

Table 7: Strains for mating type determination

Strain	Genotype	Source
YR312	Mat a *his1-123* test strain for mating type determination	H. Rudolph, Stuttgart
YR320	Mat α *his1-123* test strain for mating type determination	H. Rudolph, Stuttgart

3.1.2 *Escherichia coli*

Table 8: *Escherichia coli* strains used in this study

Name	Genotype	Source
DH5α	F' (Φ *80* (*ΔlacZ*) *M15*) *Δ* (*lacZYA-argF*) *U169 recA1 endA1 hsdR17* r_k- m_k + *supE44 thi-1 gyrA relA*	(Hanahan, 1983)
BL21 (DE3) pLysS	F' *dcm ompT hsdSB (rB-, mB-) gal λ (DE3); pLysS (CamR)*	Stratagene
BL21 (DE3)-RIPL	F' *ompT hsdS (rB-, mB-) dcm+ Tet+ Gal λ (DE3) endA Hte; argU prol CamR; argU ileY leuW Strep/SpecR*	Stratagene

3.1.3 Plasmids

Table 9: Plasmids used in this study

Name	Genotype	Source
GFP-Atg8	pRS316 CEN6 URA3 GFP-Atg8	(Suzuki, 2001)
Pgk1-GFP	pRS316 CEN6 URA3 Pgk1-GFP	(Welter, 2010)
mito-GFP	pRS316-Su9-mtDHFR-GFP	This study
GST-shp1	pGEX-4T3-Shp1	This study
GST-shp1-UBX	pGEX-4T3-Shp1-UBX	This study
GST-shp1-UBA	pGEX-4T3-Shp1-UBA	This study
NLSmcherry	pYX242 2µ LEU2 TPI Nab2NLS-2m cherry	B. Timney and M. Rout
RFP-Atg8	pRS313 Cen6 HIS3 RFP-Atg8	S. Bremer
GFP-Atg9	CEN6 URA3 MET25 GFP-Atg9	(Meiling-Wesse, 2004)
pUG35	pUG35 CEN6 URA3	J. H. Hegemann
pRS316	pRS316 CEN6 URA3	(Sikorski and Hieter, 1989)
GFP-Atg8-FG	pRS316 CEN6 URA3 GFP-Atg8-FG	(Suzuki, 2001) (Kirisako, 2000)
pOm45-GFP	pRS316 CEN6 URA3 Om45-GFP	this study
pIdh1-GFP	pRS316 CEN6 URA3 Idh1-GFP	this study
GFP-Osh1	pRS416 CEN6 URA3 GFP-Osh1	(Loewen, 2003)
pFA6-natNT2	natNT2	(Janke, 2004)
PFA6a-HIS3MX6	HIS3MX6	(Longtine, 1998)
PFA6a-kanMX6	kanMX6	(Longtine, 1998)
pHO	for mating type switch; pGal	unknown

3.1.4 Oligonucleotides

Table 10: Oligonucleotides used in this study

acquired by purchase from: www.eurofins.com

Name	Sequence (5'-3')
shp1Δ::natNT2	
shp1_S1f:	ATATATAAGAAACGTCGGTAGCACAACAATTAACTCATTATTTAGGTATGCGTACGCTGCAGGTCGAC
shp1_S2r:	ATATTAAGTTGAAGTCTTTTCCCGTTTCTGTTTTTGTATATTTATGCTCAATCGATGAATTCGAGCTCG

Name	Sequence (5'-3')
atg1Δ::natNT2	
atg1_ko_fw	CCCCATATTTTCAAATCTCTTTTACAACACCAGACGAGAAATT AAGAAAATG CGTACGCT GCAGGTCGAC
atg1_ko_rev	GCAGGTCATTTGTACTTAATAAGAAAACCATATTATGCATCAC TTAATCGATGAATTCGAGCTCG
doa4Δ::natNT2	
Doa4_ko_frw	GTGCACGCTTCCAAAGTTTTTTTTACTATTTGATACATGCTTAA GTTATGCGTACGCT GCAGGTCGAC
Doa4_ko_rev	CGGAAAAAAAGTGTATAGACAACGGTTTTCAGTTATTTATTCA AATGAATCAATCGATGAA TTCGAGCTCG
vac8Δ::natNT2	
Vac8-his _fw	CTATAAGGGTGTTCTTTCTTCTGTACTATATATACATTTGCAAC TATGCGGATCCCGGGTTAATTAA
Vac8-his rev	AAAATTTTGATAAAAATTATAATGCCTAGTCCCGCTTTTGAAG AAAATCAGAATTCGAGCTCGTTTAAAC
pAG25	
Nat_frw	AGC TTG CCT TGT CCC CGC CG
Nat_rev	TCG ACA CTG GAT GGC GGC GT
control primer	
NAT_1r	CCTCCATGTCGCTGGCCG
1f Shp1 XbaI	TCCGCCTATCTAGACATAACTTATTTACATAGTGCC
atg1_1_fw	GGGGAAACAGAGAACAGTAC
atg1_2_rev	CCCATCCAGGTATAAAAGAGC
atg1_3_rev	GCCTTTGCGGCCAGAGATTCC
Doa4_1_frw	CTTCGGTAGT ATAGGGCAG
Doa4_2_rev	GATGGAAATA ATGATATGCC
Doa4_3_rev	CACCAGAATG TCCAACAGGA C
Vac8_K1fw:	CGGTAAGGAAGTGGGATCTGTAGCG
Vac8_K2rev:	CCGAACAACCCCGGTTCGAATCCG
Vac8_K3rev:	CGAGCTTGGATTGTTGTTGCTCCCC
Vac8_K4fw	CTTTTCGTCACTGACGGGTCCCTGC
Vac8_K5rev	CCCACCATCAGAGGACGAAGAGAG
Idh1-GFP f	GAATTGGAGCTCCACCGCGGTGGCGGCCGCTCTAGAAC TAGTGGATCC GCTGTAGTTGATGTGGTTGGG
Idh1-GFP/OM45-GFP r	CTCGAGGTCGACGGTATCGATAAGCTTGATATCGAATTCCTG CAGGCAACCTGACCTACAGGAAAG
OM45-GFP f	GAATTGGAGCTCCACCGCGGTGGCGGCCGCTCTAGAACTAGT GGATCCGTATAGCACATCCAGGAATGG
Sequence primer	
Prs316seq	GATGTGCTGCAAGGCGATTAAG
OM45seq1	GTCGAGTTCCTTGAAGAGGAG
OM45seq2	GCAAAGCATCTTCAATTGG
OM45seq3	GCCAGAGGTTTAGAAGGATG
IDH1seq1	GATTTCTTTACTCTACCGTAG
IDH1seq2	GAAGGGTGTCAAGACTAG
IDH1seq3	GTTCCAGACATGTTGGTTTAG

Name	Sequence (5'-3')
mt-DHFR	
Su9 for	TCTAGAGGATCCATGGCCTCCACTCGTGTCCTCG
Su9 rev	GTCGACAAGCTTGTCTTTCTTCTCGTAGACTTCAAAC
GST-shp1-construct	
GST-SHP1-Eco	AGTAGGAATGAATTCGATGGCGGAAATACCTGATGAAAC
GST-SHP1-Xho	AAGTAGGAATCTCGAGTCATGCCCATCTTTGCACGAC
GST-SHP1^{-UBA}-Eco	AGTAGGAATGAATTCGCAAAAGGATAGAAGAGAGGAAGC
GST-SHP1-UBX-Xho	AAGTAGGAATCTCGAGTCAGTCCGGCATGGGTTGTTCCTG
Sequence	
Shp1 Seq1f	CCTTCTCCACCAACTCTTCG
Shp1 Seq1r	CGAAGAGTTGGTGGAGAAGG
Shp1 Seq2f	GATTCCGTGATGACGAAGAC
Shp1 Seq2r	GTCTTCGTCATCACGGAATC
Shp1 Seq3f	GCCAAAGACTAGGATCTCC
Shp1 Seq3r	GGAGATCCTAGTCTTTGGC
Chromosomal integration	
cOM45-GFP for	ATGGAATGATAAGGGTGATGGTAAATTCTGGAGCTCGAAAAA GGACGGTCGACGGATCCCCGGGTT
cOM45-GFP rev	GTATATATGTTATGCGGGAACCAACCCTTTACAATTAGCTATC TAATCGATGAATTCGAGCTCGTT
cOM45_b_fw	TGATAAGGGTGATGGTAAAATCTGGAGCTCGAAAAAGAACCG GATCCCCGGGTTAATTAA
cOM45_b_rev	GAGAAACATGTGAATATGTATATATGTTATGCGGGAACCAGA ATTCGAGCTCGTTTAAAC
IDH1-GFP for	CTACTACTGACTTCACGAATGAAATCATCAACAAATTATCTAC CATGGGTCGACGGATCCCCGGGTT
IDH1-GFP rev	TGAACACACTTAAGTTGCAGAACAAAAAAAAGGGGAATTG TTTTCATCGATGAATTCGAGCTCGTT
control primer	
K-OM45	CGCGCTTCTGGGCGTATCTC
K-GFP	GACAGGGCCATCGCCAATTGG
K-GFP	GGCGGTCGTTTCACCGTCAC

3.1.5 Media

3.1.5.1 YPD-medium, pH 5.5

YPD is a rich medium for yeast cultures and contains:

1 % Bacto® Yeast Extract
2 % Bacto® Pepton
2 % D-glucose

3.1.5.2 CM-medium, pH 5.6

CM-medium is a synthetic medium for yeast cultures consisting of:

0.67 %	Yeast Nitrogen Base w/o amino acids
2 %	D-glucose
0.0117 %	L-alanine 0.0117% L-methionine*
0.0117 %	L-arginine 0.0117% L-phenylalanine
0.0117 %	L-asparagine 0.0117% L-proline
0.0117 %	L-aspartic acid 0.0117% L-serine
0.0117 %	L-cysteine 0.0117% L-threonine
0.0117 %	L-glutamine 0.0117% L-tyrosine
0.0117 %	L-glutamic acid 0.0117% L-valine
0.0117 %	L-glycine 0.0117% myo-inositol
0.0117 %	L-isoleucine 0.00117% p-aminobenzoic acid

Depending on selection conditions the following supplements were added:

0.3 mM	L-histidine
0.4 mM	L-tryptophan
1.7 mM	L-leucine
0.3 mM	adenine
1 mM	L-lysine
0.2 mM	uracil**

Depending of the intended growth conditions of the cells different carbon sources were added:

2 %	D-glucose	or
2 %	Lactate	

* For overexpression experiments using a MET25 promoter L-methionine was excluded from the drop out mix.
** Uracil was resuspended in 0.5 % sodium hydrogen carbonate solution.

3.1.5.3 SD-N-medium

Nitrogen free SD (-N)-medium was used for nutrient starvation of yeast cells:

0.67 % Yeast Nitrogen Base w/o amino acid and w/o ammonium sulfate
2 % D-glucose

3.1.5.4 1% potassium acetate

Potassium acetate is a medium used for sporulation (tetrade formation) or can also be used for carbon starvation:

1 % potassium acetate

3.1.5.5 MV-medium, pH 5.5

For determination of the mating type of a haploid yeast strain, MV-medium was used:

0.67 % Yeast Nitrogen Base w/o amino acids
2 % *D*-glucose

3.1.5.6 YPL-medium, pH 5.5

YPL is a rich medium for yeast cultures (similar to YPD) to enhance the synthesis of mitochondria and contains:

1 % Bacto® Yeast Extract
2 % Bacto® Pepton
2 % lactate

3.1.5.7 YPG-medium, pH 5.5

1 % Bacto® Yeast Extract
2 % Bacto® Pepton
2 % D-galactose

3.1.5.8 LB-medium, pH 7.5

As standard growth medium for *E. coli* cultures LB-medium was used.

1 % Bacto® Trypton
0.5 % Bacto® Yeast extract
0.5 % sodium chloride

For plasmid selection: 75 µg / ml ampicillin was added.
For the use of BL21 (DE3) cells: 25 µg/ml was added.

3.1.5.9 SOC-medium, pH 7.5

For regeneration of electroporated *E. coli* cells SOC-medium was used

2 %	Bacto® Trypton
0.5 %	Bacto® Yeast extract
0.4 %	D-glucose
10 mM	sodium chloride
10 mM	magnesium sulfate
10 mM	magnesium chloride
2.5 mM	potassium chloride

3.1.5.10 Enriched sporulation medium

1%	potassium acetate
0.1%	Bacto® Yeast extract
0.05 %	D-glucose
0.01 %	Amino-acids supplement powder mixture for sporulation*
2 %	Bacto agar

*Amino-acids supplement for sporulation medium:

0.2 %	L-histidine
1 %	L-leucine
0.2 %	L-lysine
0.2 %	L-uracil

3.1.5.11 SD medium for SGA

0.17 %	yeast nitrogen base w/o amino acids or ammonium sulfate
0.1 %	MSG (L-glutamic acid sodiumsalt hydrate, Sigma),
0.2 %	amino-acids supplement powder mixture*,
5 %	40 % D-glucose
	additional antibiotica/ amino acids for selection**

*Amino acids supplement powder mixture for synthetic media (complete)/ (DO – his/arg/lys)/ (DO – leu/arg/lys)

0.3 %	L-adenine (Sigma)
0.2 %	uracil (ICN)
0.2 %	L-inositol
0.02 %	para-aminobenzoic acid (Acros 5Organics)
0.2 %	L-alanine
0.2 %	L-arginine
0.2 %	L-asparagine
0.2 %	L-aspartic acid
0.2 %	L-cysteine
0.2 %	L-glutamic acid
0.2 %	L-glutamine
0.2 %	L-glycine

0.2 %	L-histidine
0.2 %	L-isoleucine
1 %	L-leucine
0.2 %	L-lysine
0.2 %	L-methionine
0.2 %	L-phenylalanine
0.2 %	L-proline
0.2 %	L-serine
0.2 %	Lthreonine
0.2 %	L-tryptophan
0.2 %	L-tyrosine
0.2 %	L-valine (Fisher)

**

100 µg/l	canavanine
100 µg/l	thialysine
200 µg/l	G418
100 µg/l	clonNAT

3.1.6 Antibodies

Table 11: Anibodies used in this study
TBST is containing 20 mM Tris/HCl pH 7.6; 137 mM sodium chloride; 0.1% Tween 20 (w/v)

Name	Dilution	Source
Mouse-Anti-GFP	1:2000 in TBST + 1% milk	Roche, Mannheim
Mouse-Anti-PGK	1:10000 in TBST	Molecular Probes, Leiden, NL
Rabbit-Anti-Ape1p	1 :3000 in TBST + 1% milk	Eurogentech, Belgium
Rabbit-Anti-Aut7	1:10000 in TBST	M. Thumm
Mouse-Anti-CPY	1:10000 in TBST	Molecular Probes, Leiden, NL
anti-mouse-HRPO-conjugate	1 : 10000 in TBST + 1% milk	Dianova, Hamburg
anti-rabbit-HRPO-conjugate	1 : 5000 in TBST + 1% milk	Medac, Hamburg

3.1.7 Kits

Table 12: Kits used in this study

Name of product	Source
Wizard Plus SV Minipreps DNA purification System	Promega
QIAquick Gel Extraction Kit	Quiagen, Hilden
QIAquick PCR Purification Kit	Quiagen, Hilden
QIAquick Nucleotide Removal Kit	Quiagen, Hilden
Rodeo ECL Western Blot Detection	USB
ECL PLUS Western Blotting Detection Reagents	Amersham, GE Healthcare

3.1.8 Chemicals

Table 13: Chemicals used in this study

Chemicals	Source
Acetic acid	Riedel-De Haën, Seelze
Acetone	Roth, Karlsruhe
Adenine	Roth, Karlsruhe
Agarose	Roth, Karlsruhe
Ammoniumpersulfat	Roth, Karlsruhe
Ampicillin	Roth, Karlsruhe
Bacto Peptone	Becton Dickinson, Heidelberg
Bacto Tryptone	Becton Dickinson, Heidelberg
Bacto Yeast Extract	Becton Dickinson, Heidelberg
Bromphenolblue	Riedel-De Haën, Seelze
BSA 100x	NEB, Frankfurt
Canavanin	Sigma, Deisenhofen
CH_3CO_2K (acetic acid)	Merck, Darmstadt
Chloramphenicole	Roth, Karlsruhe
Chloroforme	Roth, Karlsruhe
Chymostatin	Merck, Darmstadt
clonNat (nourseotricine)	Werner BioAgents, Jena
CompleteTM protease inhibitor	Roche, Mannheim
Cupric sulfate	Sigma, Deisenhofen
D-Galactose	Sigma, Deisenhofen
D-Glucose	Roth, Karlsruhe
DMSO	Sigma, Deisenhofen
DNA-marker (1 kb)	NEB, Frankfurt
DNAse 1	Invitrogen, Karlsruhe
dNTP	NEB, Frankfurt
D-Sorbitol	Roth, Karlsruhe
DTT	Roth, Karlsruhe
ECL	USB, Santa Clara, CA
ECL™ plus	GE Healthcare, München

Chemicals	Source
EDTA	Roth, Karlsruhe
Ethidium bromide	Roth, Karlsruhe
EtOH	Roth, Karlsruhe
Fidely Taq	USB, Santa Clara, CA
FM4-64	Invitrogen, Karlsruhe
G418/Kanamycin	Roth, Karlsruhe
Glusulase	PerkinElmer, Hamburg
Glycerine	Roth, Karlsruhe
Glycine	Roth, Karlsruhe
Hepes/KOH	Roth, Karlsruhe
Herring sperm DNA	Promega, Madison, USA
HiDye	Sigma, Deisenhofen
Hoechst 33342	Molecular Probes, Freiburg
IPTG	Roth, Karlsruhe
Isopropanol	Roth, Karlsruhe
KCl	Roth, Karlsruhe
KCl	Merck, Darmstadt
KH2PO4	Roth, Karlsruhe
Lactate	Sigma, Deisenhofen
L-alanine	Sigma, Deisenhofen
L-arginine	Sigma, Deisenhofen
Lasparagine	Sigma, Deisenhofen
L-aspartic acid	Sigma, Deisenhofen
L-cysteine	Sigma, Deisenhofen
Leupeptine	Sigma, Deisenhofen
L-glutamic acid	Sigma, Deisenhofen
L-glutamic acid sodiumsalt hydrate	Sigma, Deisenhofen
L-glutamine	Sigma, Deisenhofen
L-glycine	Sigma, Deisenhofen
L-histidine	Sigma, Deisenhofen
ligation buffer 1x	NEB, Frankfurt
L-isoleucine	Sigma, Deisenhofen
Lithium acetate	Sigma, Deisenhofen
L-leucine	Sigma, Deisenhofen
L-lysine	Sigma, Deisenhofen
L-methionine	Sigma, Deisenhofen
L-tryptophan	Roth, Karlsruhe
Magnesium chloride	Roth, Karlsruhe
Magnesium sulfate	Roth, Karlsruhe
Methanol	Applichem, Darmstadt
Na_2HPO_4	Roth, Karlsruhe
NaCl	Roth, Karlsruhe
NA-desoxylat	Roth, Karlsruhe
NaOH	Roth, Karlsruhe
Paraquat	Sigma, Deisenhofen
Pefablock	Sigma, Deisenhofen
PEG 3350	Sigma, Deisenhofen
Phe TE	Roth, Karlsruhe
Phe/Chl	Roth, Karlsruhe
PMSF	Roth, Karlsruhe

Chemicals	Source
Poly-*L*-lysine	Sigma, Deisenhofen
DNA polymerase (Taq)	NEB, Frankfurt
DNA polymerase (Fideli Taq)	USB, Santa Clara, CA
Precision Plus Protein All Blue Standards	Biorad, Munich
Protease inhibitor cocktail	Sigma, Deisenhofen
Protogel (30 %)	Biozym, Hessisch Oldendorf
Rapamycin	LCLabs, Woburn, USA
Restriction ezymes	NEB, Frankfurt
RNAseA	Applichem, Darmstadt
SDS	Sigma, Deisenhofen
Sepharose/slurry	GE Healthcare, München
Sequencing buffer	Applied Biosystems, Darmstadt
Skim milk powder	Granovita GmbH, Heimertingen
ß-ME	Roth, Karlsruhe
T4-Ligase	NEB, Frankfurt
TCA	Roth, Karlsruhe
Temed	Roth, Karlsruhe
Thialysin	Sigma, Deisenhofen
Tris	Roth, Karlsruhe
Triton X-100	Roth, Karlsruhe
Tween 20	Sigma, Deisenhofen
Uracil	Sigma, Deisenhofen
Vent Taq	NEB, Frankfurt
Yeast Nitrogen Base w/o amino acids	Becton Dickinson, Heidelberg
Yeast Nitrogen Base w/o amio acids w/o ammonium sulfate	Becton Dickinson, Heidelberg

3.1.9 Consumables and equipment

Table 14: Consumables and equipment used in this study

Name of product	Source
Agarose gel equipment	Bio RAD Mini-SUB Cell GT
Autoclave	Adolf Wolf; Sanoclav
Autoclave DX200	Systec
Bench	BDK Luf- u. Reinraumtechnik GmbH
Blot shaker	GFL 3019
Centrifuge	Eppendorf 5804
Centrifuge (refridgerating)	Eppendorf 5404R
Centrifuge (small)	Eppendorf 5415 D
Centrifuge (small; refridgerating)	Eppendorf 5415 R
Chemical balance	Sartorius universal
Cuvettes	Sarstedt cuvettes no. 67.742

Name of product	Source
Cuvettes for electroporation	peq lab; 2mm elektroporationsküvetten
Electroporator	Eppendorf; Electroporator 2510
Freezer (-20 °C)	Liebherr
Freezer (-80 °C)	Heareus; Hera freeze
French pressure cell press	SIM AMINCO
Gel dokumentation	UV solo; Transilluminator
Incubator (24/ 37 °C)	Haraeus Kelvitron-t
Incubator (small)	Eppendorf Thermomixer comfort
Incubator shaking (24/37 °C)	New Brunswich Scientific; Innova 4200
LAS 3000	Fujifilm
Micromanipulator	ZEISS
Microscope	ZEISS
Microscope Δ vision, Olympus IX71	Olympus; Δ vision Applied Precision, Inc
Microscope slides (76x26 mm)	Menzel-Gläser
Microscope cover slips	Menzel-Gläser
Multivortex	IKA vibrax VXR basic
PCR machine	Sensquest; Labcycler
PCR machine	Eppendorf; Mastercycler gradient
pH meter	Microprocessor pH Meter pH537
Photometer	Eppendorf Biophotometer
Photometer	Amersham Ultrospec 100 pro
Pinning tools	V & P Scientific, Inc. (San Diego, CA)
Pipettes	Eppendorf research
Powersuplies	BioRAD; PowerPac HC
PVDF membrane	Amersham Hybond-P; GE Healthcare
Refrigerator (4 °C)	Bosch/ Liebherr
Screen Roboter	Tecan; freedom evo
OmniTrays	Nunc
SDS-PAGE equipment	Bio RAD Mini Protean cell
Sorvall centrifuge	Beckman router J2-MC
special accuracy weighing machine	Sartorius handy
Pipette tips, petri dishes, ...	Sarstedt/ Eppendorf
Sterile filter	Whatman; vacuflo, disposal vacuum filtration system
Transilluminator	Biometra TI 1
Vaccumpump	Diaphragm vacuum pump
Vortex	Bender & Hobein AG; Genie 2
Western Blot equipment	Bio RAD Trans Blot Cell
Western Blot equipment (small)	Bio RAD Mini Trans Blot Cell
Glassbeads	Schütt, Göttingen

3.2 Cell biological methods

3.2.1 Cultivation of *S. cerevisiae*

For preculture, yeast strains were inoculated with a sterile toothpick from an agar plate in liquid medium and grown over night (12-14 h) at 30 °C. For main-cultures the cells were diluted (depending on growth ability and requested OD_{600}) in liquid media and grown over night (12-14 h) at 30 °C. Special growth conditions needed to be adapted for some experiments, e.g. main-cultures for mitophagy experiments (see 3.4.5.3; up to 72 h in media containing 2 % lactate).

3.2.2 Storage of *S. cerevisiae*

Yeast cells could be stored on agar plates at 4 °C up to one month. For long time storage yeast cells were cultured in liquid medium over night, transferred in 30 % glycerol and frozen at -80 °C.

3.2.3 Cultivation of *E. coli*

For culturing of *E. coli* cells LB medium was used. The cells were inoculated in 5 ml LB and were incubated over night at 37 °C.

3.2.4 Storage of *E. coli*

E. coli cells could be stored for a few days in liquid culture or an LB agar plates at 4 °C. For long time storage 500 µl of *E. coli* liquid culture were transferred in 500 µl 15 % glycerol and frozen at –80 °C.

3.2.5 Mating of haploid yeast cells

For mating of two different haploid strains (Mat a and Mat α), 500 µl of precultured cells were mixed by plating on agar plates or in liquid culture and incubated for at least 4 hours at 30 °C. Developing zygotes were taken up by a micromanipulator and separated from haploid cells.

3.2.6 Mating type switch

To switch the mating type, cells were transformed (see 3.3.3) with pHO plasmid. After two days of growth on selection medium one of the clones was grown over night in liquid YPG medium. The next day a 1:100 000 dilution of the culture was plated on YPD agarose. The grown colonies were tested for growth ability on CM -ura selection medium and colonies not able to grow could now be tested for mating type (see 3.2.7).

3.2.7 Mating type determination

To determine the mating type of a haploid cell, YR312 (Mat a) and YR320 (Mat α) containing the *His1* allele were used as tester strains (Table 7). Both strains were applied on a MV-medium agar plate in two separate lines. The strain of interest was streaked through each of the tester strain lines and the plates were incubated for 2 days at 30 °C. The strain of interest is only able to mate with the tester strain of contrary mating type, resulting in a diploid strain growing on MV-medium.

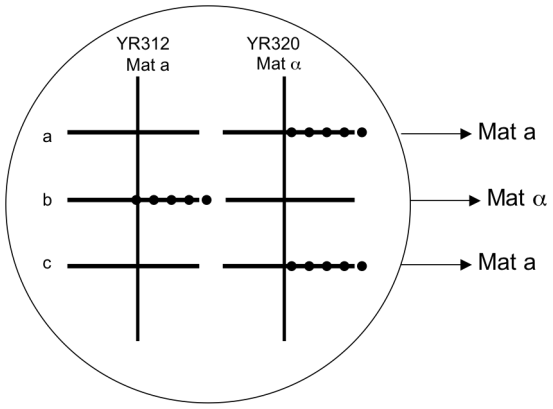

Figure 9: Scheme of mating type determination

3.2.8 Sporulation of yeast cells

For sporulation of diploid cells a preculture was inoculated and cultured over night at 30 °C. On the next day the cells were transferred into enriched sporulation medium (see 3.1.5.10) or 1 % potassium acetate medium and incubated for 5 days at 24 °C.

3.2.9 Separation of haploid tetrads

Sporulation of diploid yeast cells caused the formation of 4 haploid spores with a wrap (ascus) or so called tetrads. Therefore this method can be used to create haploid cells with different allele combinations out of a heterozygote diploid mother cell.

To separate haploid tetrads 200 µl of a sporulated culture was washed with H_2O by centrifugation and resuspended in 200 µl H_2O. 4 µl glusulase was added and incubated for 5 min at 30 °C while cautious shaking. Afterwards 800 µl of H_2O was added and incubated over night at 4 °C. The next day, 6 µl of the cells were dropped on the top of an YPD plate and scattered carefully in one line to the bottom of the plate. After a few minutes of drying the tetrads could be taken up and divided by a gently knocking using a micromanipulator (ZEISS).

3.2.10 Microscopy

Light microscopy is a very powerful tool in science and probably the easiest and most rapid way to register macroautophagy by the direct visualisation of intravacuolar autophagic bodies (Prick and Thumm, 2008). For visualisation of yeast the cells either a light microscope (Zeiss Axioskope 2 or an inverted microscope (DeltaVision Spectris; Applied Precision)) were used. Both microscopes were equipped with a 100x objective.

3.2.10.1 Test for the accumulation of autophagic bodies inside the vacuole

The test for the accumulation of autophagic vesicles can be used for the detection of autophagic defects in deletion strains (Prick and Thumm, 2008).

Wild type cells treated with 1 mM of the protease inhibitor PMSF are no longer able to breakdown the autophagic bodies in the vacuole. Using a 100x objective these vesicles can be observed as little wafting dots in the vacuole. In cells lacking compounds of the autophagic machinery as in the negative control *atg1*Δ, no autophagic bodies can be observed. In contrast, autophagic vesicles are visible in *pep4*Δ cells lacking the breakdown machinery, even without the addition of PMSF.

3.2.10.2 Fluorescence microscopy

As a substantial part of this study, cells containing a fluorescence signal (e.g. GFP, RFP) were visualised and evaluated. The pictures were taken using a Zeiss Axioskope 2 with an

AxioCam MRm and interpreted with by AxioVision software 4.5 (Zeiss) or the pictures were examined by an inverted fluorescence microscope (DeltaVision Spectris; Applied Precision) and analysed using soft-WoRx (Applied Precision, LLC). All fluorescence pictures were taken with corresponding filter sets: FITC, TRITC and DAPI.
For microscopy 5 µl of yeast cells of interest were dropped on a glass slide and covered with a cover slip.

3.2.10.2.1 Staining of the nucleus using Hoechst 33324

The use of Hoechst 33324 is a very useful tool to stain nuclear DNA. Cells of interest were cultured to OD_{600} 0.5 – 6. 10 µl/ml of 2 mM Hoechst 33324 stock solution was added and the cells were further incubated for 15 min at 30 °C and used for microscopy.

3.2.10.2.2 Staining of endosome and vacuole using FM4-64

Cells of interest were cultured to OD_{600} 0.5 – 6. After sedimentation at RT for 5 min at 2000 rpm, the cells were resuspended in required medium of corresponding amount containing 2µl of FM4-64 stock solution (1 mg/100 µg DMSO) and further incubated at 30 °C for 30 min. Afterwards they were transferred to fresh medium and used for microscopy (see 3.2.10.2) after a certain growth or starvation time (Prick and Thumm, 2008).

3.2.11 Synthetic genetic array

The Synthetic Genetic Array analysis (SGA) is a powerful high-throughput technique for exploring synthetic lethality. SGA allows the systematic construction of double mutants using a combination of mating and selection and was developed using the model organism *S. cerevisiae*. In SGA methodology a query gene deletion mutant is crossed to an entire genome deletion library consisting of 5000 viable deletion mutants available for yeast *S. cerevisiae* (Euroscarf; deletion mutant array (DMA); $x_{(DMA)}\Delta$::KanMX4), to identify synthetic lethality, yielding to functional information of the query gene and the interacting genes. The result of such a screen highlights genes with similar function, which tend to interact with each other and genes with similar patterns of genetic interactions, which often encode products that tend to work in the same pathway or complex (Tong, 2001; Tong and Boone, 2006).

3.2.11.1 Generation of the query strain

All strains of interest had to be generated. BY4741 *atg8*Δ*, atg15*Δ and *atg21*Δ were chosen for screening and therefore furthermore mentioned as *query*Δ. Fore use in the screen, every query strain (deletion mutant) had to be mated with Y8205 (MAT α *can1*Δ::STE2pr-his5 *lyp1*Δ::STE3pr-LEU2 *ura3*Δ*0 leu2*Δ*0 his3*Δ*1 met15*Δ; www.utoronto.ca/boonelab) to include several genetic attributes for selection during the screen and the zygotes were separated from haploid cells (see 3.2.5).

In the next step kanamycin resistance cassette (KanMX4) had to be switched to a nourseothricin resistance cassette (NatMX4). The method described in the literature (Tong and Boone, 2006) did not result in a successful switch, therefore the nourseothricin resistance cassette (NatMX4) was amplified by PCR using the plasmid pAG25 and the respective primers (Table 10). The resulting product was used for tranformation by homologue recombination (see 3.3.2). Afterwards the diploid strain containing NatMX4 was sporulated for 5 days in enriched sporulation medium (see 3.2.8).

The genetic modifications passed by Y8205 to the progeny allowed the subsequent selection for the haploid progeny of mating type a *query*Δ::NatMX4 *can1*Δ::STE2pr-his5 *lyp1*Δ::STE3pr-LEU2 *ura3*Δ*0 leu2*Δ*0 his3*Δ*1 met15*Δ by SD-leu/arg/lys + 100 µg/l can/lyp medium. As STE3pr-LEU2 reporter is only activated in MAT α cells, the use of medium lacking leucine allowed the selection for cells of mating type α and the further lack of arginine and lysine and the addition of 100 µg/l canavanin (can; a toxic analogue for arginine (Hoffmann, 1985)) and 100 µg/l thialysine (lyp; a toxic analogue to lysine (Sychrova and Chevallier, 1993) ensured the elimination of diploids (Mat a/α) and inhibited the growth of false positive Mat α/α diploid mutations. This furthermore allowed to skip an additional step for separating the tetrads.

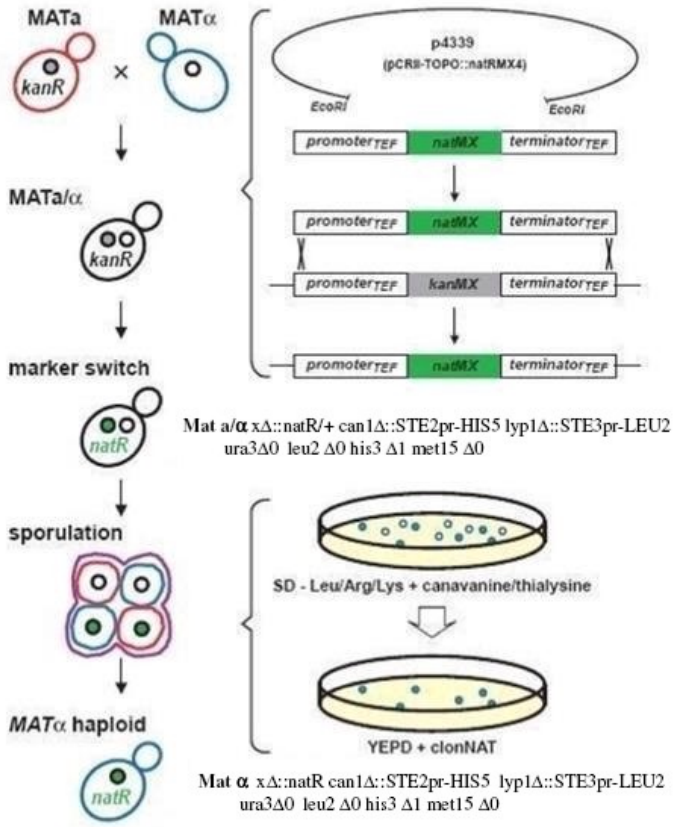

Figure 10: Preparation of the query strain

Deletion strain of interest (query strain) is prepared for the screen by mating with Y8250, switching of the resistance cassette (KanMX4 to NatMX4), sporulation and selection for the haploid progeny containing the deletion and the nourseothricin resistance ((Tong and Boone, 2006); modified).

3.2.11.2 SGA - screen

The screen, consisting of 5 pinning steps, was done with the whole deletion library available at Euroscarf, using a freedom evo screen roboter from Tecan in the laboratory of Prof. Braus (Department of Molecular Microbiology & Genetics, University of Göttingen), or manual pinning tools (96 floating pin E-clip style manual replicator (VP408FH) and 384 floating pin E-clip style manual replicator (VP384F)) purchased from V & P Scientific, Inc. (San Diego, CA). All pinning steps were done on OmniTrays (Nunc).

On the first day, the query strain (*query*Δ::NatMx4) and DMA ($x_{(DMA)}$Δ::KanMX4) were mated on YPD medium. After one day of growth, the colonies were transferred sporulation medium. After 5 days of sporulation the colonies were transferred to SD-his/arg/lys + 100 µg/l can/lyp medium to select for haploid progeny of mating type a, allowed by the resulting lowest level of inappropriate expression of *HIS3* in Mat α and Mat a/α cells. Also in this step the addition of 100 µg/l can/ and 100 µg/l lyp ensured the elimination of diploids (Mat a/α) and inhibited the growth of false positive Mat a/a diploid mutations. On the next day, the

colonies were transferred to SD-his/arg/lys medium containing 200µg/l G418 and 100 µg/l can/lyp for selection ($x_{(DMA)}$Δ::KanMX4). The last step included the switch to SD-his/arg/lys medium containing 100 µg/l clonNAT, 200µg/l G418 and 100 µg/l can/lyp, resulting in the gowth of the haploid double mutant of mating type a (*query*Δ::NatMx4 $x_{(DMA)}$Δ::KanMX4 *can1*Δ::STE2pr-his5 *lyp1*Δ::STE3pr-LEU2 *ura3Δ0 leu2Δ0 his3Δ1 met15*Δ) after two days of selection.

Two colonies per double mutant were pinned on the OmniTray plate and every plate was done in dublicates. This kind of double control resulted in about 53 plates containing 384 (192 x 2) colonies for each round.

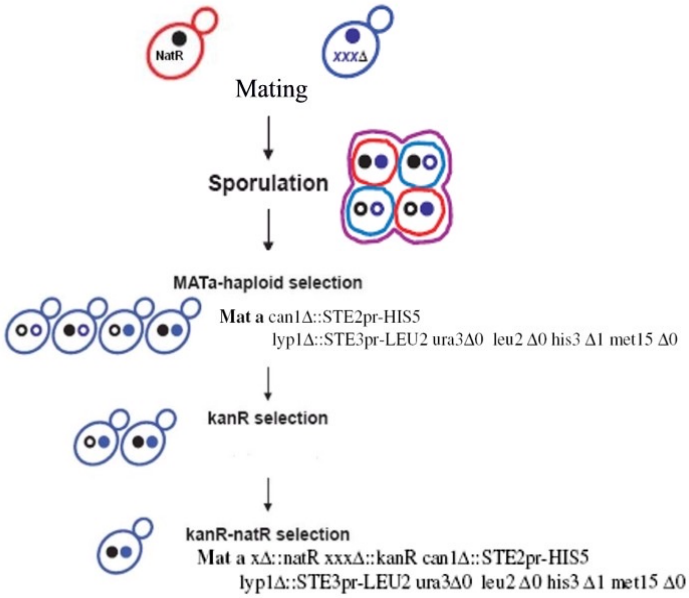

Figure 11: Synthetic genetic array methodology

Query strain containing nourseothricin resistance (*query*Δ::NatMX4) and deletion strains containing kanamycin resistance ($x_{(DMA)}$Δ::KanMX4) are mated, sporulated and the resulting haploid Mat a progeny are selected for double mutants ((Tong and Boone, 2006); modified)

3.3 Molecular biological methods

3.3.1 Isolation of chromosomal DNA

For isolation of yeast chromosomal DNA, a 2 ml over night culture was inoculated. The next day cells were spun down at 14000 rpm for one minute and washed with 500 µl H_2O. The pellet was resuspended in 200 µl breaking buffer (10 mM Tris/HCl, 100 mM NaCl, 1 mM EDTA, 1 % SDS and 2 % TritonX-100) 200 µl glass beads and 200 µl Phe/Chl (50 % (v/v) Phe TE, 50 % (v/v) chloroforme) were added and mixed for 20 min at 4 °C. Afterwards 200 µl H_2O were added and the sample was centrifuged at 14000 rpm for 10 min at room temperature. 300 µl of the upper phase were transferred to a new 1.5 ml reaction tube and the DNA was precipitated for 10 min at -20 °C by addition of 1 ml EtOH (100 %). After centrifugation at 14000 rpm for 10 min at 4 °C the supernatant was discarded and the pellet resuspended in 400 µl H_2O + 3 µl RNaseA (10 mg/ml). The RNA was digested for 5 min at 37 °C and the DNA again precipitated by adding 1 ml EtOH and 10 µl 5 mM ammonium acetate for 10 min at -20 °C. After centrifugation at 14000 rpm for 10 min at 4 °C the pellet was dried for a few minutes at 37 °C and resuspended in 30 µl H_2O.

3.3.2 Transformation of DNA

A preculture of the cells of interest was prepared. On the next day 10 to 50 ml main culture were inoculated with a dilution of 1:10. After an incubation of 2 - 6 hours at 30 °C the cells were harvested at an OD_{600} 0,5 - 0,8 by centrifugation at 2000 rpm for 5 min, fallowed by two washing steps with water and one with LiOAc-Sorb (100 mM lithium acetate, 10 mM Tris/acetate pH 8.0, 1 mM EDTA, 1 M D-Sorbitol). Furthermore the cells were resuspended in 100 - 500 µl LiOAc-Sorb and incubated at 30 °C for 15 min. Afterwards 50 µl of the cells were added to 5 µl herring sperm DNA (10 mg/ml), 300 µl PEG in Li-TE (100 mM lithium acetate, 10 mM Tris/acetate pH 8.0, 1 mM EDTA, 40 % (v/v) PEG 3350) and 3-10 µl of the DNA to be transformed. After an incubation step at 30 °C for 30 min the cells were heat shocked at 42 °C for 15 min, sedimented at 2000 rpm for 1 min and spread on selection medium. In case of DNA transformation for knock out by homologues recombination an additional incubation for 2 hours in YPD medium was necessary.

3.3.3 Transformation of plasmid-DNA

For transformation of plasmid DNA ("Quick and dirty"), cells from an agar plate were resuspended in 300 µl PEG in Li-TE-buffer (100 mM lithium acetate; 10 mM Tris/acetate pH 8.0; 1mM EDTA, 40 % (v/v) PEG 3350). 5 µl herring-sperm DNA (10 mg/ml) and 1 - 5 µl plasmid DNA were added and the sample was incubated as described in chapter 3.3.2.

3.3.4 Preparation of electrocompetent *E. coli*

Plasmid tranformation in *Escherichia coli* is a standard procedure in the field of molecular biology (see 3.3.5), but can only be performed in competent cells.

For competent *E. coli* cells (Table 8), a main culture of 600 ml LB-medium was inoculated 1 : 100 from an overnight culture and incubated at 37 °C up to an OD_{600} of 0.6 - 0.7, cooled down for 10 min on ice and spun down at 6500 rpm for 8 min at 4 °C. The cells were washed tree times with 0.5 l H_2O and 20 ml cold 10 % (v/v) glycerol. After these washing steps the cells were resuspended in 2 ml cold 10 % (v/v) glycerol and aliquoted (usually 40 µl) and stored at -80 °C.

3.3.5 Plasmid transformation in *E. coli*

In this study electroparation was used for transformation of plasmid DNA in *E. coli* cells. By an electric impulse the cell membrane is made permeable to DNA (Hanahan, 1991; Sheng, 1995).

Prepared electrocompetent *E. coli* (see 3.3.4) cells were thawn carefully on ice, 1 - 2 µl of the DNA to be transformed was added. The reaction was transferred to a pre-chilled electroporation tube and electroporated at 2500 V. Afterwards 900 µl SOC-medium were added and the sample was incubated for 1 hour at 37 °C at 220 rpm. After the incubation the cells were spun down, resupended in 100 µl H_2O, spread on LB-plates containing 45 µg/ml ampicillin and incubated over night at 37 °C.

3.3.6 Isolation of plasmid DNA from *E. coli*

To isolate small amounts of clean DNA the Wizard Plus SV Kit from Promega was used as described in the manufacturer's manual.

3.3.7 Restriction of DNA

DNA was digested with specific restriction enzymes to analyse DNA or prepare DNA for ligation (see 3.3.10). 1 - 5 µl DNA, 1.5 µl buffer (10 x concentrated), 1.5 µl BSA (10 x concentrated) if needed and 2 - 10 U enzyme were used (∑ = 15 µl). The reaction was incubated for 1 - 2 hours at optimal enzyme temperature (normally 37 °C). All reactions were done following the manufacturers advice from NEB. The reaction was mixed with 1.5 µl of DNA sample buffer (1 M Tris/HCl H 8.0; 50 % (v/v) glycerol; 0.1 % (w/v) bromphenolblue) and tested by using DNA agarose gel electrophoreses. For preparative digestions all standard reactions were scaled up and used for DNA gel extraction (see 3.3.9).

3.3.8 DNA agarose gel electrophoresis

The DNA agarose gel electrophoresis is a standard method to separate DNA fragments by size using their behaviour in an electric field (Brody and Kern, 2004). Dependent on the size of these fragments agarose gels with an concentration of 0.8 to 1.5 % (w/v) agarose with 1 µg / ml ethidiumbromide (to allow the detection of the DNA under UV-light (254 nm)) in TAE buffer (40 mM Tris/acetate pH 8.1; 2 mM EDTA; 0.114 % acetic acid) were prepared in an electrophoresis chamber containing TAE buffer. Furthermore the DNA samples were prepared with DNA sample buffer (1 M Tris/HCl pH 8.0; 50 % (v/v) glycerol; 0.1 % (w/v) bromphenolblue), loaded on the agarose gel and separated for 20 - 30 min by running up to a voltage of 120 V. For determination of DNA fragment size a standard ladder was loaded (TriDye 1 kb, NEB) (Table 15).

Table 15: Standard Tri Dye 1 kb

Fragment	1	2	3	4	5	6	7	8	9	10
Size (kb)	10	8	6	5	4	3	2	1.5	1	0.5

3.3.9 DNA gel extraction

To purify DNA fragments from agarose gels the QIAEX II Gel Extraction Kit from Qiagen was used as described in the manufacturer's manual.

3.3.10 Ligation of DNA fragments

For ligation of DNA fragments into a vector, 2 - 6 µl insert DNA (prepared by restriction; see 3.3.7), 0.5 - 3 µl vector DNA (prepared with corresponding restriction enzymes), 2.5 U T4-DNA-ligase and 1µl ligation buffer (10 x concentrated) were filled up to 10 µl with H_2O and incubated overnight at 16 °C. The next day 1 - 2 µl of the sample could be transformed into *E. coli* (see 3.3.5).

3.3.11 Polymerase chain reaction (PCR)

The polymerase chain reaction (PCR) is a method to amplify a DNA sequence by using a DNA polymerase (Saiki, 1988). For 100 µl PCR reaction, 10 µl PCR buffer (10 x concentrated), 100 pmol per oligonucleotide (forward and reverse; Operon), 1 µl template DNA, 1 µl dNTP mix (25 mM each dNTP), 1 - 2 µl DMSO and up to 5 U Taq DNA polymerase were mixed. Small fragments were amplified using the Taq DNA polymerase (NEB) and longer DNA fragments by using the proof reading polymerase Fideli Taq (USB). After a first step of DNA denaturation, 30 cycles of denaturation, annealing and elongation followed, completed by a last step of elongation. The exact program, concerning temperature and duration of cycles, was specially designed for each experiment, depending on the properties of the oligonucleotides and product size. The synthesised product could be evaluated by using the method of agarose gel electrophoresis (see 3.3.8).

3.3.12 Sequencing of DNA

For control, new cloned constructs were prepared for sequencing. 1 µl of template DNA, 1 µl sequencing mix (polymerase; dNTP mix with fluorescent dyes; 30 mM magnesium chloride and buffer substances), 1 µl oligonucleotide (1 : 100; compared to usual PCR), 1.5 µl sequencing buffer and 6 µl H_2O were used for PCR reaction. The PCR program included a 10 s denaturation step at 95 °C, 25 cycles of annealing for 5 s at 50 °C and elongation for 4 min at 60 °C. The PCR product was precipitated by addition of 1 µl 3 M sodium acetate (pH 5.2), 1 µl 125 mM EDTA and 50 µl ethanol (100 %, RT). After centrifugation at 13000 rpm for 10 min at RT, the sediment was washed with 70 % ethanol and dried for a few minutes. 15 µl HiDye (formamide) were added to stabilise the DNA. The reactions were analysed by the department of developmental biology of the Georg-August-Universität Göttingen.

3.3.13 Construction of knock out strains

For construction of knock out strains, the method of homologous recombination was used. Homologous recombination is a type of genetic recombination in which nucleotide sequences are exchanged between two similar or identical molecules of DNA. Using well-directed primers for construction of the new DNA- cassette, specific DNA sequences can be specifically exchanged (Figure 12).

The knockout construct, synthesised by a PCR reaction using corresponding primers (Table 10) (Longtine, 1998; Janke, 2004), was adopted for competent yeast transformation (see 3.3.2).

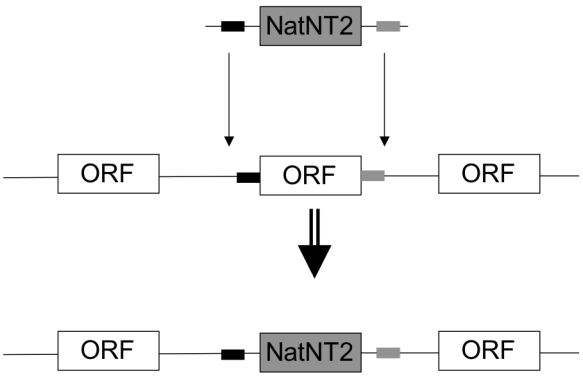

Figure 12: Scheme for construction of a knockout strain
((Tong and Boone, 2006); modified)

3.3.14 Chromosomal C-terminal fusion with a GFP-taq

A common approach is furthermore the chromosomal fusion of the gene of interest with a GFP taq. Most GFP fusion strains are available at Invitrogen (www.invitrogen.com), others were generated in this thesis. For example the chromosomal GFP-fusion of Om45 (Kanki, 2009a). Similar to knock out strain construction, the method of homologue recombination was used, including the PCR reaction using corresponding primers (Table 10) and the competent yeast transformation (see 3.3.2) (Longtine, 1998).

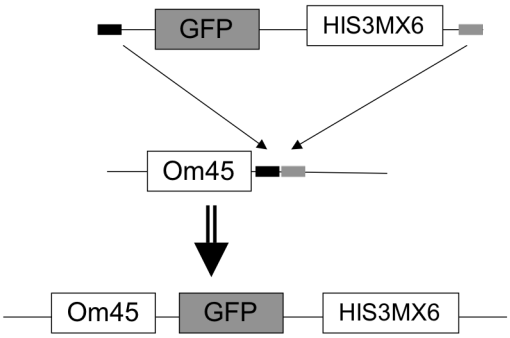

Figure 13: Scheme for the construction of chromosomal Om45-GFP
((Huh, 2003); modified)

3.3.15 Plasmid construction

several plasmids were constructed in this study

Om45-GFP/ Idh1-GFP

The plasmids pOm45-GFP and pIdh1-GFP were constructed by homologues recombination for use in mitophagy experiments. Therefore the vector pRS316 and specific primers, containing the purposed intersection for pRS316 (Table 10), were used. These primers were used for a PCR (see 3.3.11) reaction to amplify Om45-GFP, which had to be integrated into pRS316. As template 5 µl of chromosomal DNA isolated from Om45-GFP/Idh1-GFP (Invitrogen) were used. The resulting DNA fragment was purified by gel electrophoresis (3.3.8). Furthermore 6.5 µl of the resulting DNA fragment and 3.5 µl of Sma I digested pRS316 were used for competent yeast tranformation into matching knock out strains (*om45*Δ*/ idh1*Δ).

The grown yeast colonies were used for plasmid rescues: 1.5 ml of an over night preculture were centrifuged at 14000 rpm for 1 min at room temperature. After washing with 500 µl H_2O, the cells were resuspended in 200 µl breaking buffer (100 mM NaCl, 10 mM Tris/HCl, 1 mM EDTA, 1 % (w/v) SDS, 2 % (v/v) Triton-X-100; ph 8.0). 200 µl glass beads and 200 µl Phenol/Chloroform (50 % (v/v) Phenol, 50 % (v/v) Chloroform) were added and the reaction was mixed at 4 °C for 5 min. The cells were centrifuged at 14000 rpm for 10 min and 50 µl of the upper phase were transferred into a new reaction tube. The DNA was then precipitated at -20 °C for 20 min by adding 140 µl ethanol (100 %, ice cold) and 5 µl 3 M sodiumacetate/acetic acid (pH 5.2). After an additional centrifugation step for 10 min at 14000 rpm, the supernatant was removed and the sediment was washed with 70 % ethanol (cold) and dried at room temperature. Afterwards the plasmid DNA was resuspended in 30 µl

H_2O and could be stored at -20 °C or used for transformation in electrocompetent *E. coli* cells and subsequently for sequencing (see 3.3.12).

su9mtDHFR-GFP (mito-GFP)

Another plasmid, which was constructed in this study is su9-mt-DHFR-GFP, to detect mitophagy, furthermore referred to mito-GFP.

The use of well-directed primers (Table 10) in PCR to amplify a Su9-DHFR sequence (AG Rehling; Biochemistry II; Göttingen), containing specific restriction sites at the beginning and the end, allowed the insertion of this fragment (digested with BamH I and Hind III) into the vector pUG35 by ligation. Resulting in a plasmid encoding the Su9-DHFR sequence followed by a GFP-tag under control of a MET promoter.

GST-Shp1

For pull down experiments (see 3.4.7) recombinant GST-fusions of Shp1 were needed.

First step for construction of the plasmids encoding the recombinant GST-Shp1 was a polymerase chain reaction (see 3.3.11) using chromosomal wild type DNA as template and according primers (Table 10), containing restriction sites for Eco R I and Xho I and a vector - gene overlapping sequence. The resulting PCR products were treated with the restriction enzymes Eco R I and Xho I (see 3.3.7) and ligated in frame into the EcoR I and Xho I – restricted vector pGEX-4T-3 (Amersham) (see 3.3.10). The ligation product was transformed into electrocompetent *E. coli* cells (DH5α) (see 3.3.5) and tested for mutations by sequencing (see 3.3.12). Positive plasmids without mutations were transformed in *E. coli* BL21 (DE3) RIPL cells (Table 8) and used for pull down experiments (see 3.4.7).

3.4 Protein biochemical methods

3.4.1 Alkaline lysis

For protein lysates via alkaline lysis as described in literature (Horvath and Riezman, 1994), 2 OD_{600} of cells were used. The cells were centrifuged and resuspended in 1 ml of cold H_2O, 150 µl of lysis solution (925 µl of 2 M NaOH (4 g in 50 ml) and 75 µl ß-ME) were added and the reaction was incubated on ice for 10 min by vortexing every 2 minutes. To stop the reaction, 150 µl 50 % TCA were added and the lysed cells could be stored at -20 °C over night or incubated on ice for 10 min. Afterwards the tubes were centrifuged at 10000 g for 10 min at 4 °C, supernatants were removed and the pellets were washed with acetone and dissolved in 100 µl 1x Laemmli buffer (6 x Laemmli buffer pH 6.8: 0.35 M Tris/HCl, 10.28 % SDS, 36 % Glycerol, 5 % ß-ME (add freshly), 0.012 % bromphenoleblue) by conscientious shaking at 30 °C for 20 min. After centrifugation at 10 000 g for 5 min, the samples were used for SDS-PAGE (see 3.4.3) or could be stored at -20 °C.

3.4.2 Cell lysis for the detection of Atg8-PE

The lipidation of Atg8, via an ubiquitin like conjugation system (see 2.2.1.2) and the delipidation via Atg4, are necessary for autophagosome formation (Kirisako, 2000). Strains defective in autophagy therefore were tested for impairment in the lipidation of Atg8.
To detect the connection of Atg8 to phosphatidylethanolamine (PE), cells have to be disrupted in a very smooth manner, using a modified method for cell lysis (Suzuki, 2001).

60 OD_{600} were harvested, centrifuged at 3000 rpm for 3 min at RT and the supernatant was discarded. The cell pellet could be stored on ice (or -20 °C) or directly resuspended in 500 µl lysismix (500 µl lysis buffer (50 mM Hepes/KOH pH 7.5, 140 mM NaCl, 1 mM EDTA, 10 % glycerin, 0.05 % Na-desoxylat, 2 % Triton X-100, 0.1 % SDS) containing furthermore 10 µl 100 mM PMSF, 20 µl 50 x complete (1 tab in 1 ml lyse buffer) and 1 µl 1000x inhibitormix (1 µg/ml Pepstatin; 1 µg/ml leupeptin; 20 µg/ml chymostatin; 20 µg/ml antipain; 1 mM benzamidin; 10 µg/ml aprotinin in DMSO)). Afterwards 200 µl glass beads were added and the sample was vortexed for 10 min at 4 °C, centrifuged 5 min at 3000 rpm and 200 µl of the supernatant were transferred into a new reaction tube. After the addition of 40 µl 6x laemmli buffer (pH 6.8: 0.35 M Tris/HCl; 10.28 % SDS; 36 % glycerol, 5 % ß-ME

(added freshly); 0.012 % bromphenoleblue) the samples were used for SDS-PAGE (see 3.4.3) or could be stored at -20 °C.

3.4.3 SDS-PAGE

The so called SDS-PAGE (sodium dodecyl sulfate polyacrylamide electrophoresis) is a technique to separate proteins according to their electrophoretic mobility (Laemmli, 1970). First a separating gel (Table 16) was prepared. For polymerisation APS and Temed were added. After filling the gel into the designated equipment, it was covered with a thin layer of isopropanol. After the polymerisation and the further displacement of the isopropanol, the stacking gel could be coated on the separating gel (Table 16). Subsequent to the polymerisation of the stacking gel, 10 - 15 µl of the prepared samples and, for further determination of the size of the proteins, a standard ladder (Precision Plus Protein All Blue Standard, BioRad) (Table 17) were loaded. The gel was run up to a voltage of 150 V.

Table 16: Contents of SDS-PAGE

Separating gel	2 x 7%	2 x 8%	4 x 8%	2 x 10%	2 x 12%	2 x 15%
H_2O	5,1 ml	4,7	9,4	3,9	3,4	2,4
1,5M Tris (pH 8.8)	2,5 ml	2,5	5	2,5	2,5	2,5
Protogel	2,3ml	2,7	5,4	3,5	4	5
SDS	100 µl	100	200	100	100	100
APS	100 µl	100	200	100	100	100
TEMED	5 µl	5	10	5	5	5

Stacking gel	2
H_2O	6,1 ml
0,5 M Tris (pH 6.8)	2,5 ml
Protogel	1,3 ml
SDS	100 µl
APS	100 µl
TEMED	10 µl

Table 17: Precision Plus Protein All Blue Standard

Line	1	2	3	4	5	6	7	8	9
Size (kDA)	250	150	100	75	50	37.5	25	15	10

3.4.4 Western Blot

To blot the proteins separated by SDS-PAGE on PVDF-membranes based on the established standard method of western blot (Renart, 1979; Towbin, 1979). The wet blot system from BioRad was used. The SDS-gel, the PVDF-membrane and whatmanpaper were inserted into the blot chamber from BioRad (Figure 14) and filled up with wet blot buffer (192 mM glycin, 25 mM Tris and 20 % methanol). The transfer time was chosen to be at least 4 hours or over night at 4 °C with 70 mA per 45 cm^2 membrane size. Afterwards the PVDF-membranes were incubated in TBST buffer (20 mM Tris/HCl pH 7.6; 137 mM sodium chloride; 0.1% Tween 20 (w/v)) containing 10 % (w/v) skim milk powder) for 30 min - 1 h at RT or overnight at 4 °C to block all unspecific binding sites on the membrane. The blots were washed 3 times with 25 – 50 ml TBST for 5 min. Furthermore the membranes were incubated in TBST buffer containing the primary antibody (Table 11) for at least two hours at RT or overnight at 4 °C. The immunoblots were washed 6 times with 25 - 50 ml TSBT buffer for 5 min and then incubated in TBST buffer containing 1 % skim milk powder (w/v) and the secondary antibody (Table 11) for 45 min. After six times of 5 min washing steps with TBST, the blots were developed with ECL (USB) or ECL™ Plus (Amersham) following the manufacturer´s advice. Afterwards the immunoblots were analysed using a LAS-3000 (Fujifilm). Quantitative statistics from blots were done using the AIDA Software, Version 4.06.116.

For the detection using another antibody, the immunoblots were stripped by shaking in 10 % acetic acid for 10 min followed by three washing steps with TBST for 10 min. Afterwards the immunoblots were incubated for 30 min - 1 h in TBST containing 1 % slim milk powder, washed and incubated with the primary antibody of interest (see above).

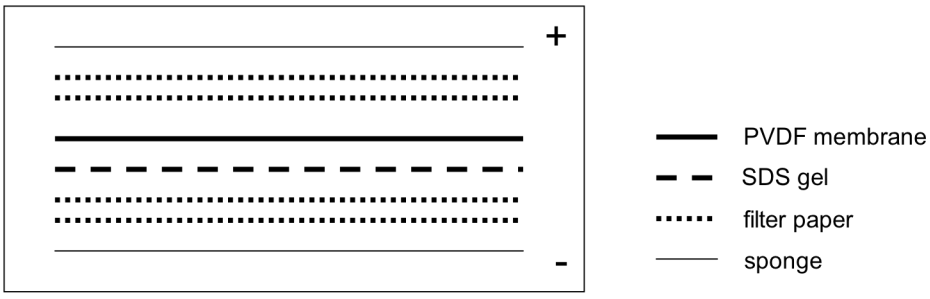

Figure 14: Scheme of western blot equipment

3.4.5 Measurement of autophagy dependent degradation of GFP-fused proteins

3.4.5.1 Macroautophagy

For measurement of autophagy dependent degradation of GFP-fused proteins the strains of interest were transformed with GFP-Atg8 (~39 kDa) or Pgk1-GFP (~71 kDa) and treated as described in literature (Meiling-Wesse, 2002; Klionsky, 2007; Welter, 2010). Upon dlivery of GFP-Atg8 or Pgk1-GFP into the vacuole, the proteins are rapidly degraded, whereas the released free GFP remains relatively stable. Accordingly, the appearance of free GFP can be used to monitor autophagy (Klionsky, 2007).
Cells were grown in a main culture to stationary phase. 20 OD_{600} were washed with SD-N medium, resuspended in 2 ml of SD-N and incubated at 30 °C. 200µl (2 OD_{600}) cells were taken at defined time points (0, 2, 4 and 6 h) and alkaline lysed (see 3.4.1).

3.4.5.2 PMN

For measurement of the selective piecemeal microautophagic degradation of the nucleus, the strains of interest were transformed with GFP-Osh1 (~180 kDa) and treated as described (see 3.4.5.1) (Krick, 2008b).

3.4.5.3 Mitophagy

Two methods for detection of mitophagy by western blot were used. In the strains of interest GFP was chromosomally integrated after the Om45 locus (Om45-GFP::HIS3X6; see 3.3.14) (~71 kDa) (Kanki, 2009a) or they were transformed with the plasmid mito-GFP (~48 kDa) (constructed in this thesis, see 3.3.15). Cells were grown for preculture in selection medium containing 2 % glucose over night and transferred to main-culture medium containing 2 % lactate* (0.5 OD_{600} / ml). The next day 0.05 mM H_2O_2, 2 mM paraquat or 0.2 µg/ml rapamycin were added to 20 OD_{600} cells and incubated at 30 °C. 2 OD_{600} cells were taken at defined time points (0, 2, 4, 6 h) and alkaline lysed (see 3.4.1) or the cells were grown up to 72 h in main culture and 2 OD_{600} cells were taken at defined time points (24, 48 and 72 h) and alkaline lysed.

*For cells transformed with the plasmid mito-GFP, main culture medium furthermore lacking methionine (-Met) was used.

3.4.6 Pull down of GST-Shp1

((Wu, 2006); (Smith and Johnson, 1988); modified)

3.4.6.1 Purification of recombinant GST-Shp1

For preculture, 10 ml LB containing 75 µg/ml ampicillin and 25 µg/ml chloramphenicol were inoculated with *E. coli* cells containing the GST-Shp1 construct. The next day, the cultures were diluted 1 : 10 and incubated at 30 °C for 2 hours. Afterwards the expression of recombinant protein was induced by adding 0.2 mM IPTG and an incubation for additional 4 hours at 30 °C.

The cells were harvested by centrifugation at 5000 rpm for 10 min and solubilised using a french press (SIM AMINCO). Therefore the sediments were resuspended in 5 ml PBS (140 mM NaCl, 2.7 mM KCl, 10 mM Na_2HPO_4, 1.8 mM KH_2PO_4) and 15 µl 0.2 M PMSF, 150 µl 10 % Triton X100, 3 µl DNAse 1, 11.25 µl Complete, 0.45 µl Leupeptin, 4.5 µl Pefablock and 2.7 µl 0.5 M EDTA were added. The cell solution was treated with the french press for three times on ice and afterwards used for coupling to the sepharose matrix (see 3.4.6.2).

3.4.6.2 Coupling of GST-fusion protein to sepharose

To couple the GST-fusion protein to the sepharose matrix, 100 µl 50 % slurry was added to the cell lysates and incubated at 4 °C for 30 - 50 min while shaking constantly. The matrix was sedimented at 500 g for 5 min. The supernatant was carefully removed and the sediment was washed with 500 µl PBS (140 mM NaCl, 2.7 mM KCl, 10 mM Na_2HPO_4, 1.8 mM KH_2PO_4) three times and finally resuspended in 500 µl PBS.

3.4.6.3 Native cell extracts

For the assembly of native protein extracts, cells expressing GFP-Atg8 were prepared for preculture and the next day inoculated in main culture in a dilution of 1 : 100.

On day 3, 40 OD_{600} of the cells were harvested and washed with H_2O by centrifugation for 5 min at 4 °C. The cell pellet was resupended in 1 ml lysis buffer (100 mM NaCl; 50 mM Tris/HCl pH 7.5; 5 mM $MgCl_2$; 1 mM EDTA; 5 % Glycerol; added freshly: 100 mM PMSF, 1000 x inhibitor-mix, 25 x Complete (Roche)), added to 0.2 ml glass beads and vortexed 15 min at V_{max} and 4 °C. After this cell lysis the tube was centrifuged at 5000 rpm for 5 min at 4 °C and the supernatant could be used for GST-pull down experiments or stored at -80 °C.

3.4.6.4 GST-Pull down

For the GST-pull down experiment 500 µl (20 OD_{600}) of native cell extract were incubated with the prepared GST-column for 4 h at 4 °C while shaking. Afterwards the beads were sedimented at 500 g for 5 min at 4 °C, the supernatant was removed and the GST-beads were washed three times with lysis buffer at 500 g for 5 min at 4 °C. For elution of the bound proteins 200 µl of elution buffer (10mM red. glutathione; 50 mM Tris/HCl pH 8.0) were added and the beads were sedimented at 500 g for 5 min at 4 °C and the supernatant was taken. After repeating the elution for 2 times the eluates were pooled and precipitated using 50 % TCA, incubated on ice for 20 min and centrifuged at 13000 rpm for 10 min at 4 °C. The pellet was washed with acetone, dried for a few minutes and resuspended in 50 µl laemmli buffer.

4. Results

4.1 Synthetic Genetic Array

The Synthetic Genetic Array analysis (SGA) is a powerful high-throughput technique for exploring synthetic lethality. It allows the systematic construction of double deletion mutants of a query strain and an entire genome deletion library. The identification of synthetic lethality highlights genes with similar function or genes with similar patterns of genetic interactions (Tong, 2001; Tong and Boone, 2006).

To ensure the preparation of the query strain, mating and sporulation steps were controlled via microscopy. Figure 15 represents the zygotes generated by mating (A) and the resulting spores generated by incubation of the diploid cells in enriched sporulation medium (B). The spores were plated on medium selecting for the haploid progeny containing the required genetic attributes. Query strains deleted in *ATG8, ATG15, ATG18* and *ATG21* were generated (see 3.2.11.1).

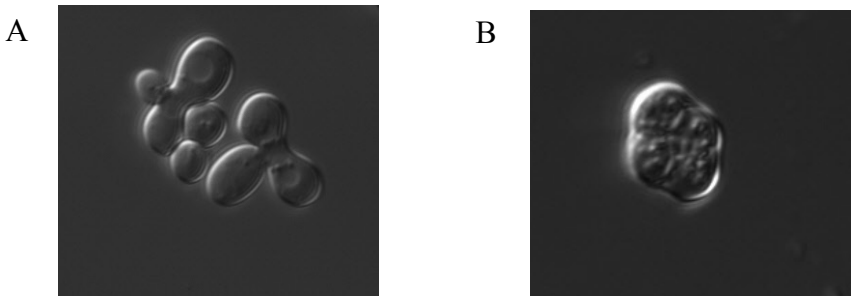

Figure 15: Mating and sporulation for query strain generation was controlled by microscopy
(A) The mating of Y8205 and the deletion strain of interest resulted in zygotes without any abnormality; (B) the incubation for 5 days in enriched sporulation medium resulted in spores of common character

All generated query strains were used for the SGA screen as described in chapter 3.2.11.2. The last step of the screen, the selection for the haploid progeny of mating type a containing the double deletion (*query*Δ::NatMX4 and $x_{(DMA)}$Δ::KanMX4), was arranged by the use of SD-his/arg/lys medium containing 100 µg/l clonNAT, 200 µg/l G418, 100 µg/l can and 100 µg/l lyp. A total of 53 plates had to be evaluated concerning double deletions resulting in synthetic lethality. Figure 16 shows two of the OmniTray plates after the last selection step of the screen. Two colonies per double deletion were pinned on one OmniTray plate and every plate was done in duplicates. Therefore, single colonies without growth could be ignored. When both colonies, pinned on one plate, were not able to grow, the double mutant was

nominated as synthetic lethal. The synthetic lethality was confirmed by the same growth phenotype on the second, identic control plate. All detected synthetic double deletions are listed in table 18.

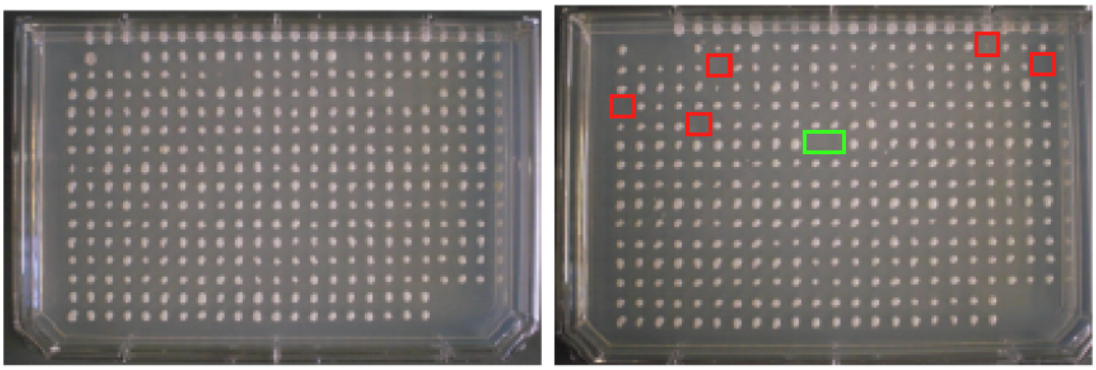

Figure 16: SGA plates

Representative OmniTray plates after the last selection step: SD-his/arg/lys medium containing 100 µg/l clonNAT, 200µg/l G418 100 µg/l can and 100 µg/l lyp, resulting in haploid progeny of mating type a with double deletion (*query*Δ::NatMX4 and $x_{(DMA)}$Δ::KanMX4); on the right: single colonies without growth are marked with a red box, both colonies of one double deletion mutant defective in growth are marked with a green box.

Table 18: Strains occurring as synthetic lethal in SGA

query strain *query*Δ::NatMX4	**DMA strain** $x_{(DMA)}$Δ::KanMX4	
*atg15*Δ	YDR234W	*lys4*Δ
	YOR302W	*yor302w*Δ
	YOR303W	*Cca1*Δ
	YOL058W	*arg1*Δ
	YOR323c	*pro2*Δ
	YOR258W	*hnt3*Δ
	YGL033W	*hop2*Δ
	YIL094c	*lys12*Δ
	YEL057c	*yel057c*Δ
	YCR010c	*ady2*Δ
	YPL125W	*kap120*Δ
	YNL053W	*msg5*Δ
	YMR143W	*rps16A*Δ
*atg18*Δ	YMR280c	*cat8*Δ
	YNL242W	*atg2*Δ
	YJL122W	*alb1*Δ
*atg8*Δ	YOL127c	*hmo1*Δ
	YLL0026W	*hsp104*Δ
***atg21*Δ**	**YDR323c**	***vac1*Δ**
	YJL178c	***atg27*Δ**

For confirmation of the synthetic lethality of the double deletion *atg21*Δ *vac1*Δ and *atg21*Δ *atg27*Δ in the screen (Table 18; bold), these double deletions were generated again in a separate experiment.

The double mutants were generated by conventional mating (see 3.2.5), sporulation (see 3.2.8) and selection steps, using media similar to the SGA-screen (see 3.2.11.2). Both double deletion combinations presented neither a synthetic lethality nor a defect in growth of colonies on SD-his/arg/lys medium containing 100 µg/l clonNAT, 200 µg/l G418, 100 µg/l can and 100 µg/l lyp, selecting for the haploid progeny of mating type a (*query*Δ::NatMX4 $x_{(DMA)}$Δ::KanMX4).

For further control of the *atg21*Δ *atg27*Δ double deletion in a second yeast background, *atg27*Δ::HIS3 cells of the WCG background were also mated with *atg21*Δ::KAN of the WCG background. The resulting diploids were sporulated (see 3.2.8), tetrads were separated (see 3.2.9) and examined for growth ability on medium lacking histidine and containing 200 µg/l G418. The tetrad separation of these diploid double mutant resulted in the growth of four different haploid cells, including the double deletion (*atg21*Δ::KAN *atg27*Δ::HIS3) without any viability or growth defect.

4.2 Detection of nonselective bulk autophagy using Pgk1-GFP

For the detection of autophagy by western blot, GFP-Atg8 is the common marker protein. In this study the cytosolic 3-phosphoglycerate kinase Pgk1 could be introduced as novel marker protein (Welter, 2010). To detect the autophagic degradation of Pgk1-GFP, the plasmid pRS316-Pgk1-GFP was constructed in the Thumm laboratory and used for experiments in this study.

Cells expressing Pgk1-GFP were starved up to 6 hours in SD-N medium and samples were taken at defined time points (0, 2, 4 and 6 h). The cells were alkaline lysed and treated for immunoblotting using anti-GFP antibody, as also described in Welter *et al.* (2010). Upon delivery of Pgk1-GFP into the vacuole, Pgk1 is rapidly degraded, whereas the released GFP remains relatively stable. Accordingly, the appearance of free GFP can be used to monitor unselective autophagy.

In wild type cells a clear signal for free GFP was detected. *ATG21* deleted cells showed a reduction in signal quantity compared to wild type cells. *ATG1* deleted cells, deficient in autophagy, and *pep4*Δ cells, deficient in intravacuolar proteolysis, were used as controls (Figure 17 (A)). The signal intensities of the western blot bands were quantified using AIDA software. The ratio between free GFP and Pgk1-GFP was calculated, taking wild type cells (6 h) as 100 %. The resulting values of three independent experiments are displayed in figure 17 (B). Figure 17 (C) highlights the values after 6 hours of starvation.

A

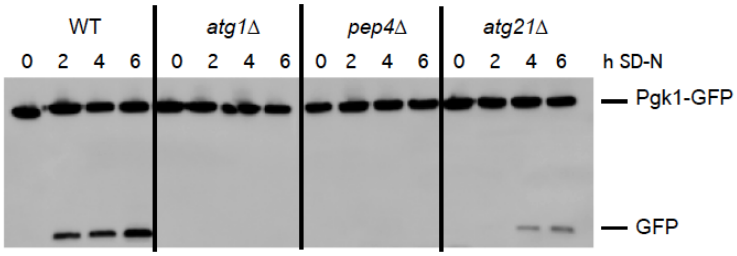

B

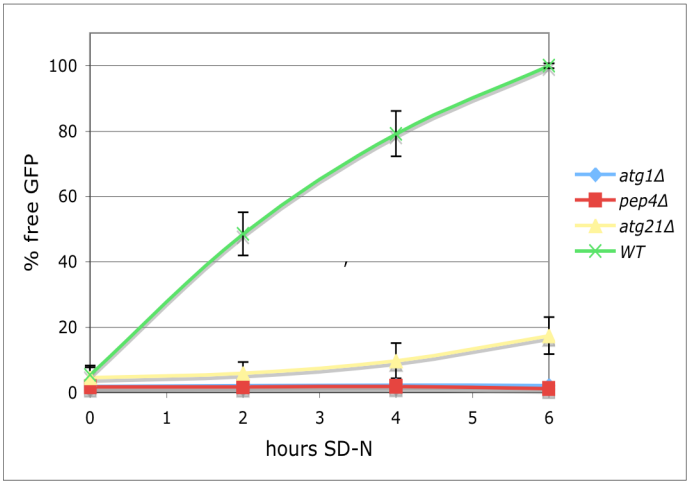

C

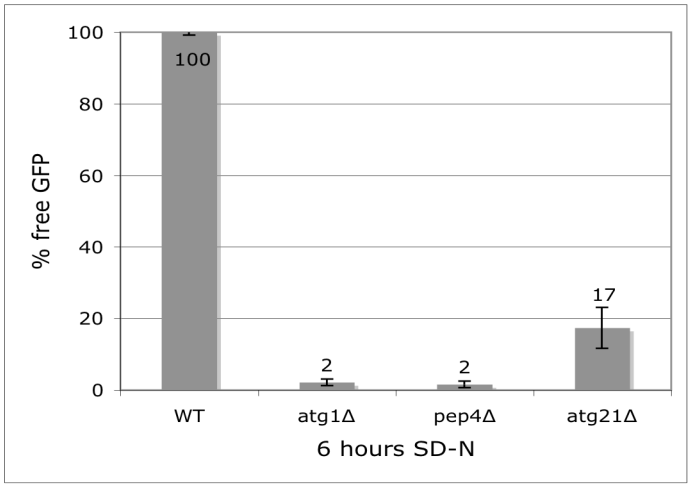

Figure 17: Monitoring unselective autophagy using Pgk1-GFP

(A) Wild type (WT), *atg1*Δ, *pep4*Δ and *atg21*Δ cells expressing Pgk1-GFP were starved in SD-N, samples were alkaline lysed and immunoblotted. Using a monoclonal mouse anti-GFP antibody and a peroxidase-coupled secondary antibody, Pgk1-GFP (~71 kDa) and free GFP (~26 kDa) were detected.
(B) Quantification of signal intensities by AIDA software. The value of wild type cells starved for 6 hours was set to 100 % (n = 3).
(C) Values of free GFP of cells starved for 6 hours are presented.

The degradation of Pgk1-GFP was also shown in fluorescence microscopy experiments (Figure 18). Wild type, *atg1*Δ, *pep4*Δ and *atg21*Δ cells expressing Pgk1-GFP were starved for 4 hours in SD-N medium containing 1 mM PMSF, to avoid vacuolar proteolysis. Using a DeltaVision spectris fluorescence microscope equipped with a FITC filter, a high amount of free floating autophagic bodies inside the vacuole were observed in wild type cells. In *atg1*Δ cells, used as negative control, no autophagic bodies appeared in the vacuole, while in *pep4*Δ cells, unable for degradation of vacuolar vesicles, a clear accumulation of autophagic bodies was observed. A small amount of green vesicles was found in *atg21*Δ cells, supporting the observation in the western blot analysis.

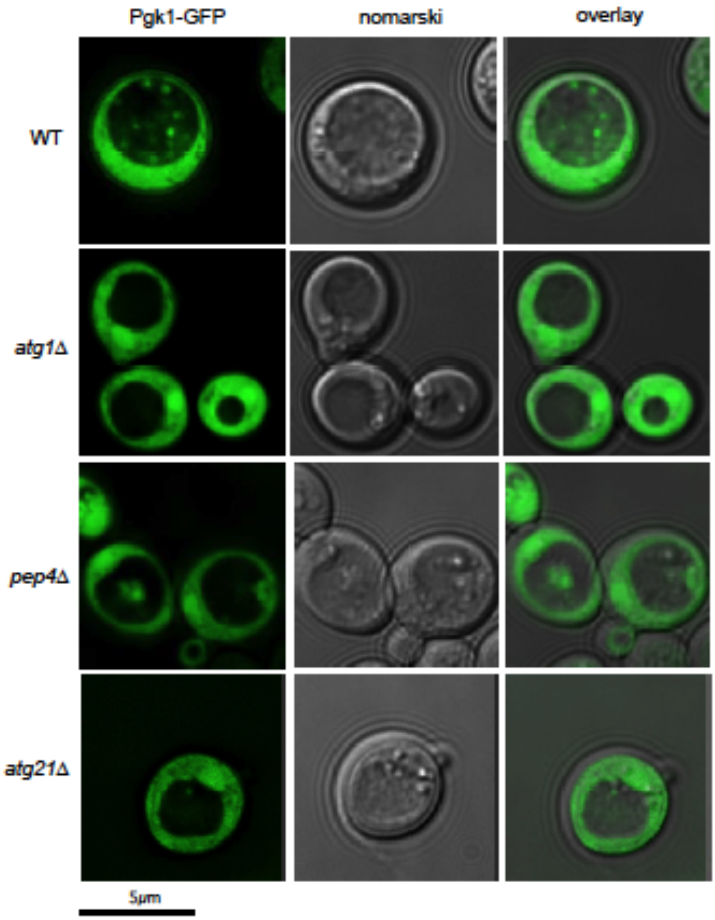

Figure 18: Fluorescence microscopy of cells expressing Pgk1-GFP

Wild type (WT), *atg1*Δ, *pep4*Δ and *atg21*Δ cells (WCG) expressing Pgk1-GFP were starved for 4h in SD-N medium containing 1 mM PMSF. The cells were observed by fluorescence microscopy using a DeltaVision microscope (FITC filter) and the accumulation of autophagic bodies in the vacuole was analysed.

4.3 Cdc48 and its cofactor Shp1 are needed for functional autophagy

Cdc48 and Shp1 (also termed Ubx1) are required for autophagosome biogenesis (Krick, 2010).

4.3.1 Shp1 is the exclusive cofactor of Cdc48 needed for autophagy

The requirement of Cdc48 for autophagy was shown by the use of the standard GFP-Atg8 degradation assay (see 3.4.5.1) (Bremer, 2009).

Cdc48 is known to be involved in different pathways (ERAD, UFD). Caused by this diversity in function, many cofactors of Cdc48 have been identified (overview see (Buchberger, 2010). To elucidate the need for autophagy and to confirm former results (Bremer, 2009), strains deleted in these cofactors and regulators were tested for functional autophagy.

Members of the UBX domain protein family are known to act as Ccd48 regulators (Schuberth, 2004). Therefore *Ubx1* to *Ubx6* deletion strains were tested in the standard GFP-Atg8 degradation assay for their involvement in autophagy (see 3.4.5.1).

After 4 hours of starvation in SD-N medium, decreasing signal for GFP-Atg8 and increasing signal of free GFP was detectable in wild type cells, whereas in the negative control *atg1*Δ, no free GFP was detected. Furthermore *ubx1*Δ (*shp1*Δ) cells showed a clear reduction of free GFP in contrast to the other deletion strains of the UBX protein family *ubx2*Δ, *ubx3*Δ, *ubx4*Δ, *ubx5*Δ and *ubx6*Δ.

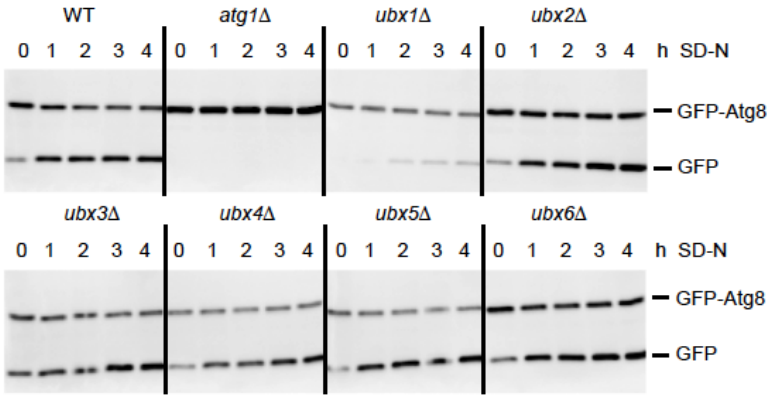

Figure 19: Ubx1 but no other UBX domain protein is required for autophagy

Wild type (WT), *atg1*Δ and *ubx1*Δ - *ubx6*Δ cells expressing GFP-Atg8 were starved in SD-N, samples were alkaline lysed and immunoblotted. Using a monoclonal mouse anti-GFP antibody, GFP-Atg8 (~39 kDa) and free GFP (~26 kDa) were detected.

In the next step, it was analysed if the ubiquitin-proteasome system, represented by the substrate-processing Cdc48 cofactors Ufd2 and Ufd3, the ubiquitin ligase Ufd4 and the proteasome regulator Ufd5, is required for macroautophagy.

As Ufd1, a crucial substrate-recruiting cofactor, is an essential protein, a strain containing a point-mutation in the *UFD1* allele (ufd1-1) was used for GFP-Atg8 degradation assay experiments (Figure 20 (B)). Ufd1-1 and all further tested strains, deleted in one of the proteasome related cofactors or regulators of Cdc48 (*ufd2*Δ - *ufd5*Δ), showed normal starvation induced degradation of GFP-Atg8, comparable to wild type cells (Figure 20 (A)).

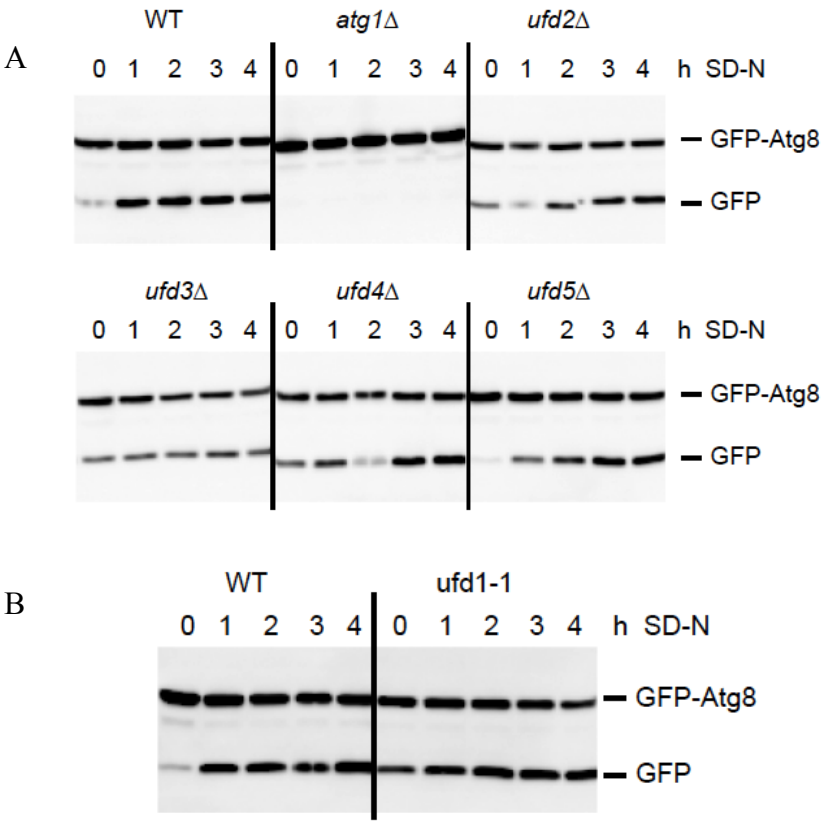

Figure 20: Ufd proteins are not required for autophagy

(A) Wild type (WT), *atg1*Δ and *ufd2*Δ - *ufd5*Δ cells, (B) wild type and ufd1-1 cells expressing GFP-Atg8 were starved in SD-N, samples were alkaline lysed and immunoblotted. Using a monoclonal mouse anti-GFP antibody, GFP-Atg8 (~39 kDa) and free GFP (~26 kDa) were detected.

Furthermore the ERAD component Der1 and the Cdc48 substrate-processing cofactor Otu1 were tested for intact autophagy.

Both of the tested strains *der1*Δ and *otu1*Δ showed normal degradation of GFP-Atg8 comparable to wild type cells, while in the negative control *atg1*Δ no signal for GFP was detected (Figure 21).

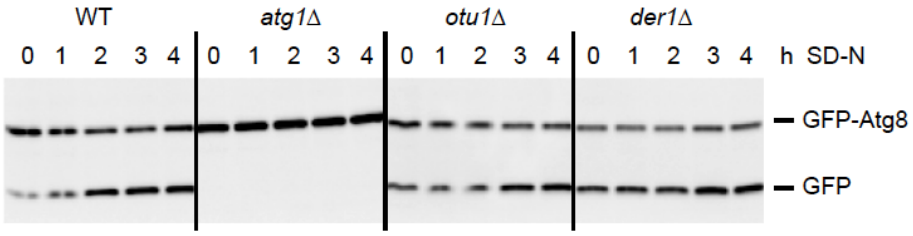

Figure 21: Otu1 and Der1 are not required for autophagy

Wild type (WT), *atg1*Δ, *der1*Δ and *otu1*Δ cells expressing GFP-Atg8 were starved in SD-N, samples were alkaline lysed and immunoblotted. Using a monoclonal mouse anti-GFP antibody, GFP-Atg8 (~39 kDa) and free GFP (~26 kDa) were detected.

Furthermore Doa4 was tested for the involvement in autophagy. Doa4 is an ubiquitin isopeptidase, required for recycling of ubiquitin from proteasome-bound polyubiquitinated proteins. The deletion of *DOA4* depletes the cellular ubiquitin level (Swaminathan, 1999; Ren, 2008).

The WCG *doa4*Δ strain was generated by homologous recombination in this thesis (see 3.3.13) and the cells were used for GFP-Atg8 degradation assays. These assays resulted in the detection of free GFP signal in *doa4*Δ cells, comparable to wild type cells.

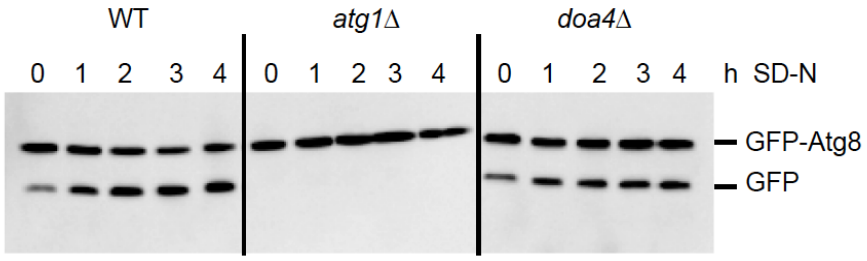

Figure 22: Macroautophagy is not affected in *doa4*Δ cells

Wild type (WT), *atg1*Δ and *doa4*Δ cells (WCG) expressing GFP-Atg8 were starved in SD-N, samples were alkaline lysed and immunoblotted. Using a monoclonal mouse anti-GFP antibody, GFP-Atg8 (~39 kDa) and free GFP (~26 kDa) were detected.

4.3.2 Shp1 is needed for autophagy but not for the Cvt pathway and CPY maturation

As an additional method, the involvement of Ubx1/Shp1 in autophagy was tested in a degradation assay using Pgk1-GFP as marker protein (see 4.2) (Welter, 2010).

Wild type, *atg1Δ* and *shp1Δ* cells were transformed with Pgk1-GFP. Stationary grown cells were starved in SD-N up to 6 hours, samples were taken (0, 2, 4 and 6 h), treated for immunoblot as previously described and visualised using a monoclonal mouse anti-GFP antibody. In this Pgk1-GFP degradation assay Pgk1-GFP and free GFP were detected in wild type cells. In contrast, *shp1Δ* and *atg1*Δ cells showed no signal for free GFP.

Furthermore the blots were reprobed with a polyclonal rabbit anti-ApeI antibody to detect a potential dysfunction in the Cvt-pathway. However, the maturation of aminopeptidase1 (Ape1) was not impaired in *shp1*Δ cells compared to wild type cells.

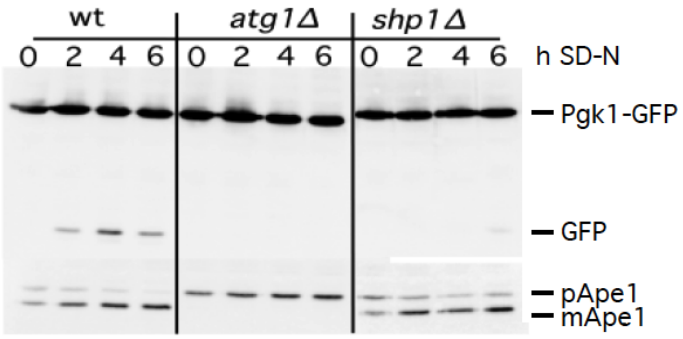

Figure 23: Shp1 is required for autophagy but not for the Cvt-pathway
Wild type (WT), *atg1*Δ and *shp1*Δ expressing Pgk1-GFP were starved in SD-N, samples were alkaline lysed and immunoblotted. Using a monoclonal mouse anti-GFP antibody, Pgk1-GFP (~71 kDa) and free GFP (~26 kDa) were detected, prApe1 (~62 kDa) and mApe1 (~57 kDa) were detected using a polyclonal rabbit anti-Ape1 antibody.

Ape1 can be matured either selectively via the Cvt pathway or unselectively via autophagy, dependent of the growth phase and supply of nutrients. Also the carboxypeptidase Y (CPY) is synthesised as a prepro-form and travels through the ER and Golgi to the vacuole in an autophagy-independent manner (Conibear and Stevens, 1998).

To test the involvement of Shp1 in these pathways, wild type, *shp1*Δ, *atg1*Δ, *atg21*Δ and *pep4*Δ cells of different growth phases (logarithmic (log) and stationary (stat)) and starved cells were tested for maturation of Ape1 and CPY.

Figure 24 shows, that the maturation of Ape1 and CPY in *shp1*Δ cells occurs comparable to wild type cells. The control strains *atg1*Δ and *pep4*Δ are blocked in maturation of Ape1 and

*pep4*Δ cells are also blocked in maturation of CPY. In *atg21*Δ cells, where the Cvt pathway is blocked, the maturation of Ape1 was only observed under starvation conditions.

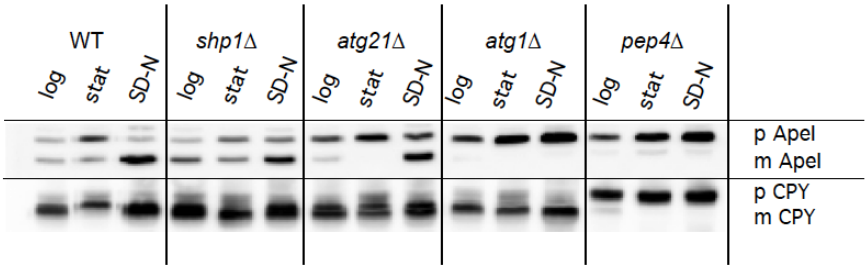

Figure 24: The maturation of Ape1 and CPY occurs normal in *shp1*Δ cells
Samples of wild type (WT), *shp1*Δ, *atg1*Δ, *atg21*Δ and *pep4*Δ cells in logarithmic and stationary growth phase and starved in SD-N medium were taken, alkaline lysed and immunoblotted. prApe1 (~62 kDa) and mApe1 (~57 kDa) were detected using a rabbit anti-Ape1 antibody and pCPY (~69 kDa) and mCPY (~61 kDa) were detected using a mouse anti-CPY antibody.

4.3.3 No accumulation of autophagic bodies occurs in *shp1*Δ cells

Another standard method in the field of autophagy is the visualisation of intravacuolar vesicles by microscopy (see 3.2.10.1). Therefore *shp1*Δ cells in the WCG background were generated by homologues recombination in this study (see 3.3.12). Wild type, *pep4*Δ, *atg1*Δ and *shp1*Δ cells of WCG background were starved in SD-N medium. Additional cultures of wild type, *pep4*Δ, *atg1*Δ and *shp1*Δ cells were treated with 1 mM PMSF to inhibit vacuolar proteinase B. The cells were used for microscopy (see 3.2.10.1). Distinct to other vesicles, also transported to the vacuole (e.g. MVB vesicles), autophagic bodies can be observed as little swirling dots in the vacuole.

Figure 25 (A) displays yeast cells after starvation for 4 hours in SD-N. Wild type cells treated with 1 mM PMSF showed various autophagic bodies inside the vacuole, cells without PMSF exhibited an empty vacuole caused by the degradation of autophagic bodies by vacuolar proteases. The positive control *pep4*Δ, defective for the breakdown of vesicles, showed an intense accumulation of autophagic bodies. In contrast, the autophagy deficient control cells *atg1*Δ showed no vesicles inside the vacuole. *SHP1* deleted cells also showed no accumulation of autophagic bodies in the vacuole, even not with PMSF treatment. For statistic interpretation 200 cells of each strain (with and without 1 mM PMSF) were monitored and evaluated concerning the accumulation of vesicles (Figure 25 (B)).

A

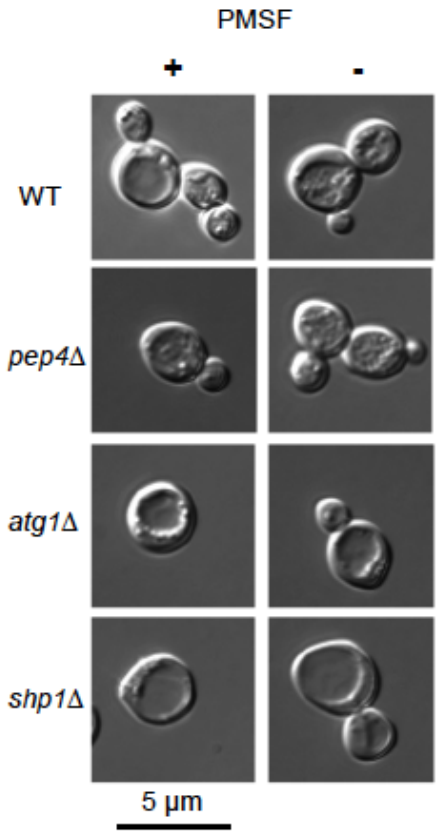

B

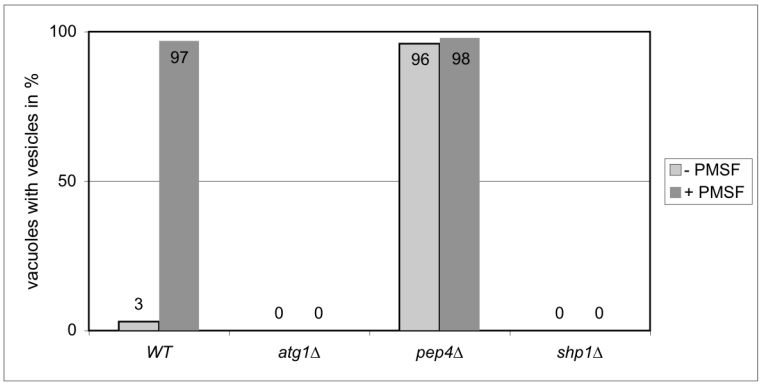

Figure 25: No vacuolar accumulation of autophagic bodies in *shp1*Δ cells

(A) Wild type (WT), *pep4*Δ, *atg1*Δ and *shp1*Δ cells were starved in SD-N for microscopy. Additional cultures of wild type and shp1Δ cells were treated with 1 mM PMSF to inhibit vacuolar proteases.
(B) Wild type (WT), *atg1*Δ, *pep4*Δ and *shp1*Δ cells (treated/ not treated with 1mM PMSF) containing autophagic bodies in the vacuole after starvation for 4 hours in SD-N were counted and evaluated.

4.3.4 The formation of the PAS occurs normal in *shp1*Δ cells

A very important step during autophagy is the formation of the pre-autophagosomal structure (PAS), where the autophagic core machinery assembles (Suzuki, 2001; Kim, 2002). Besides Atg8, which is integrated via PE into the membrane during autophagosome formation, also the transmembrane protein Atg9 is known to be involved in autophagosome biogenesis.

Therefore both proteins are qualified marker proteins for the PAS in microscopy (Reggiori, 2004a; Reggiori, 2005; Klionsky, 2007).

The formation of the PAS was observed in *shp1*Δ cells in fluorescence microscopy using GFP-Atg8 (Figure 26 (A)). For statistic evaluation, cells containing clear green dots, representing the PAS, were counted. 200 cells either expressing GFP-Atg8 or GFP-Atg9 were analysed. Two independent experiments were done (n = 2). *SHP1* deleted cells showed no reduction in PAS formation compared to wild type cells using both marker proteins (Figure 26 (B)).

A

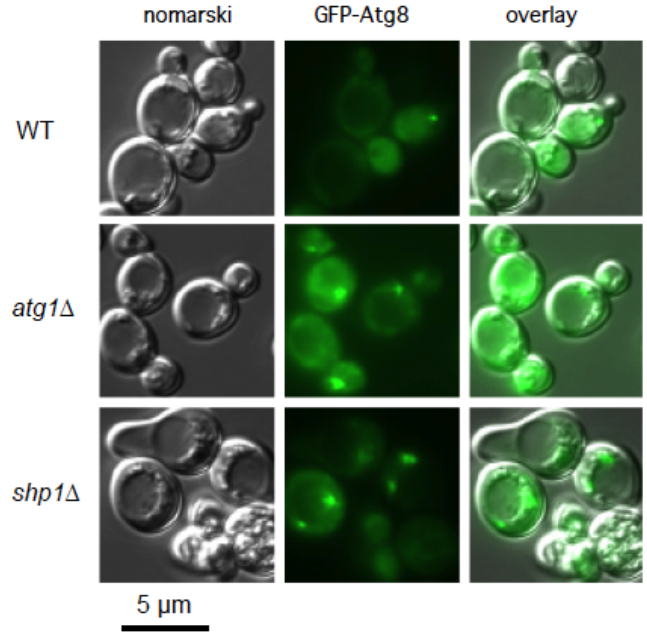

B

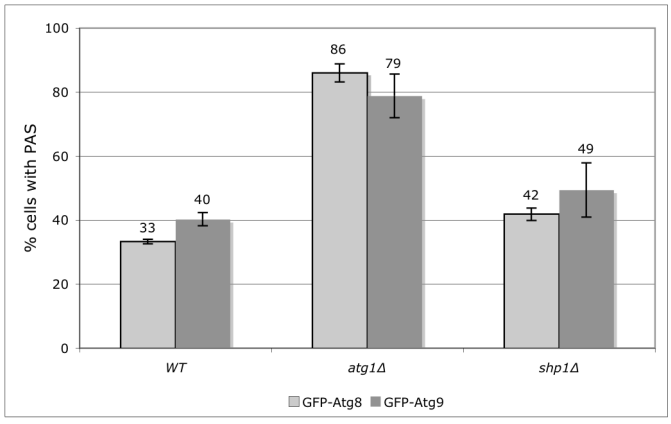

Figure 26: The formation of the PAS occurs normal in *shp1*Δ cells

(A) Wild type (WT), *atg1*Δ and *shp1*Δ cells expressing GFP-Atg8 were starved in SD-N medium. The PAS represented by GFP-Atg8 was visualised in fluorescence microscopy

(B) Wild type (WT), *atg1*Δ and *shp1*Δ cells expressing GFP-Atg8 or GFP-Atg9 containing a clear green PAS dot were counted. 200 cells were counted in two independent experiments (n=2)

4.3.5 Lipidation of Atg8 occurs normal in *shp1*Δ cells

Atg8 is conjugated via an ubiquitin like conjugation system to phosphatidylethanolamine (PE) (Kirisako, 2000) (see 2.2.1.2). This lipidation and also the delipidation are necessary for effective autophagosome expansion and formation (Nakatogawa, 2007). Therefore *shp1*Δ cells were tested for Atg8 lipidation in western blot analysis.

Comparable to wild type cells, the lipidation occurred slightly retarded in *shp1*Δ cells, similar to *atg21*Δ cells. *ATG7* deleted cells, unable for Atg8-conjugation (Ichimura, 2000; Kirisako, 2000), showed no lipidated Atg8. The control strain *atg8*Δ showed no signal at all.

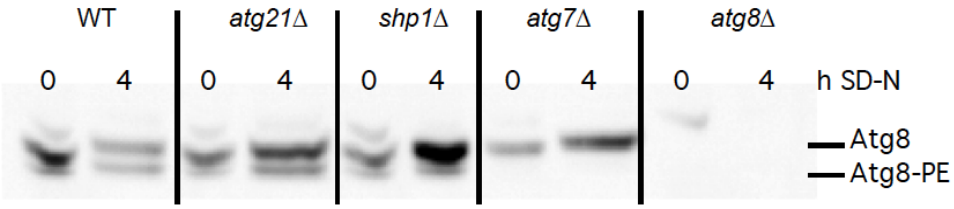

Figure 27: The lipidation of Atg8 occurs normally in *shp1*Δ cells
Wild type (WT), *atg21*Δ, *shp1*Δ, *atg7*Δ and *atg8*Δ cells were starved for 4 hours in SD-N. Samples were taken after 0 and 6 hours of starvation, alkaline lysed and immunoblotted. Using a monoclonal rabbit anti-Atg8 antibody, Atg8 (~14 kDa) and Atg8-PE were detected. To ensure an adequate separation of the signals, a 12 % SDS gel containing 6 M Urea was used.

4.3.6 Pull down experiments of recombinant GST-Shp1

A split ubiquitin assay gave first incidence for a potential interaction between Shp1 and Atg8. This interaction has been proven by coimmunoprecipitation and pull down experiments using recombinant GST-Atg8 (Krick, 2010). For further investigations, pull down experiments using recombinant GST-Shp1 were done in this study. Shp1 is known to possess an N-terminal UBA and a C-terminal UBX domain (see 2.2.5.1). Therefore full length GST-Shp1, as well as a GST-Shp1 construct lacking the UBX domain and a GST-Shp1 construct lacking the UBA domain, were generated. The three GST-fusion proteins were purified (see 3.4.6.1) and used for pull down experiments by incubation with crude extract of cells expressing GFP-Atg8 (see 3.4.6.4).

The purification of recombinant GST-Shp1 was optimised by the use of *E. coli* BL21 RIPL cells for expression and a following cell disruption by french press. Figure 28 (A) exhibits samples of *E. coli* BL21 RIPL cells ahead of treatment with IPTG (1), samples of *E. coli* cell

suspension before cell disruption by french press (2), samples taken after cell disruption (3) and samples of GST-coupled sepharose beads (4).

For pull down, crude cell extracts (L) from either *pep4*Δ cells expressing GFP-Atg8 (B) or *atg4*Δ *atg8*Δ cells expressing GFP-Atg8-FG (C) (see 5.3.2) were incubated with GST-Shp1/-UBX/-UBA and GST coupled sepharose beads. After incubation, the supernatant (S) was discarded and the beads were washed four times (W). By addition of Laemmli buffer, the GST-fusions and the interacting proteins of the crude cell extract were solubilised (PD). Samples were loaded on SDS-PAGE and immunoblotted. The resulting immunoblots incubated with GFP antibody showed a clear signal for GFP-Atg8/-FG in lysate (L= 2.5% input) and supernatant (S), but not in a sample taken from the last washing step (W). Furthermore, a clear signal for GFP-Atg8/-FG could be detected in the pull down samples (PD) of each GST-Shp1 construct, but not in the negative control using only GST (Figure 28 (B) and (C)).

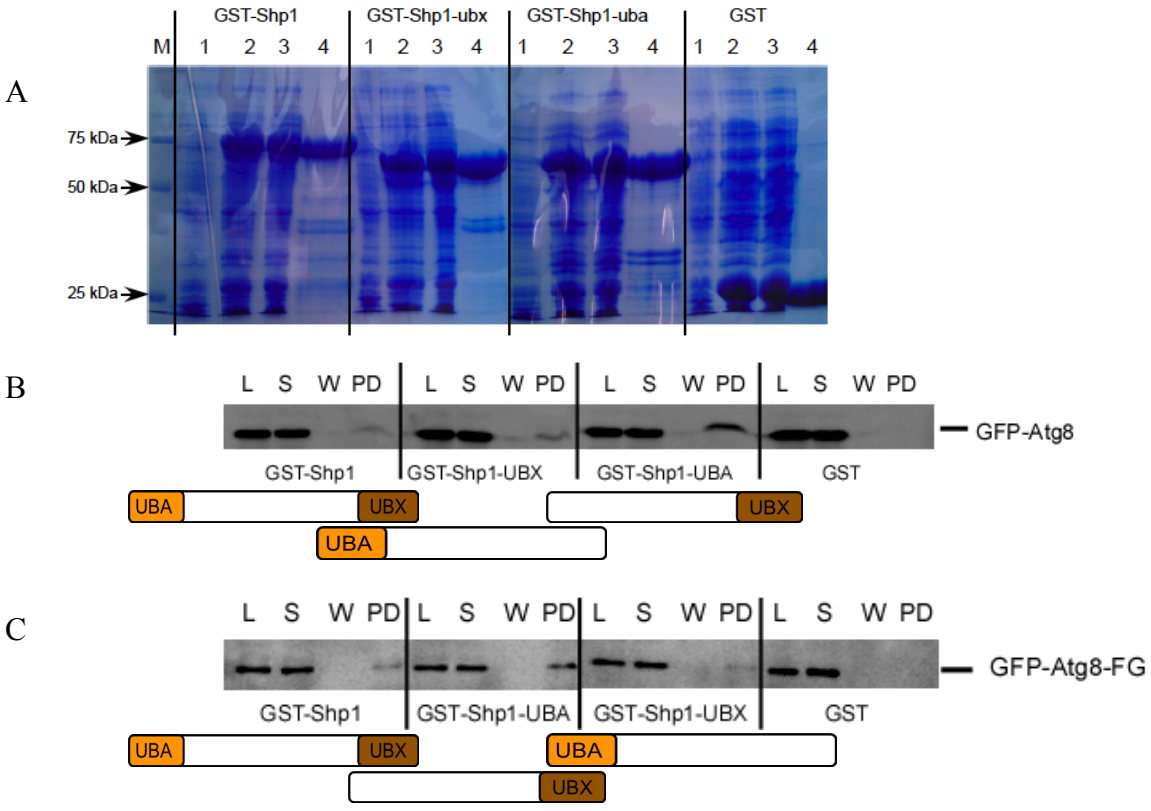

Figure 28: Pull down experiments with recombinant GST-Shp1

(A) Purification of GST-Shp1 constructs and coupling to Sepharose beads was monitored by SDS-PAGE: Precision Plus Protein All Blue Standard (M); BL21 RIPL ahead of IPTG addtition (1); BL21 RIPL suspension used for cell disruption by French Press (2); extract after cell disruption (3) and fraction of GST-linked sepharose beads (4).

(B) (C) 2.5 % of the crude cell lysate was loaded (L), the GST fusion proteins were incubated with lysates from WCG *pep4*Δ cells expressing GFP-Atg8 (A) or WCG *atg4*Δ *atg8*Δ cells expressing GFP-Atg8-FG (B), supernatant (S), wash (W) and pull down (PD) were used for immuno-blotting. Monoclonal mouse anti-GFP antibody was used for detection.

4.4 Mitophagy in *S. cerevisiae*

Mitochondria play a significant role in a lot of important metabolic processes, ranging from energy production to cell death. As a consequence, they are at the same time the major source of cellular reactive oxygen species (ROS), which cause oxidative damage to, for instance, mitochondrial DNA. Therefore a quality control of mitochondria is very important to maintain cellular homeostasis (Nieminen, 2003; Keeble and Gilmore, 2007). In addition to the oxidant defence system (Jamieson, 1998), the selective degradation of mitochondria via autophagy termed mitophagy might fulfil this indispensable role.
In this study, methods for the induction and detection of mitophagy should be established.

4.4.1 Chromosomal integration of Om45-GFP

To enable the detection of mitophagy with plasmid-encoded marker proteins, similar to the marker proteins GFP-Atg8 or Pgk1-GFP for the detection of unselective autophagy, Om45-GFP and Idh1-GFP were constructed (see 3.3.15).
The use of these plasmids for degradation assays did not result in autophagic degradation depended on Atg1 and Pep4 (data not shown), therefore GFP was chromosomally integrated at the Om45 locus via homologous recombination in some strains of interest, as described (Kanki, 2009a) (see 3.3.13). These strains were used for degradation assays (see 3.4.5.3). The cells were grown up to 3 days in YPL medium, containing lactate as sole carbon source, samples were taken at 24, 48 and 72 hours, alkaline lysed and immunoblotted.
Wild type cells expressing Om45-GFP showed a weak GFP signal after 48 hours growth in YPL, which increased after 72 hours. In contrast, the negative controls *atg1*Δ and *pep4*Δ showed no free GFP, due to their defects in autophagic degradation or vacuolar breakdown, respectively.

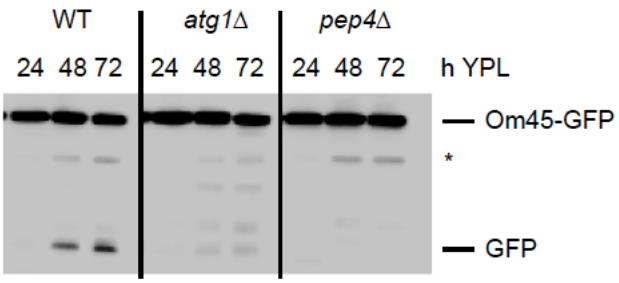

Figure 29: Monitoring mitophagy by western blot using Om45-GFP
Wild type (WT), *atg1*Δ and *pep4*Δ cells chromosomally expressing the mitochondrial Om45-GFP were grown up to 3 days in YPL medium. Samples were taken at 24, 48 and 72 hours, alkaline lysed and immunoblotted. Using monoclonal mouse anti-GFP antibody Om45-GFP (~70 kDa) and GFP (~26 kDa) were detected. *unspecific crossreaction

4.4.2 The pre-autophagosomal structure localises to mitochondria

Up to now, it is still unclear if the mitochondrial cargo is transported to the PAS or if the PAS assembles at the mitochondria.

Wild type and *atg1*Δ cells chromosomally expressing Om45-GFP were used for fluorescence microscopy. The cells, additionally expressing the PAS marker RFP-Atg8, were observed in a DeltaVision microscope after starvation of 5 hours in SD-N medium.

Both strains, wild type and *atg1*Δ, showed clear red punctate structures, representing the PAS, in close proximity to mitochondria, indicating the specific recruitment of the autophagic machinery for initiation of mitophagy.

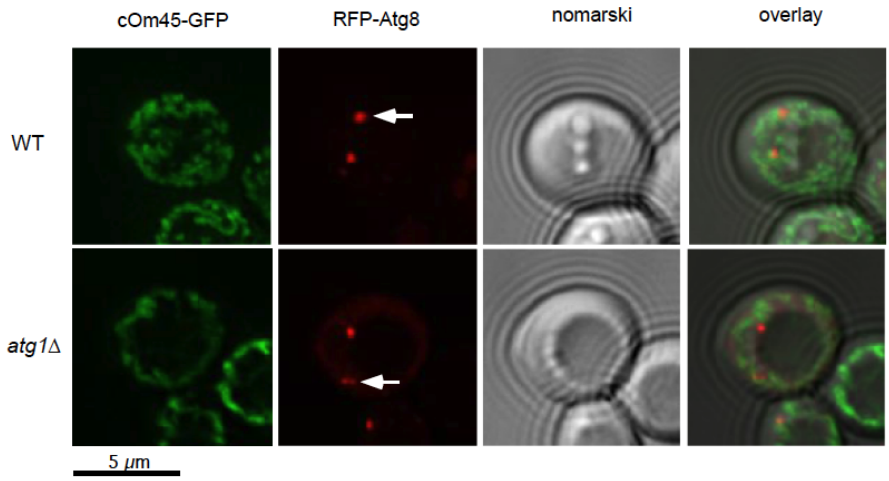

Figure 30: Localisation of the PAS at mitochondria
Wild type (WT) and *atg1*Δ cells (WCG) chromosomally expressing Om45-GFP and RFP-Atg8 from plasmid were cultured in CM -ura + 2 % lactate for 3 days and visualised by fluorescence microscopy using a DeltaVision microscope equipped with FITC and TRITC filters. The white arrow indicates a PAS-like structure distant from the vacuole.

4.4.3 Construction of mito-GFP

Chromosomal tagging of Om45 is laborious (Kanki, 2009a), therefore a plasmid based assay should be established. Su9-mt-DHFR was inserted into the vector pUG35 containing a GFP sequence under control of the MET25 promoter (mito-GFP) (see 3.2.10.2).

The mito-GFP plasmid was transformed in WCG wild type cells. These cells were grown to log phase in CM –ura –met + 2 % lactate and visualised using a DeltaVision microscope equipped with a FITC filter. Under these conditions mito-GFP showed green tubular structures representing mitochondria (Figure 31 (A)).

Furthermore wild type, *atg1*Δ and *pep4*Δ cells transformed with mito-GFP were grown up to 3 days in CM –ura –met + 2% lactate medium, samples were taken at 24, 48 and 72 hours, alkaline lysed and immunoblotted.

After 48 h of growth, wild type cells showed a clear signal for free GFP, increasing after 72 hours of growth. In contrast, the negative controls *atg1*Δ and *pep4*Δ showed no signal (Figure 31 (B)).

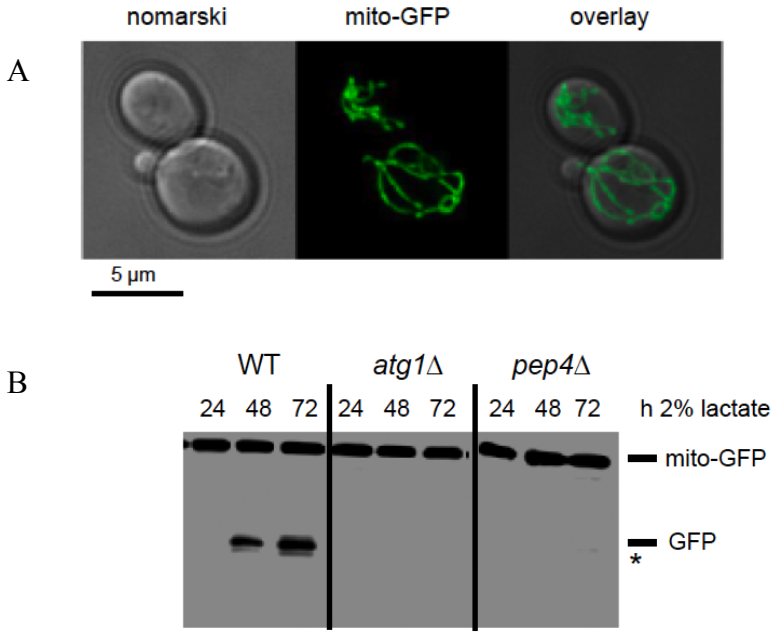

Figure 31: Fluorescence microscopy and western blot analysis of cells expressing mito-GFP

(A) Wild type (WCG) cells expressing mito-GFP were grown over night in CM-ura-met + 2 % lactate and GFP was visualised by fluorescence microscopy using a DeltaVision microscope equipped with a FITC filter.

(B) Wild type (WT), *atg1*Δ and *pep4*Δ cells expressing mito-GFP were grown up to 3 days in CM-ura-met + 2% lactate medium. Samples were taken 24, 48 and 72 hours, alkaline lysed and immunoblotted. Using monoclonal mouse anti-GFP antibody mito-GFP (~48 kDa) and GFP (~26 kDa) were detected. *unspecific crossreaction

4.4.4 Different methods to induce mitophagy

Kanki *et al.* (2009a) described two different conditions to induce mitophagy in *S. cerevisiae* cells grown on non-fermentable carbon source. One method is the induction by amino acid starvation, which means the shift of the cells grown to mid log phase from a nonfermentable carbon source to nitrogen starvation medium containing glucose. The other method is the above used induction at post-log phase, meaning a prolonged incubation for up to 3 days in lactate as sole carbon source. In recent publications these two conditions have led to some discrepancies concerning the requirement of different proteins for mitophagy (Kanki, 2009b; Okamoto, 2009). Aim of this study was the confirmation and establishment of different conditions to reliably induce mitophagy and to analyse the requirement of individual Atg-proteins.

As control for variations in the general autophagic machinery caused by e.g. growth conditions, cells expressing Pgk1-GFP were included for visualisation of unselective autophagy (Welter, 2010). To ensure an adequate separation of the GFP signal and crossreactions, 10 % SDS gels containing 6 M urea were used for all experiments using mito-GFP. Post-log phase induced mitophagy by cultivation of the strains up to 3 days in lactate medium led to a clear signal of free GFP in wild type cells for both mitophagy (Figure 32 (A)) and unselective autophagy (Figure 32 (B)). No signal was observed in *atg18*Δ cells, used as negative control. *ATG13* deleted cells showed a block for unselective autophagy but a residual activity for mitophagy was be detected. The autophagic core protein Atg13, whose interaction with Atg1 is required for autophagy (Kamada, 2000), has already been discussed to be not essential for mitophagy (Okamoto, 2009). In agreement with literature, cells depleted in the mitophagy-specific receptor protein Atg32 showed no mitophagy, but significant unselective autophagy.

Another common method to induce autophagic processes, is the addition of rapamycin, the inhibitor of the TOR (target of rapamycin) kinase (Noda and Ohsumi, 1998). Mitophagy also depends on the autophagic core machinery including the TOR kinase (Kanki, 2009b; Okamoto, 2009). Hence, cells expressing mito-GFP or Pgk1-GFP were grown to mid log phase and treated with 0.2 µg/ml rapamycin. Samples were taken at 0, 2, 4 and 6 hours and treated as previously described. This method led to a clear signal for free GFP in wild type cells for both mitophagy (Figure 33 (A)) and unselective autophagy (Figure 33 (B)), but not in *atg18*Δ cells. *ATG13* deleted cells showed a block for unselective autophagy but a weak activity for mitophagy could be detected. The additional control *atg32*Δ showed no signal for mitophagy, in contrast to almost normal unselective autophagy.

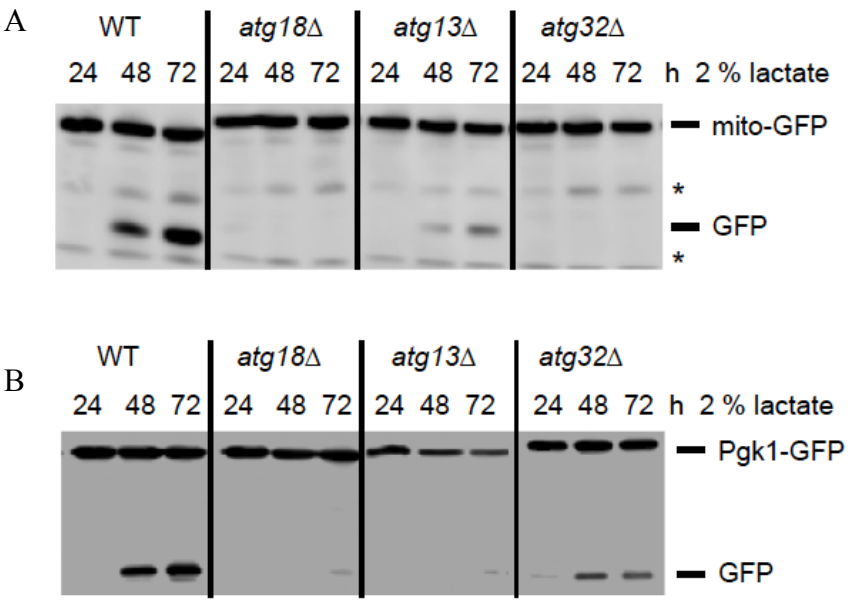

Figure 32: Incubation for 3 days in lactate medium induces mitophagy

Monitoring mitophagy (A) and unselective autophagy (B) by western blot using cells (BY4742) expressing mito-GFP or Pgk1-GFP. Wild type (WT), *atg18*Δ, *atg13*Δ and *atg32*Δ cells were grown up to 3 days in CM –ura –met + 2% lactate. Samples were taken at 24, 48 and 72 hours, alkaline lysed and immunoblotted. Using a monoclonal mouse anti-GFP antibody, mito-GFP (~48 kDa), Pgk1-GFP (~71 kDa) and free GFP (~26 kDa) were detected. (A) 10 % SDS gels containing 6 M urea were used. *unspecific crossreaction

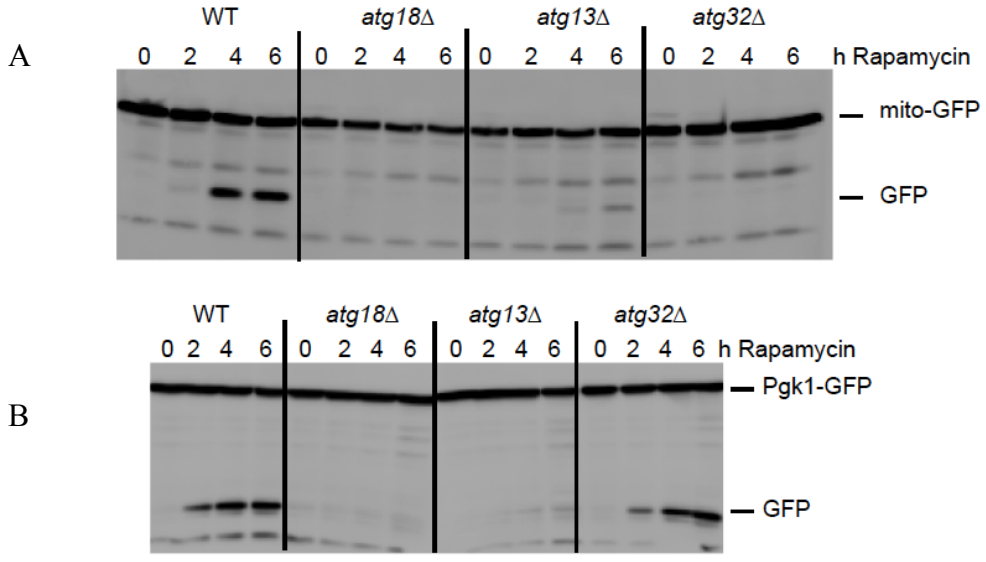

Figure 33: Rapamycin induces mitophagy

Monitoring mitophagy (A) and unselective autophagy (B) by western blot using cells (BY4742) expressing mito-GFP or Pgk1-GFP. Wild type (WT), *atg18*Δ, *atg13*Δ and *atg32*Δ were grown in lactate medium lacking methionine to mid-log growth phase and 0.2 µg/ml rapamycin was added. Sample were taken at 0, 2, 4 and 6 hours, alkaline lysed and immunoblotted. Using a monoclonal mouse anti-GFP antibody, mito-GFP (~48 kDa), Pgk1-GFP (~71 kDa) and free GFP (~26 kDa) were detected. (A) 10 % SDS gels containing 6 M urea were used. *unspecific crossreaction

So far, using the described methods, superfluous mitochondria presented the cargo for mitophagy, but also damaged mitochondria might be a specific cargo for mitophagic degradation.

One of the major sources of reactive oxygen species (ROS) is hydrogen peroxide (H_2O_2). Several studies demonstrated different roles for H_2O_2 in many biological processes, such as apoptosis and also autophagy (Kiffin, 2006; Chen, 2009). H_2O_2 is a product of incomplete one-electron reduction of oxygen, resulting in O_2^- which is converted to H_2O_2 by the superoxide dismutase (SOD) and furthermore altered by catalases to H_2O (Chen, 2009).

In this thesis, H_2O_2 was tested as external stress factor and potential inducer of mitophagy by disturbing the intracellular conditions concerning the ROS balance.

Different concentrations of H_2O_2 were tested in wild type and *atg18*Δ cells expressing mito-GFP (Figure 34 (A)). In parallel the survival rate was analysed, to avoid effects from dead cells (Figure34 (B)). As 0.05 mM H_2O_2 led to a measurable signal of free GFP in wild type cells but not in *atg18*Δ after 3 hours of treatment and a cell survival rate of 89 %, decreasing by the addition of 0.1 mM H_2O_2 to 83 %, this concentration was used for further experiments.

0.05 mM H_2O_2 was added to cells grown to mid log phase, samples were taken at defined time points (0, 2, 4 and 6 h) and treated as previously described. Figure 34 shows that treatment with H_2O_2 led to a clear signal for free GFP in wild type cells for both mitophagy (C) and unselective autophagy (D). *ATG13* deleted cells showed a block for unselective autophagy but again a weak mitophagy activity was detected. The additional control *atg32*Δ showed no signal for mitophagy, in contrast to almost normal unselective autophagy.

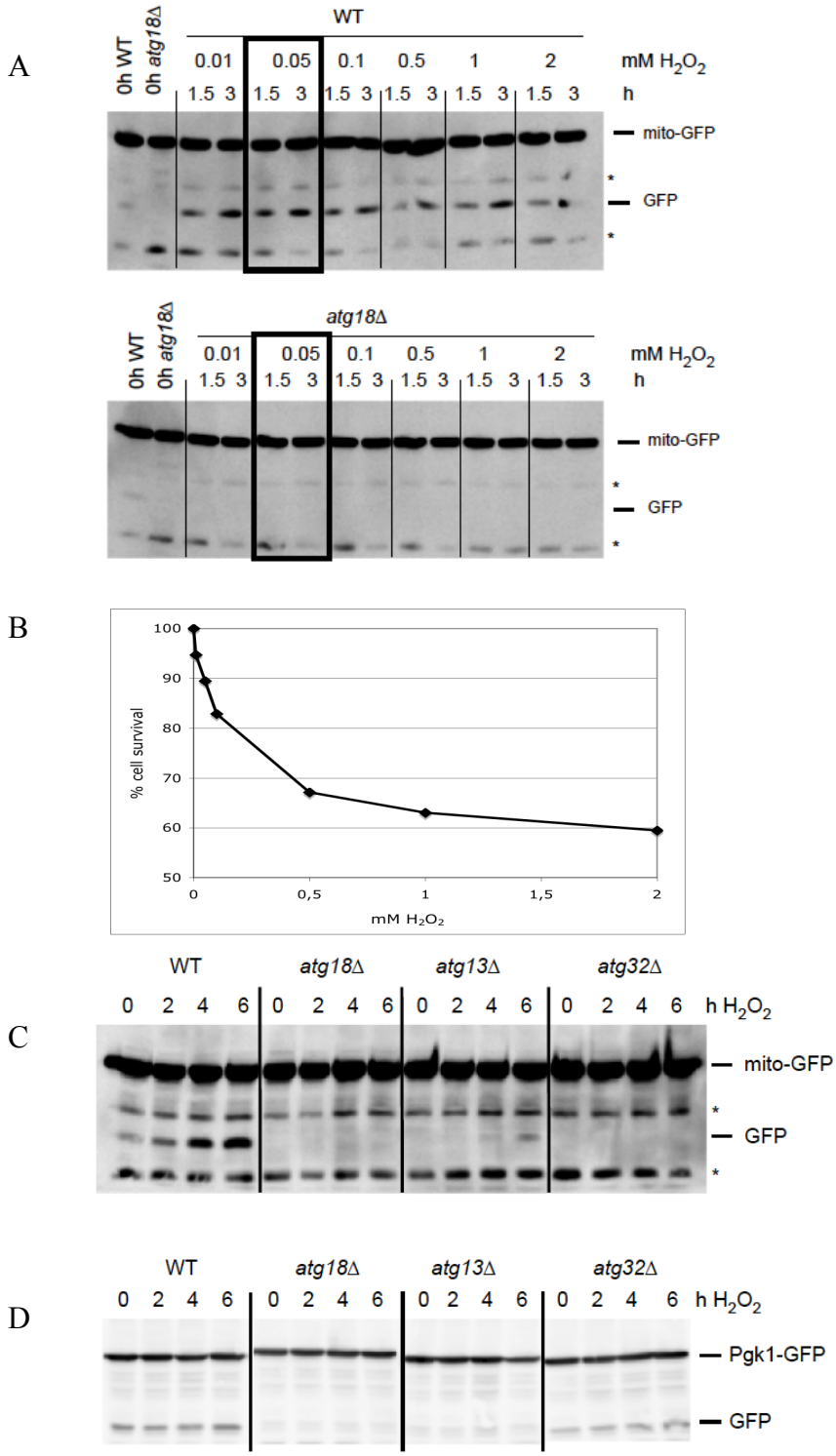

Figure 34: Mitophagy is induced by oxidative stress (H_2O_2)

(A) Different concentrations of H_2O_2 were tested in wild type and *atg18*Δ cells (BY4742) expressing mito-GFP. (B) In parallel the survival rate was analysed, to exclude excessive cell death.
(C) and (D) Monitoring mitophagy (C) and unselective autophagy (D) by western blot using cells (BY4742) expressing mito-GFP or Pgk1-GFP. Wild type (WT), *atg18*Δ, *atg13*Δ and *atg32*Δ were grown in lactate medium lacking methionine to mid-log growth phase and 0.05 mM H_2O_2 was added. Samples were taken at 0, 2, 4 and 6 hours, alkaline lysed and immunoblotted. Using a monoclonal mouse anti-GFP antibody, mito-GFP (~48 kDa), Pgk1-GFP (~71 kDa) and free GFP (~26 kDa) were detected. (A) and (C) 10 % SDS gels containing 6 M urea were used. *unspecific crossreaction

Another compound causing oxidative stress is N, N'-dimethyl-4,4'-bipyridinium dichloride (paraquat). It catalyses the formation of ROS by the acceptance of electrons from an electron donor (e.g. NADPH) and the further oxidation of an electron receptor such as dioxygen. Paraquat therefore mainly produces superoxide anions (O_2^-) and H_2O_2, yielding in the impairment of the mitochondrial function.

To test if paraquat induces mitophagy, wild type and *atg18*Δ cells expressing mito-GFP were treated with different concentrations of paraquat up to 6 hours (Figure 35 (A)). In parallel the survival rate was analysed, to exclude excessive cell death (Figure 35 (B)). As 2 mM paraquat led to a measurable signal for free GFP in western blot experiments and a cell survival rate of 84 %, decreasing by the addition of 5 mM paraquat to 81 %, this concentration was used for further experiments.

Wild type, *atg18*Δ, *atg13*Δ and *atg32*Δ cells were grown to mid log phase and treated with 2 mM paraquat. Samples were taken at 0, 2, 4 and 6 hours and treated as described previously. Figure 35 demonstrates that the addition of paraquat led to a clear signal for free GFP in wild type cells using mito-GFP (C). A very weak signal could be detected for unselective autophagy (D). *ATG13* deleted cells showed a block for unselective autophagy, but as above a very weak residual mitophagy activity was detected. The additional control *atg32*Δ showed no mitophagy but some unselective autophagy.

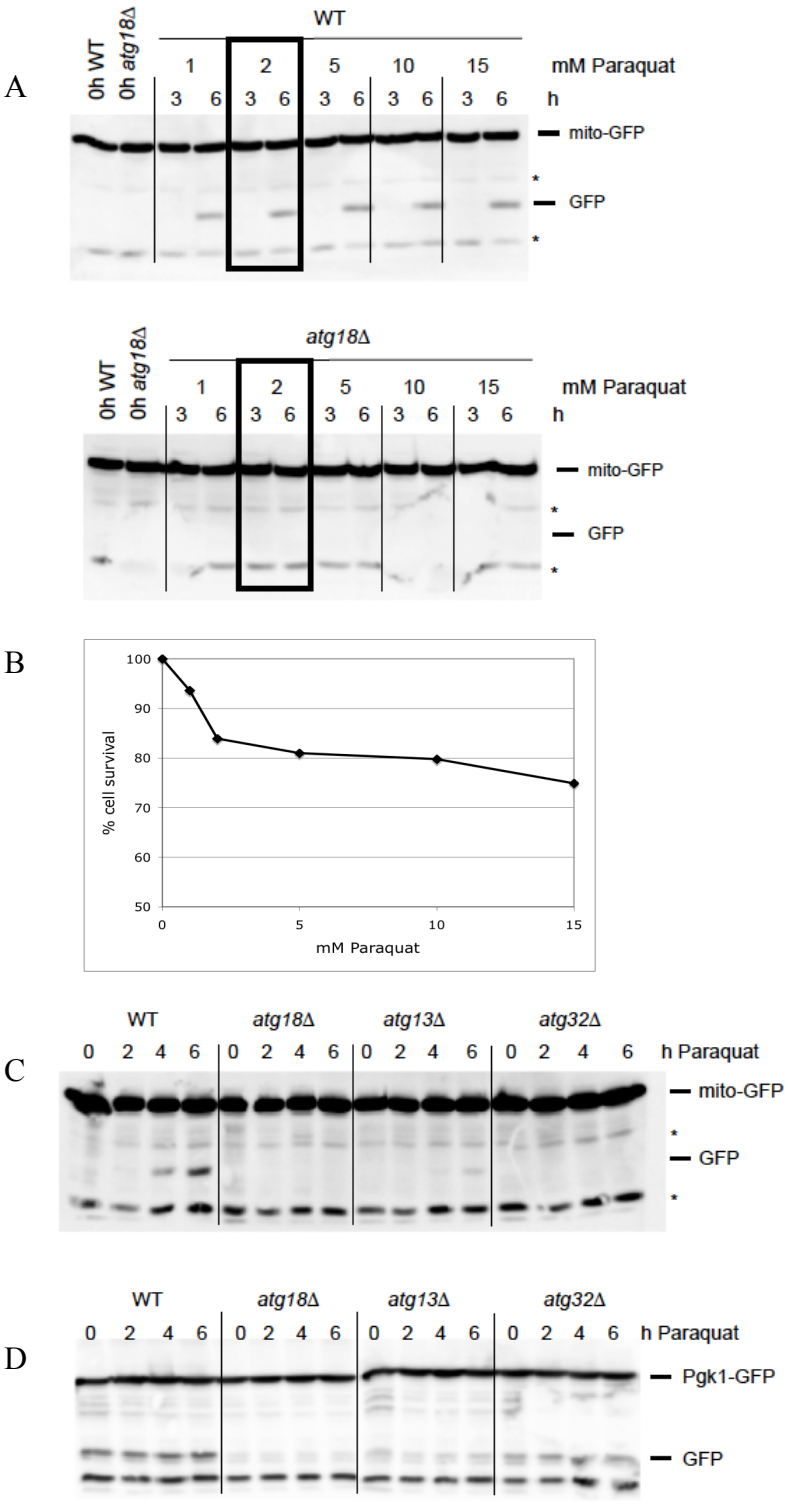

Figure 35: Paraquat induces mitophagy

(A) Different concentrations of paraquat were tested in wild type and *atg18*Δ cells (BY4742) expressing mito-GFP. (B) In parallel the survival rate was analysed, to exclude excessive cell death.
(C) and (D) Monitoring mitophagy (A) and unselective autophagy (B) by western blot using cells (BY4742) expressing mito-GFP or Pgk1-GFP. Wild type (WT), *atg18*Δ, *atg13*Δ and *atg32*Δ were cultured in lactate medium lacking methionine to mid-log growth phase and 2 mM paraquat was added. Samples were taken at 0, 2, 4 and 6 hours, alkaline lysed and immunoblotted. Using a monoclonal mouse anti-GFP antibody, mito-GFP (~48 kDa), Pgk1-GFP (~71 kDa) and free GFP (~26 kDa) were detected. (A) and (C) 10 % SDS gels containing 6 M urea were used. *unspecific crossreaction

4.4.5 Mitophagy is increased in *yme1*Δ cells

Yme1 is a subunit of the mitochondrial inner membrane i-AAA protease complex. It is responsible for the degradation of unfolded or misfolded mitochondrial proteins and therefore involved in aging and apoptotic response (Leonhard, 1996; Palermo, 2007). The accumulation of dysfunctional mitochondria in *yme1*Δ cells might therefore induce mitophagy (Campbell and Thorsness, 1998). To test if the mitophagic rate is increased in *YME1* deleted cells, wild type, *atg1*Δ and *yme1*Δ of WCG background expressing mito-GFP were grown for up to 3 days in CM –ura –met medium containing 2% lactate. Samples were taken at 24, 48 and 72 hours, alkaline lysed and used for western blots. For evaluation of mitophagy, signal intensities of mito-GFP and free GFP were quantified. The ratio of free GFP to mito-GFP was calculated. The value of wild type cells after 72 hours of growth was set to 100 %. Three independent experiments were done and the resulting values were illustrated (Figure 36). Since *atg1*Δ cells are defective in both, unselective and selective autophagy, no signal was detected in this negative control. In contrast, *yme1*Δ cells showed an increased rate of mitophagy of about 57 % after 24 hours, 113 % after 48 hours and 122 % after 72 hours of growth compared to wild type cells. After 24 hours under non starvation conditions, the mitophagy rate is already increased by 3.5 times in *yme1*Δ cells compared to wild type cells (14 %), indicating the degradation of damaged and not superfluous mitochondria.

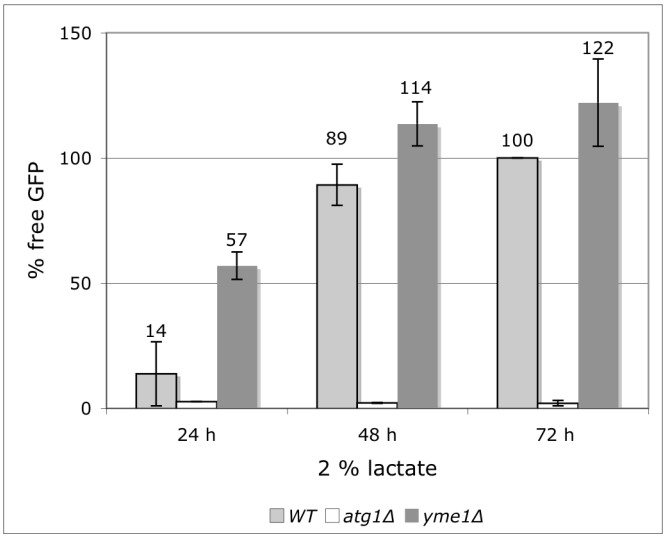

Figure 36: Quantification of mitophagy in *yme1*Δ

Wild type (WT), *atg1*Δ and *yme1*Δ (WCG background) were grown in CM –ura –met + 2 % lactate for 72 hours. Samples were taken at 24, 48 and 72 hours, alkaline lysed and immunoblotted. Using a monoclonal mouse anti-GFP antibody, mito-GFP (~48 kDa) and free GFP (~26 kDa) were detected and quantified with AIDA software. The ratio of free GFP to mito-GFP was calculated and the value of wild type cells after 72 hours of growth was set to 100 % (n = 3).

4.4.6 Part of the ESCRT machinery is required for mitophagy

As the involvement of the ESCRT machinery in PMN is discussed (Bremer, 2009), exemplary members (Table 19) were examined for their involvement in mitophagy compared to unselective autophagy in this study. Different strains, lacking one ESCRT protein and additional control strains were transformed with mito-GFP and used in the mitophagy assay, parallel to control analysis with Pgk1-GFP.

Figure 37 shows the resulting western blots. In v*ps27*Δ (ESCRT-0) and also *vps23*Δ cells (ESCRT-I) a high signal intensity of free GFP for mitophagy and for unselective autophagy similar to wild type cells was seen. The negative control *atg1*Δ exhibited no signal (Figure 37(A)). In contrast, *vps28*Δ cells showed a clear reduction in free GFP for mitophagy but not for unselective autophagy (Figure 37 (B)). Therefore further ESCRT members were tested. Compared to wild type cells, *vps24*Δ (ESCRT-III), *vps25*Δ (ESCRT-II) and *vps32*Δ (ESCRT-III) showed a clear signal reduction of free GFP for mitophagy but not of unselective autophagy. In a*tg18*Δ cells a complete block for both pathways was seen (Figure 37 (C)). Up to four independent experiments were made. The western blots were quantified using AIDA software. The calculated signal intensity of free GFP in ratio to mito-GFP or Pgk1-GFP in wild type cells after 3 days of growth was set to 100 %. Figure 37 (D) summarises the role of some ESCRT subunits in mitophagy. The quantification supports the findings that the deletion of *VPS23* and *VPS27* does not affect mitophagy. In contrast, the deletion of *VPS24*, *VPS25*, *VPS28* and *VPS32* seemed to impair mitophagy. Table 19 summarises the tested ESCRT deletion strains and their requirement for unselective autophagy or mitophagy and highlights the involvement of the ESCRT subunits II and III in mitophagy, while the ESCRT subunits 0 and I are not involved.

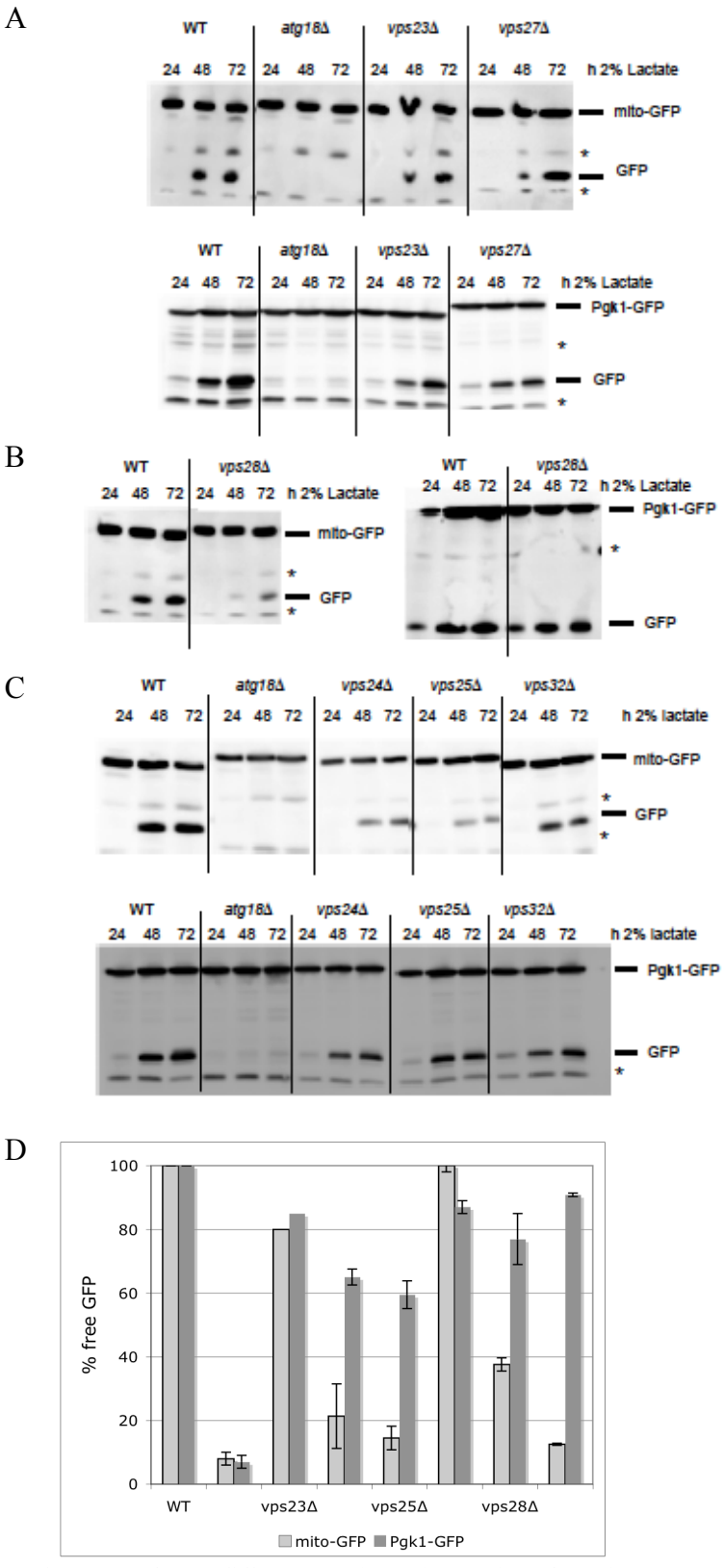

Figure 37: Part of the ESCRT machinery is required for mitophagy

(A-C) Wild type cells, *atg18*Δ and different strains deleted in one member of the ESCRT machinery (BY4742) expressing mito-GFP or Pgk1-GFP were grown up to 3 days in CM –ura –met + 2 % lactate, samples were taken at 24, 48 and 72 hours, alkaline lysed and immunoblotted. Using a monoclonal mouse anti-GFP antibody, mito-GFP (~48 kDa), Pgk1-GFP (~71 kDa) and free GFP (~26 kDa) were detected. 10 % SDS gels containing 6 M urea were used. *unspecific crossreaction

(D) The western blots were quantified using AIDA software. The calculated signal intensity of free GFP in ratio to mito-GFP or Pgk1-GFP in wild type cells after 3 days of growth was set to 100 % ($1 \leq n \geq 4$).

Table 19: Summary of tested ESCRT mutants

All tested ESCRT deletion mutants are listed including quantification values of unselective autophagy and mitophagy

strain		unselective autophagy	mitophagy
*atg18*Δ		**7 %**	**8 %**
*vps23*Δ	ESCRT-I	**85 %**	**80 %**
*vps24*Δ	ESCRT-III	**65 %**	**21 %**
*vps25*Δ	ESCRT-II	**60 %**	**15 %**
*vps27*Δ	ESCRT-O	**87 %**	**100 %**
*vps28*Δ	ESCRT-I	**77 %**	**38 %**
*vps32*Δ	ESCRT-III	**91 %**	**13 %**

4.4.7 Doa4 is involved in mitophagy but not in unselective autophagy

Doa4, an ubiquitin isopeptidase, is required for recycling of ubiquitin from proteasome-bound polyubiquitinated proteins. The deletion of *Doa4* depletes the cellular ubiquitin level (Swaminathan, 1999; Ren, 2008). In mammalian cells, ubiquitin plays an irreplaceable role in designating mitochondria for mitophagy (Matsuda, 2010). Probably, a decrease of the cellular ubiquitin level also affects mitophagy in *S. cerevisiae*. Therefore a role of Doa4 in mitophagy was tested. In addition to the control cells wild type, *atg18*Δ and *atg32*Δ, *doa4*Δ cells were transformed with mito-GFP and used for the mitophagy assay, parallel to the same strains expressing Pgk1-GFP. Figure 38 (A) shows a clear reduction of the signal for free GFP for mitophagy in *doa4*Δ cells compared to wild type cells.

Quantification was done by AIDA software and the calculated signal intensity of free GFP in ratio to mito-GFP or Pgk1-GFP in wild type cells after 3 days of growth was set to 100 % (Figure 38 (B)). The two negative controls *atg18*Δ, blocked in all autophagic pathways, and *atg32*Δ, selectively blocked for mitophagy (Kanki and Klionsky, 2009; Okamoto, 2009), showed no free GFP signal for mitophagy. In d*oa4*Δ cells the signal of free GFP appeared strongly reduced for mitophagy. Unselective autophagy was only reduced in *doa4*Δ cells. Wild type and *atg32*Δ cells showed normal autophagy rates. Six independent experiments were done. The quantification of these western blots, which was done for exact evaluation of the signal for free GFP (Figure 38 (B)), confirmed the slight reduction of the GFP-signal for unselective autophagy in *doa4*Δ cells (65 %; SEM = 11) compared to wild type cells and the more significant reduction for mitophagy (37 %; SEM = 11).

A

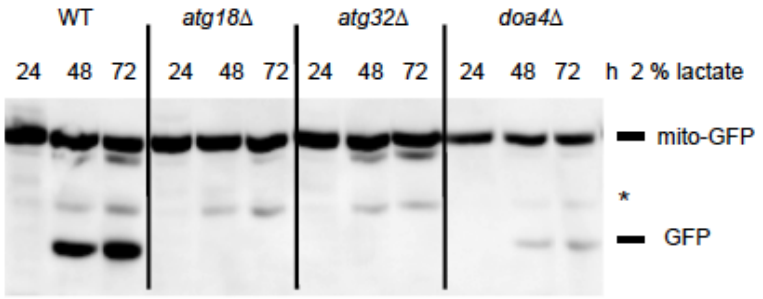

B

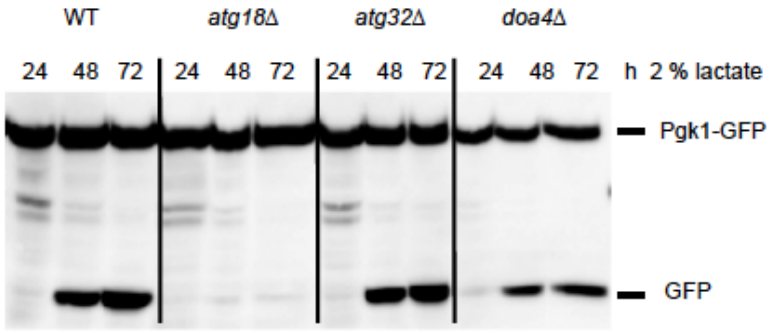

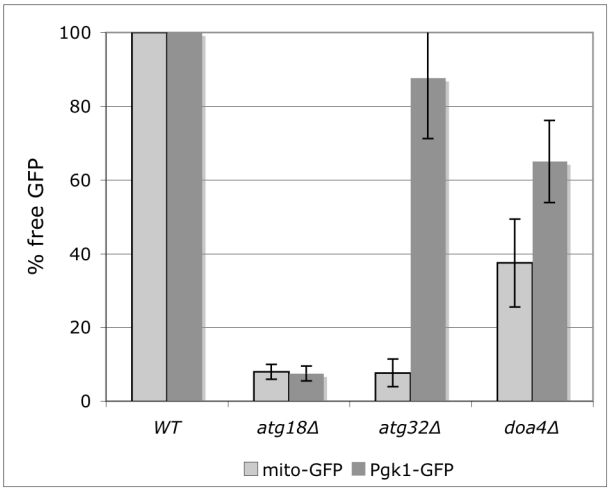

Figure 38: Doa4 is needed for mitophagy

(A) Monitoring mitophagy and unselective autophagy by western blot using cells expressing mito-GFP or Pgk1-GFP. Wild type (WT), *atg18*Δ, *atg32*Δ and *doa4*Δ cells were grown for 3 days in CM –ura –met + 2 % lactate. Samples were taken at 24, 48 and 72 hours, alkaline lysed and immunoblotted. Using a monoclonal mouse anti-GFP antibody, mito-GFP (~48 kDa), Pgk1-GFP (~71 kDa) and free GFP (~26 kDa) were detected. 10 % SDS gels containing 6 M urea were used. *unspecific crossreaction (B) GFP signals were quantified using AIDA software and the ratio of free GFP to mito-GFP or Pgk1-GFP in wild type cells after 3 days of growth was set to 100 % (n = 6).

4.5 Piecemeal microautophagy of the nucleus

Piecemeal microautophagy of the nucleus PMN is the selective microautophagic degradation of parts of the nucleus, which requires a subset of autophagic proteins (Roberts, 2003; Krick, 2008b).

Osh1, a member of the OSH family in yeast and a homologue of mammalian oxysterol-binding protein (OSBP) (Levine and Munro, 2001), may function in nonvesicular lipid trafficking. Osh1 is targeted to nucleus-vacuole (NV) junctions through physical interaction with Nvj1. Due to the interaction with NV junctions, Osh1 exhibits a substrate for PMN and is therefore a commonly used marker protein (Millen, 2009).

Besides the PMN dependent degradation of proteins involved in the formation of NV junctions (Roberts, 2003; Kvam, 2005), at the current state of research, a specific nuclear cargo for PMN is still unknown and is a major focus of investigation.

4.5.1 Screen for selective PMN cargos

In this thesis, 79 strains expressing different GFP fusion proteins (Table 5; Invitrogen) were tested for their autophagic degradation by the detection of free GFP in western blot analysis (similar to 3.4.5). Aim of this experiment was to find a specific PMN cargo. The set of the chosen GFP fusion proteins mainly included proteins of the nucleus and the nucleolus and further included proteins of other organelles such as mitochondria and the ER as controls. Exemplary for all strains used in this experiments, nucleolar located proteins are shown (Figure 39).

All strains were starved in SD-N up to 6 hours and samples were taken at 0 and 6 hours. The cells were alkaline lysed and used for western blot analysis. Chromosomally expressed Pgk1-GFP was used as control for the induction of unselective autophagy and showed normal amounts of free GFP. Surprisingly, no degradation of any of the nucleolar proteins was detected.

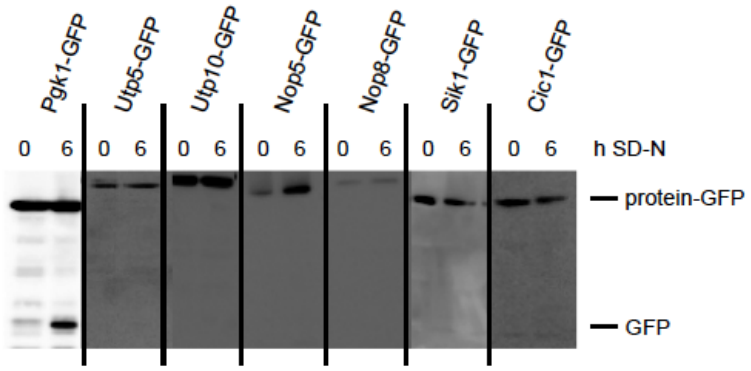

Figure 39: Western Blot analysis for the identification of specific PMN cargos

Different strains expressing nucleolus-located proteins with a GFP-tag and a strain chromosomally expressing Pgk1-GFP were starved for 6 hours. Samples were taken after 0 and 6 h, alkaline lysed and immunoblotted. Using a monoclonal mouse anti-GFP antibody, GFP signals (Pgk1-GFP (~71 kDa), Utp5-GFP (~98 kDa), Utp10-GFP (~226 kDa), Nop5-GFP (~82 kDa), Nop8-GFP (~82 kDa), Sik1-GFP (~83 kDa), Cic1-GFP (~69 kDa) and free GFP (~26 kDa)) were detected.

4.5.2 Microscopic analysis of nucleolar GFP fusion proteins

Different GFP-tagged nucleolus proteins (Invitrogen) were used for microscopic analysis. The cells were incubated with FM4-64 for staining of the vacuolar membrane (see 3.2.10.2.2), starved in SD-N medium containing 1 mM PMSF up to 4 hours and visualised using a DeltaVision microscope (FITC, TRITC) (Figure 40).

In contrast to Utp5-GFP and Utp10-GFP, which showed no green signal outside of the nucleolus, additional GFP signals inside the vacuole were detected in Nop8-GFP cells. Sik1-GFP expressing cells presented a conspicuous contact of Sik1-GFP to the vacuolar membrane, while in Cic1-GFP expressing cells, some small green fluorescent vesicles released into the vacuole were observed (Figure 40).

Nog1, a nuclear GTP-binding protein, is tethered in a complex to the nucleolus upon nutrient starvation or rapamycin treatment (Honma, 2006). Therefore cells chromosomally expressing Nog1-GFP (Invitrogen) were also used for microscopy.

The cells were incubated with FM4-64 and starved for 4 hours in SD-N containing 1 mM PMSF. Using the DeltaVision microscope equipped with FITC and TRITC filter system, PMN structures in Nog1-GFP cells were monitored. PMN-like structures, formed like green noses, budding from the nucleolus into the vacuole were observed in about 30 % of the cells (Figure 41).

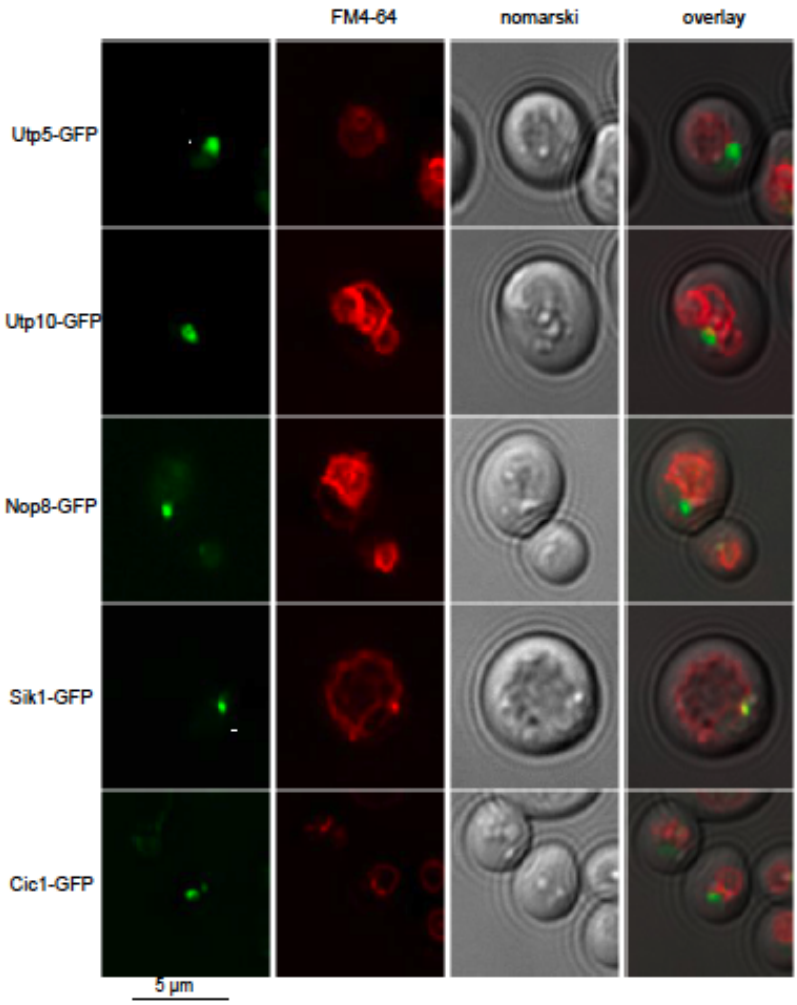

Figure 40: Microscopic analysis of strains expressing nucleolar GFP fusion proteins

Strains chromosomally expressing different nucleolar GFP fusion proteins (Invitrogen) were starved for 4 hours in SD-N medium containing 1 mM PMSF. The vacuoles were stained with FM4-64 (red).

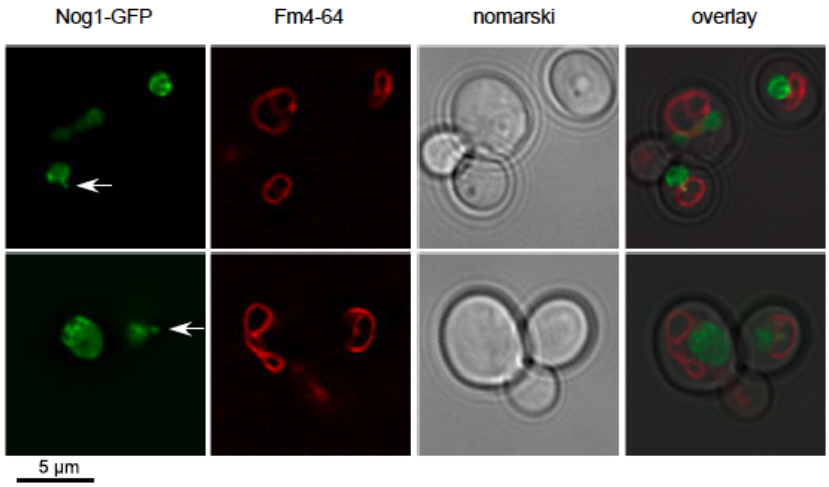

Figure 41: PMN structures in Nog1-GFP

Cells chromosomally expressing Nog1-GFP (Invitrogen) were starved for 4 hours in SD-N medium containing 1 mM PMSF. The vacuoles were stained with FM4-64 (red). Clear green PMN-like structures pinching off the vacuolar membrane are marked with a white arrow.

4.5.3 Nucleus-vacuole junctions localise at the nucleolus

Up on initiation of PMN, the cells form nucleus-vacuole junctions. These junctions can be visualised by GFP-tagged Osh1, which is targeted to NV junction through a physical interaction with Nvj1 (Kvam and Goldfarb, 2004). Sik1 (Nop56) is involved in rRNA processing and is located inside the nucleolus (Dragon, 2002; Bogomolnaya, 2004). Therefore cells chromosomally expressing Sik1-RFP were used for visualisation of the nucleolus in microscopy. To detect NV junctions and determine their localisation, these cells were transformed with Osh1-GFP.

The cells were starved for 4 hours in SD-N and visualised by using the DeltaVision microscope equipped with a FITC and TRITC filter system. Figure 42 (A) demonstrates the localisation of the NV junctions at the nucleolar part of the nucleus in wild type and *atg1*Δ cells. In the negative control *vac8*Δ, no NV junctions were observed.

Counting more than 350 wild type cells in 5 independent experiments allowed a statistic evaluation. 70.6 % (SEM = 0.6 %) of NV junctions localised at the nucleolar part of the nucleus (Figure 42 (B)). These results indicated a specific uptake of nucleolar material by PMN.

A

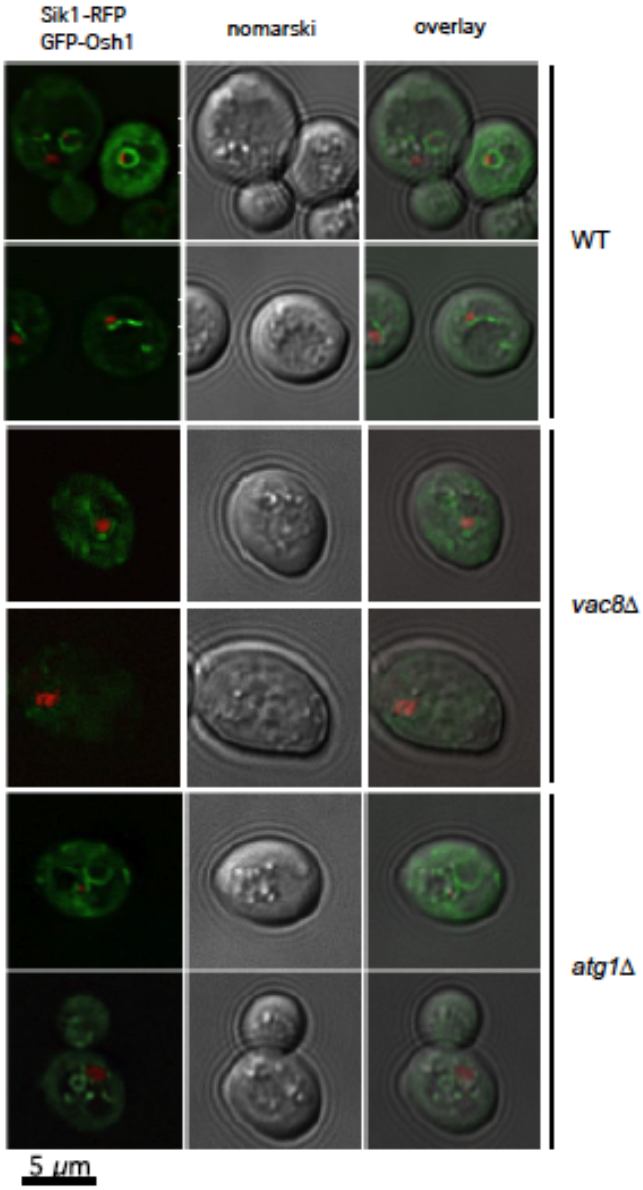

B

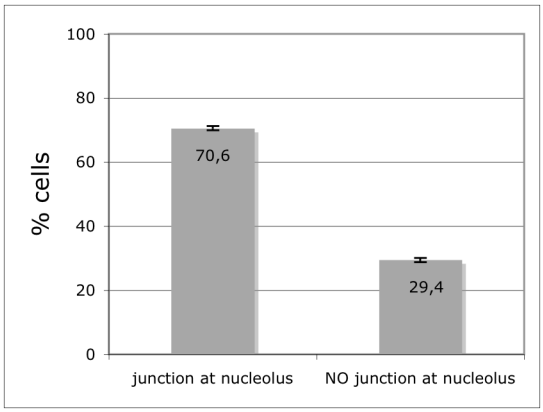

Figure 42: Nucleus-vacuole junctions localise adjacent the nucleolus

(A) Sik1-RFP cells containing Osh1-GFP were examined with the DeltaVision microscope (using FITC and TRITC filter). Wild type and *atg1*Δ cells chromosomally expressing Sik1-RFP showed clear green nucleus-vacuole junctions, while in *vac8*Δ these junctions are absent.

(B) NV junctions were counted in 350 wild type cells in 5 independent experiments. 70.6 % of NV junctions localised at the nucleolus (SEM = 0.6; n = 5).

4.5.4 The PAS localises at the nucleolar part of the nucleus

For the detection of the pre-autophagosomal structure (PAS), cells chromosomally expressing the nucleolar Sik1-RFP were transformed with GFP-Atg8. The cells were starved for 4 hours in SD-N medium. The visualisation of these cells using a DeltaVision microscope equipped with a FITC and TRITC filter system, presented a localisation of several PAS dots in close proximity to the nucleolus (Figure 43 (A)). Counting more than 100 cells in two independent experiments allowed a statistic evaluation resulting in 22.9 % (SEM = 7.5 %) cells exhibiting PAS dots in close proximity to the nucleolus (Figure 43 (B)).

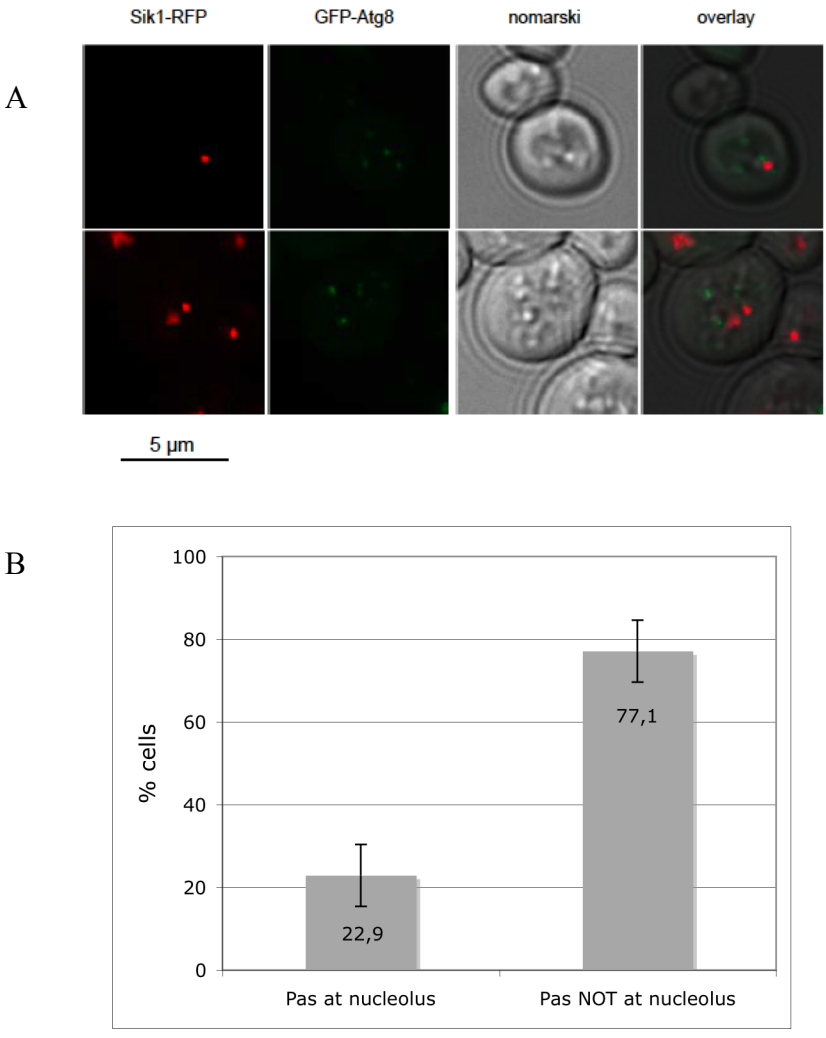

Figure 43: The pre-autophagosomal structure localises partially at the nucleolus

(A) Sik1-RFP (representing the nucleolus) cells expressing furthermore GFP-Atg8 (representing the PAS) were starved in SD-N for 5 hours and examined under the DeltaVision microscope (equipped with FITC and TRITC filter).

(B) More than 100 cells were monitored for occurrence of the PAS at the nucleolar part of the nucleus. 22.9 % of the PAS dots in close proximity to the nucleolus were observed (SEM = 7.5; n = 2).

5. Discussion

The yeast, *Saccharomyces cerevisiae,* provides many advantages as a model organism for scientific research, such include the fast growth combined with the easy cultivation and non-pathogenicity. Furthermore, yeast cells are easy to handle for transformation (see 3.3.2/3.3.3). A wide range of yeast vectors is commercially available (e.g. 2µ plasmids), which allow the expression of yeast and also foreign genes. *S. cerevisiae* provides the advantage of using homologues recombination for the precise deletion or modification of single genes (see 3.3.13/3.3.14). Standard methods for measuring gene expression, the identification of protein-protein interaction, as well as the analysis for functional relationships between different genes and/or their products (e.g. SGA methodology; see 3.2.11) allow the identification of cellular functions of single genes/proteins or their complexes. The resulting information can in most cases be transferred to higher eukaryotic cells, making *S. cerevisiae* a very useful model organism.

5.1 Synthetic Genetic Array (SGA)

The SGA methodology is a powerful high-throughput technique to explore synthetic lethality allowing the systematic production of double deletions by crossing the entire genome deletion library available for *S. cerevisiae* (DMA) with a deletion mutant of interest (query strain). When two genes show a synthetic lethal interaction, it often reflects that the gene products impinge on the same essential function (A. Tong and C. Boone (2007) not published, see: www.utoronto.ca/ boonelab/sga_technology).

To benefit from the optimised conditions for the SGA methodology (Tong, 2001; Tong and Boone, 2006), the strain Y8205 (Boone Lab; University of Toronto, Canada; www.utoronto.ca/boonelab) was used for the generation of the query strains in this thesis. Y8205 carries a range of different genetic advantages such as a STE3pr-LEU2 reporter, which is activated only in MATα cells. After mating of the query strain with Y8205, the kanamycin resistance cassette should be switched into a nourseothricin resistance to enable the use of the deletion library (KanMX6). As the method described in literature (Tong and Boone, 2006) resulted not in a successful switch, the NAT resistance cassette was amplified by PCR (using the plasmid pAG25 as template and corresponding primers) and inserted by homologues recombination. The comprised STE3pr-LEU2 reporter enabled the further selection for only haploid MATα meiotic progeny using medium lacking leucine.

This modified query deletion mutant was used for the presented screen with the entire deletion mutant library available for *S. cerevisiae* (Euroscarf). The different selection steps after mating and sporulation of each different deletion combination was simplified by further genetic attributes, resulting out of crossing with the Y8205 strain. The STE2pr-HIS3 reporter, mainly induced in Mat a cells (A. Tong and C. Boone (2007) not published, see: www.utoronto.ca/ boonelab/sga_technology), allowed the selection of haploid progeny of mating type a (Mat a) using medium lacking histidine. Furthermore, the deletion of *CAN1* and *LYP1* also ensured the selection for haploid cells of mating type a by the elimination of diploids (Mat a/α) and growth inhibition of false positive Mat a/a diploid mutants. *CAN1* encodes an arginine permease that allows canavanine, a toxic analogue for arginine, to enter and kill cells (Hoffmann, 1985). *LYP1* encodes a lysine permease that allows, similar to canavanine, thialysine (a toxic analogue for lysine) to enter the cells resulting in death of the cells (Sychrova and Chevallier, 1993). Diploid cells (mat a/α) still carry a wild-type copy of the *CAN1* and *LYP1* genes and are killed by the treatment with 100 µg/l canavanine and 100 µg/l thialysine. A possible mitotic recombination, resulting in a crossover event of the Mat locus and therefore in Mat a/a diploids, is also repressed under canavanine and thialysine treatment (Tong and Boone, 2006). The protocol recommended by Tong and Boone (2006) was furthermore modified in the step of sporulation, by omitting the proposed 200 µg/l G418, to reduce false positive kanamycin resistance mutants. Using these optimisation strategies, the potential of false negative SGA hits was drastically reduced. Nevertheless, the screen procedure containing at least 5 pinning steps, led to false positive synthetic lethal double deletions, mainly caused by problems with pinning of the spores on selection medium and sporulation defects in some deletion strains. 53 plates containing 384 colonies (2 x 192 different combinations) had to be analysed for positive double deletions, represented by synthetic lethality (Figure 15, Table 18, chapter 4.1). Double deletion strains of interest were furthermore examined by separate re-mating of the single deletion strains, followed by sporulation, separation of the tetrads and analysis of the growth phenotype.

In this study it was screened for synthetic lethality of a double deletion of *atg21*Δ $x_{(DMA)}$Δ. Atg21 and its homologues Atg18 and Ygr223c are phosphoinositide binding proteins that contain seven WD-40 repeats and are predicted to fold as seven bladed ß-propellers. WD-40 repeat proteins are thought to serve as stable platforms for protein-protein interaction, thereby mediating the assembly of multiprotein complexes. Atg18, Atg21 and Ygr223c are required for different subsets of autophagic processes. Atg21 is strictly required for the Cvt-pathway, efficient unselective autophagy and PMN (Barth, 2001; 2002; Krick, 2006; Krick,

2008a). Atg21 is further involved in lipidation and effective recruitment of Atg8 to the PAS during the Cvt pathway. Atg18 localises to the PAS and the vacuolar membrane. Its localisation requires Atg2 and PtdIns3P, synthesised by the Vps34 complex I, containing Atg14. A PAS localisation of Atg21 and Ygr223c is still under investigation. All three homologues are recruited to the endosomal compartment via PtdIns3P, generated by the Vps34 complex II, containing Vps38. Therefore an endosomal function of all three homologues distinct from autophagy has been suggested (Dove, 2004; Meiling-Wesse, 2004; Strømhaug, 2004; Krick, 2008a).

To get more hints for a potential role of Atg21 inn autophagy and its putative role in endocytosis, which might be shared with Atg18 and Ygr223c, the BY4741 *atg21*Δ strain was chosen as query strain in the SGA screen. The double deletions strains *atg21*Δ *vac1*Δ and *atg21*Δ *atg27*Δ resulted in a synthetic lethal phenotype. These double deletion strains of interest were further examined by separate remating of the single deletion strains, followed by sporulation, separation of the tetrads and evaluation of the growth phenotype. The generated *atg21*Δ::NatMX4 query strain was mated with *vac1*Δ cells and *atg27*Δ cells and selected for the haploid double deletion progeny by using the conditions of the original screen. To exclude the modifications needed for the SGA methodology and provide a further control, *atg21*Δ::KanMX6 cells and *atg27*Δ*::*HIS3 cells of the WCG background were used in addition to the BY4741 background used in the screen.

Vac1 is an effector of the Rab GTPase Vps21 at the endosome. It interacts with the GTP-bound Vps21 that functions in Golgi-to-endosome transport and with Vps45, bound on its t-SNARE Pep12, at the endosomal membrane. Therefore Vac1 might functionally couple Vps21 and Vps45 (Peterson, 1999). In *vps21*Δ and *vac1*Δ cells, GFP-Atg21 has been shown to be released from the endosomal compartment into the cytosol. The localisation of GFP-Atg18, GFP-Atg21 and GFP-Ygr223c at the endosome has been shown to require the Vps class D proteins Pep12, Vps45, Vps21 and Vac1. The synthetic lethality of the *atg21*Δ *vac1*Δ double deletion in the screen, in combination with the involvement of these endosomal components, especially Vac1, in the localisation of Atg21 and its homologues, point to a function of Atg21 in a protein trafficking pathway at the endosome (Krick, 2008a).

Atg27 has been described as PtdIns (3) phosphate-binding protein and a downstream effector of Vps34 (Wurmser and Emr, 2002). Vps34 is a main component of the two phosphatidylinositol 3-kinase complexes in *S. cerevisiae*, needed for autophagy (complex I) and the Vps pathway (complex II) (Figure 4, chapter 2.2.1.3). More recently, a sequencing error leading to a longer Atg27 protein sequence has been published. This Atg27 version does

not require the function of Vps34 or the binding to PdtIns3P for localisation at the PAS (Yen, 2007). Atg27, besides Atg23, is required for the cycling of Atg9 between the pre-autophagosomal structure, mitochondria, and the Golgi complex by interaction with Atg9 (Tucker, 2003; He, 2006; Yen, 2007). Furthermore, Atg27 is required for the Cvt pathway and efficient unselective autophagy, as described for Atg21 (Wurmser and Emr, 2002; Yen, 2007). These functional similarities in phenotype and the potential involvement of both proteins in protein trafficking pathways, makes a synthetic lethality highly reasonable.

Both double deletions, *atg21*Δ *vac1*Δ and *atg21*Δ *atg27*Δ, were of high interest for further investigations. Unfortunately, these double deletions did not show a synthetic lethal phenotype in the experiments of separate remaiting, done for confirmation of the screen results. Hence, both double deletions had to be valuated as false positive matches.

Even though this SGA method is simplified by all the genetic attributes and the work with the screen robot was very diversified, the procedure was not such effective as expected. The use of the robot should have facilitated the experiments by reducing the time of the screen. Unfortunately the robot needed to be monitored during the whole procedure. Single pins tended to fix in wrong positions, leading to the loss of colonies. Furthermore, irregularities in thickness or even slight disarrangement of the OmniTray plates in the gadget led to the loss of cells. Therefore the work with the robot was very time consuming. As an alternative to the robot, manual pin tools were used. Even though using these pin tools did not significantly reduce or extend the duration of the screen, they allowed better time management for other experiments.

5.2 Establishment of a novel assay to easily measure unselective autophagy using Pgk1-GFP

For the detection of unselective (macro-) autophagy by western blot, Atg8 and its mammalian homologue LC3 are standard marker proteins (Klionsky, 2007). In this study the cytosolic 3-phosphoglycerate kinase Pgk1 was introduced as a novel and convincing marker protein in *S. cerevisae* (Welter, 2010).

Unselective autophagy is a ubiquitous process among eukaryotes and is one of the major degradative pathways (Reggiori and Klionsky, 2002). It has been shown to be involved in several diseases like Alzheimer (Nixon, 2007; Jaeger and Wyss-Coray, 2010), Parkinson's (Xilouri, 2008) or Huntington's disease (Shibata, 2006) and is therefore of high interest in the scientific community. Methods for monitoring the autophagic rate were established in *S. cerevisiae* and also mammalian cells. The common method, also used in this study (see 3.4.5.1), is to monitor the autophagic degradation of GFP-Atg8 by western blot (Meiling-Wesse, 2002) similar to the standard method for monitoring mitophagy by detecting the degradation of Om45-GFP (Kanki, 2009a).

The autophagic degradation of GFP-Atg8 includes both, unselective and selective autophagic variants. Atg8 is known to be needed for autophagosome formation and is selectively recruited during the assembly of the autophagic core machinery. Under nutrient rich conditions, Atg8 is found intracellularly in considerable amounts, but its expression increases drastically under nutrient starvation conditions. It is conjugated to PE and thus coupled to the inner and outer membrane of the forming autophagosome. The amount of Atg8 localised to the outer membrane of the autophagosome is cleaved off by the specific protease Atg4, the part of Atg8 localised at the inner autophagosomal membrane is transported to the vacuole where it is degraded (Kirisako, 1999; Ichimura, 2000; Kirisako, 2000). Atg8 is therefore selectively recruited to the PAS during autophagosome biogenesis, thus the autophagic rate, measured via degradation of GFP-Atg8 might be overestimated. Furthermore GFP-Atg8 is degraded via both, unselective and selective autophagy. Hence, GFP-Atg8 is probably a biased marker for the quantification of the unselective macroautophagic rate.

In contrast, Pgk1 (3-phosphoglycerate kinase), the key enzyme in glycolysis and glyconeogenesis, represents a more unselective cytosolic cargo of autophagy and was therefore introduced as a novel marker protein for the detection of unselective bulk autophagy in this thesis (Welter, 2010).

Figure 17 (A) (chapter 4.2) presents western blot analysis using the marker protein Pgk1-GFP. After nutrient starvation and thereby induction of autophagy, wild type cells showed a clear autophagic degradation of the protein detected by accumulation of free GFP. In contrast the two negative controls *atg1*Δ cells, deficient in autophagy, and *pep4*Δ cells, disabled in intravacuolar proteolysis, showed no free GFP. Atg21 is essential for the maturation of proaminopeptidase I under non-starvation conditions (Cvt pathway), while unselective autophagy is only reduced in *atg21*Δ cells (Barth, 2002). As expected, a clear reduction in signal intensity for free GFP in *ATG21* deleted cells, compared to wild type cells was detected. To quantifiy western blot signals, the ratio of free GFP to Pgk1-GFP in wild type cells after 6 hours of nitrogen starvation was set to 100 %. The clear reduction in bulk autophagy in *atg21*Δ cells was calculated to less than 20 % (Figure 17 (A) and (B), chapter 4.2).

The autophagic rate of *ATG21* deleted cells was originally published to be reduced to 35 % (Meiling-Wesse, 2004). This slight discrepancy is most likely the result of using Pgk1-GFP as selective bulk autophagy substrate instead of the autophagy substrate GFP-Atg8. Although the requirement of Atg21 for mitophagy, the selective degradation of mitochondria, is still under discussion (Kanki, 2009b; Okamoto, 2009), Atg21 is known to be essential for the selective Cvt pathway and PMN (Barth, 2002; Krick, 2008b). The use of Pgk1-GFP as marker protein in degradation assays therefore reflects the rate of unselective bulk autophagy in a more acurate manner than the use of GFP-Atg8.

Additional microscopic analysis using cells expressing Pgk1-GFP were performed (Figure 18, chapter 4.2) and support the data of the western blot experiments using the same strains. To avoid the degradation of autophagic bodies by proteinase B, 1 mM PMSF was added to all strains. Wild type cells showed, besides the green fluorescent cytosol, clear green punctate structures, representing the autophagic bodies, moving around inside the vacuole. In contrast, *ATG1* deleted cells did not contain these intravacuolar vesicles. In *pep4*Δ cells an accumulation of autophagic bodies inside the vacuole was clearly visible. As already indicated by western blot quantification, in *atg21*Δ cells the amount of green fluorescent autophagic bodies was significantly reduced.

The utility of the Pgk1-GFP degradation assay can be furthermore accentuated by comparison with other common methods, such as the monitoring of autophagy by a radioactive assay, which requires the radioactive labelling of amino acids in cellular proteins (Prick and Thumm, 2008). Samples are taken at different time points of starvation and are precipitated with TCA. The TCA-soluble radioactivity, which corresponds to the degradated

proteins, is determined using a scintillation counter. Although this method provides reliable results, it is time consuming, expensive and demands for experience in handling. A further method is the use of an enzymatically inactive cytosolic variant of vacuolar alkaline phosphatase (*Pho8Δ60*), which only becomes active after its transport to the vacuole by unselective autophagy followed by maturation inside the vacuole (Noda, 1995). The autophagic rate can be determined by the measurement of enzyme activity. This assay requires the chromosomal deletion of *PHO13* for reduction of background activity and furthermore the replacement of *PHO8* by the truncated *PHO8Δ60*.

In summary, in comparison to other methods, the introduced Pgk1-GFP degradation assay exhibits an appropriate method concerning the costs, the required practise in handling and the required of time.

5.3 A complex of Ccd48, Shp1 and Atg8 is needed for autophagosome biogenesis in yeast

A recent publication, also presenting results of this study, introduces a new role for Cdc48 and its cofactor Shp1 in autophagosome biogenesis (Krick, 2010).

Until now, the mechanism of autophagosome biogenesis is poorly understood. Two of the proposed models for elongation of the phagophore by homotypic or heterotypic fusion events (Longatti and Tooze, 2009) morphologically remind on nuclear envelope expansion and postmitotic Golgi reassembly (Meyer, 2005). One model proposes that the required membrane for the growing phagophore is delivered through vesicular transport from a membrane source to the PAS. Therefore a part of the fusion machinery, also required for other vesicular fusion events would be needed, including motor proteins, Rab GTPases, their effectors and SNARE proteins. Up no now, no SNAREs or autophagy-specific Rab effectors have been identified (Ishihara, 2001; Longatti and Tooze, 2009). The other model proposes that the autophagosome is assembled by homotypic fusion of special autophagy vesicles. These vesicles are either generated in response to autophagy induction or are constantly present in the cytoplasm (Reggiori, 2004b; Longatti and Tooze, 2009; Mari, 2010). Therefore a special autophagy fusion machinery, or also a common homotypic fusion machinery instead of a heterotypic one, might be required. Such a fusion event is considered to be mediated by Cdc48 and its cofactor Shp1.

5.3.1 Shp1 is the exclusive cofactor of Cdc48 needed for autophagy

In contrast to another publication (Ishihara, 2001), Cdc48 was shown to be required for autophagy in previous experiments in the Thumm laboratory by testing the temperature sensitive mutant Cdc48-3 (Bremer, 2009). At the permissive temperature, starved cells showed normal unselective autophagy, but after the shift to the nonpermissive temperature of 38 °C, the GFP-Atg8 degradation assay has shown a strict block in autophagy, while the cellular survival has not been affected at 38 °C (Bremer, 2009; Krick, 2010).

These results made it necessary to test known cofactors of Cdc48 in the GFP-Atg8 degradation assays. Preliminary data already pointed to Ubx1/Shp1 as the only cofactor of Cdc48 needed for autophagy (Bremer, 2009). Ubx1/Shp1 is a member of the UBX protein family, consisting of 7 UBX proteins, described as general Cdc48 interacting proteins. They interact with Cdc48 via their UBX domain (Hartmann-Petersen, 2004; Schuberth and

Buchberger, 2008) and three of the proteins further possess an amino-terminal UBA domain, which has been shown to bind ubiquitinated proteins *in vivo* (Schuberth, 2004).

Indeed, the analysis of these cofactors using the GFP-Atg8 degradation assay in this thesis, confirmed Ubx1/Shp1 as the exclusive cofactor of Cdc48 needed for autophagy (Figure 19, chapter 4.3.1). *SHP1* deleted cells were additionally tested by using the established Pgk1-GFP degradation assay (Welter, 2010), also leading to the result that Shp1 is essential for autophagy (Figure 23, chapter 4.3.2).

Slide effects on proteasomal degradation of ubiquitinated proteins were reported for Shp1, therefore an involvement of the ubiquitin proteasome system had to be tested. Additional cofactors of Cdc48 were also tested for confirmation of previous experiments (Bremer, 2009). No autophagic defect was detected in cells lacking the substrate recruiting factor Ufd1, the substrate processing cofactors Ufd2 and Ufd3, the ubiquitin ligase Ufd4 or the proteasome regulator Ufd5 (Figure 20, chapter 4.3.1). Furthermore, cells lacking the ERAD component Der1 and the substrate processing Cdc48 cofactor Otu1 were tested. Otu1 is distantly related to mammalian VCIP135, which is the necessary cysteine protease for triggering membrane fusion in mitotic Golgi reassembly in mammals by deubiquitinating an unknown fusion regulator (Meyer, 2005). However, *otu1*Δ and *der1*Δ cells showed no reduction in the autophagic rate (Figure 21, chapter 4.3.1). The proteasome-deficient mutant, pre1-1 pre2-2 has been tested in previous experiments in the Thumm laboratory, without showing any effect on autophagy (Krick, 2010). All these data argue against a need for the ubiquitin proteasome system for the autophagic function of Cdc48 and its cofactor Shp1.

In this study, these findings were furthermore confirmed in a GFP-Atg8 degradation assay of *doa4*Δ cells. The deletion of *Doa4* depletes the cellular ubiquitin levels, and causes many cellular defects, including the loss of efficient MVB (multi vesicular body) sorting of some integral membrane proteins (Ren, 2008). The autophagic degradation of GFP-Atg8 was not drastically decreased in *doa4*Δ cells (Figure 22, chapter 4.3.1).

Together, the previous results and the results in this thesis showed that Cdc48 and Shp1 are required for unselective autophagy independently of ubiquitination and proteasomal degradation.

Furthermore, microscopic analysis showed that in contrast to *pep4*Δ cells, *shp1*Δ cells failed to accumulate autophagic bodies in the vacuole (Figure 25, chapter 4.3.3). The treatment of the cells with 1 mM PMSF, which inhibits the vacuolar proteinase B leading to an accumulation of autophagic bodies in wild type cells, showed the same result. These results led to the assumption that no autophagosomes reach the vacuole in *shp1*Δ cells. These results

are consistent with previous fluorescence microscopic analysis, which have demonstrated that the autophagic cargo GFP-Atg8 does not reach the vacuole in *shp1*Δ cells. Even under PMSF treatment, GFP-Atg8 positive autophagosomes have not accumulated in the vacuole (Krick, 2010).

Normal maturation of CPY in *shp1*Δ cells of different growth phases and under starvation supported to the conclusion that vacuolar proteolysis is not significantly disturbed by the deletion of *SHP1* (Figure 24, chapter 4.3.2). These results raised the idea that this deletion causes a defect in autophagosome formation or their vacuolar fusion. A protease protection assay has indicated a defective autophagosome biogenesis or closure (Krick, 2010). Moreover the maturation of Ape1, which was not impaired in *shp1*Δ cells (Figure 24, chapter 4.3.2), indicated a function of Shp1 in the elongation of the phagophore. The core protein Atg8 is known to be crucial for the control of autophagosomal size (Nakatogawa, 2007; Xie, 2008b). Therefore it was tested if the deletion of *SHP1* has an effect on the localisation of Atg8 at the pre-autophagosomal structure or its lipidation, which both are important steps while initiation of the autophagic process. The recruitment to the PAS was analysed by microscopy experiments using the PAS marker protein GFP-Atg8 and, as further control, the PAS marker protein GFP-Atg9 (Reggiori, 2004a; Klionsky, 2007). Cells expressing GFP-Atg8 were starved and PAS structures, represented by clear green punctate structures in close proximity to the vacuole, were counted. PAS dots were observed in 33 % of wild type cells, 86 % of *atg1*Δ cells and 42 % of *shp1*Δ cells. Additionally, 49 % of *shp1*Δ cells expressing GFP-Atg9 showed a PAS structure under these conditions (40.3 % of wild type and 78.9 % of *atg1*Δ cells). This wild type-like rate of PAS structures indicated, that the formation of the PAS is not influenced by Shp1 (Figure 26 (A) and (B), chapter 4.3.4). Furthermore, the lipidation of Atg8 was not impaired in *shp1*Δ cells (Figure 27, chapter 4.3.5). The increased level of Atg8, observed in *shp1*Δ cells, might be caused by the autophagic defect and the resulting enrichment of Atg8 in these cells.

5.3.2 Shp1 interacts with Atg8

In the model for mitotic Golgi reassemby in mammals, ubiquitin has been shown to be an essential factor (Meyer, 2005). Previous experiments in the Thumm laboratory has shown that ubiquitin is not needed for autophagosome formation (Krick, 2010). Furthermore, autophagosome formation has been shown to require the ubiquitin-like protein Atg8 (Nakatogawa, 2007). Therefore the ubiquitin-like protein Atg8 was thought to replace

ubiquitin in the fusion complex required for autophagosome formation and therefore to bind to Shp1.

An interaction of Shp1 and Atg8 has already been shown by coimmunoprecipitation and pull-down experiments using recombinant GST-Atg8 (Krick, 2010). In this study, this interaction was proven by pull down experiments using recombinant GST-Shp1 constructs.

Three different constructs were generated: full length GST-Shp1, GST-Shp1 lacking the C-terminal UBX domain and GST-Shp1 lacking the N-terminal UBA domain. The UBX domain is known to be a general Cdc48/p97-binding module (Hartmann-Petersen, 2004) and is described as a distant homologue of ubiquitin itself. Therefore Cdc48/p97 can either bind directly to ubiquitin or the UBX domain of the corresponding protein (Buchberger, 2001). The UBA domain has been shown to bind to ubiquitinated proteins in vivo (Schuberth, 2004). Furthermore, the human homologue of Shp1, p47, requires the binding of ubiquitinated proteins via the UBA domain for efficient p97/p47-mediated Golgi membrane function in vitro (Meyer, 2002). To prove the interaction of Atg8 with Shp1, and its dependence on the UBA or UBX domain, three different constructs (GST-Shp1 full length, GST-Shp1-UBX and GST-Shp1-UBA) were used for pull down experiments (Figure 28 (A) and (B), chapter 4.3.6).

The use of the standard protein purification protocol for the recombinant GST-Shp1 constructs resulted in their degradation. This degradation might be caused by a freezing step in the purification protocol and the followed lysozymal cell disruption using BL21 (DE3) pLys cells. Therefore an alternative purfication was tested. The constructs were transformed in BL21 RIPL cells (Table 8, chapter 3.1.2) and the cell disruption was done by french press (see 3.4.6.4). The cells were treated on ice and freezing was avoided. This optimisation led to a decreased degradation of the recombinant proteins.

The recombinant GST-Shp1 proteins were used for pull down experiments with native cell extract of *pep4*Δ cells expressing GFP-Atg8, to avoid vacuolar proteolysis (Figure 28 (A), chapter 4.3.6). In a second pull down *atg4*Δ *atg8*Δ cells expressing GFP-Atg8-FG were used for cell extract preparation (Figure 28 (B)). Atg4 removes the carboxy-terminal arginine of Atg8 to allow coupling to PE. By the use of the Atg8-FG construct, which lacks this arginine, coupling to PE is independent on Atg4. This allows the use of an *atg4*Δ strain, perhaps stabilising the Atg8-PE-Shp1 complex, which would be otherwise decomposed by Atg4 (Kirisako, 2000). Atg8-PE is described to mediate hemifusion during autophagosome formation most likely by mediating oligomerisation (Nakatogawa, 2007). Former experiments led to the suggestion that Shp1 might preferentially interact with Atg8-PE (Krick, 2010). The

postulated interaction of Atg8 with Shp1 might be enhanced in *atg4*Δ *atg8*Δ cells expressing GFP-Atg8-FG. All three different GST-Shp1 constructs showed an interaction with Atg8 in the pull down experiments. Interestingly, the recombinant GST-Shp1 lacking the N-terminal UBA domain showed a significant stronger interaction with Atg8 in five independent experiments. This observation might be explained by the inability of the GST-Shp1 construct lacking the UBA domain to bind ubiqutin. Using the full-length GST-Shp1 construct, Atg8 and ubiquitin might compete for binding to Shp1. Hence, Shp1 does not bind Atg8 via the UBA domain. In previous experiments it has been shown that the autophagic activity is not obviously affected by the depletion of the UBA domain (Krick, 2010).

Previous experiments, done in the Thumm laboratory and data of this thesis led to the model that the AAA^+ ATPase Cdc48 and its cofactor Shp1/Ubx1 are essential factors for autophagosome biogenesis (Figure 7, chapter 2.2.5.1.1) (Krick, 2010). Atg8 may act as a fusion regulator, which must be extracted by the AAA^+ ATPase Cdc48 and its adapter Shp1 from a complex with a fusion mediator. In this model, Atg8 replaces ubiquitin in a membrane fusion complex during autophagosome formation. The deubiquitination by the cysteine protease VCIP135 in mitotic Golgi reassembly (Meyer, 2005) might be replaced by the use of the cysteine protease Atg4, which delipidates Atg8-PE and leads to a release of the complex for the initiation of the fusion event.

Notably also PMN, the selective degradation of portions of the nucleus by microautophagy has been shown to require Cdc48 and Shp1 (Bremer, 2009).

5.4 Insights into mitophagy in *S. cerevisiae*

Mitochondria, the site of ATP production in aerobic cells consequently are at the same time the major source of reactive oxygen species (ROS), which damage mitochondria and also other organelles. Dysfunctional mitochondria therefore enhance oxidative stress and may also lead to the scattering of the membrane potential across the inner membrane, resulting in induction of cell death by the release of pro-apoptotic proteins (Kroemer, 2007; Tatsuta and Langer, 2008). Thus, a quality control for mitochondria is essential for cellular survival.

In humans the consequences of mitochondrial dysfunction are linked to ageing and neurodegeneration. Mitochondrial dysfunction has been shown to be involved in Parkinson's disease (PD) several decades ago (Mizuno, 1989), leading to the conclusion that mitochondrial quality control is indispensable for cellular health. The selective degradation of mitochondria by autophagy may represent such a quality management in the cell.

Indeed in the last few years, mitophagy was shown to be one of the major degradative pathways in conjunction with PD. The E3 ubiquitin ligase Parkin, which has no homologue in yeast, triggers the removal of damaged mitochondria. Its dysregulation is therefore linked to PD (Geisler, 2010). During mitophagy, Parkin has been shown to be translocated from the cytosol to uncoupled or depolarised mitochondria (Narendra, 2008). The induction of Parkin-mediated mitophagy is dependent on the activity of PINK1, a kinase, which spans the outer mitochondrial membrane (Narendra, 2008; Narendra, 2010a). The interaction of PINK1 with Parkin was found to be significantly enhanced after depolarisation of mitochondria (Geisler, 2010). After the translocation of Parkin to mitochondria, Parkin mediates the linkage of ubiquitin at Lys 27 and Lys 63 to mitochondrial substrates. One protein discussed to represent such a substrate, is the voltage-dependent anion channel 1 (VDAC1) (Geisler, 2010; Narendra, 2010b). Subsequently, ubiquitin receptors have to be recruited to mitochondria. Such a ubiquitin binding adaptor is p62 (Geisler, 2010; Narendra, 2010b), which recruits ubiquitinated cargo into autophagosomes by binding to LC3 (the mammalian homologue of Atg8) (Pankiv, 2007). Furthermore, in mammalian cells, the mitofusins MFN-1 and MFN-2 have been shown to be ubiquitinated in a PINK1- and Parkin-dependent manner, suggesting a proteasomal degradation which furthermore leads to a block in mitochondrial fusion machinery and an autophagy-dependent degradation of mitochondrial fragments (Gegg, 2010). In *Drosophila*, PINK1 is also required for the translocation of Parkin to dysfunctional mitochondria and the resulting degradation initiated by the ubiquitination of the profusin factor Mfn (Ziviani, 2010).

Also in *S. cerevisiae* studies in the last few years provided more insight into mitophagy. Two independent genetic screens identified the mitochondrial-anchored transmembrane receptor protein Atg32, which is exclusively required for mitophagy (Kanki, 2009c; Okamoto, 2009). Typical for an autophagic cargo receptor, Atg32 interacts with Atg8 via a highly conserved WXXI motif in its cytosolic (N-terminal) region (Kanki, 2009c; Okamoto, 2009). Atg19, which selectively binds to cargo proteins in the Cvt pathway, interacts via a WXXL motif with Atg8 (Shintani, 2002). The mammalian p62 binds ubiquitinated cargo and interacts with LC3, the mammalian homologue of Atg8, via a WXXL motif (Pankiv, 2007). Therefore, a similar function in cargo recognition and Atg8 interaction is plausible for Atg32 in mitophagy, especially because of a nitrogen starvation induced interaction with Atg11, which is necessary for selective cargo reporter recognition in the Cvt pathway and pexophagy (Kim, 2001).

In *S. cerevisiae,* the established Om45-GFP degradation assay presents an assured method for monitoring mitophagy, but requires the chromosomal GFP-tagging of Om45 (Kanki, 2009a).

To enable the detection of mitophagy using a plasmid-encoded marker protein, similar to the marker proteins GFP-Atg8 or Pgk1-GFP for the detection of unselective autophagy, plasmids encoding the mitochondrial proteins Om45-GFP and Idh1-GFP were constructed in this study. The use of these plasmids led degradation of the marker proteins independent from Atg1 or Pep4 (data not shown). Therefore mito-GFP was constructed by the insertion of the mitochondrial targeting sequence Su9-mt-DHFR into the vector pUG35. Similar to plasmids used in other studies (Tal, 2007; Okamoto, 2009), the mito-GFP of this study showed a localisation at mitochondria (Figure 31 (A), chapter 4.4.3) and was degraded in an autophagy-dependent manner after 48 hours growth in medium containing lactate as sole carbon source (Figure 31 (B)), indicating the induction of mitophagy after exhaustion of the carbon source. Due to the use of the pUG35 vector, the expression of mito-GFP is under control of a MET*25* promoter, thus all experiments were done in *S. cerevisiae* of WCG or BY4742 background, which allows growth in medium lacking methionine.

5.4.1 Differentiation between mitophagy of superfluous or damaged mitochondria

To monitor mitophagy in *S. cerevisiae,* Kanki *et al.* (2009a) described two different conditions to induce mitophagy. On one hand, the induction by amino acid starvation, which means the shift of the cells from a nonfermentable carbon source (lactate medium), leading to the proliferation of mitochondria, to nitrogen starvation medium containing glucose. The other method involves the induction at post-log phase meaning a prolonged incubation for up to three days in medium containing 2 % lactate as sole carbon source. Recent publications, using both conditions, have shown that Uth1, a protein primarily postulated as essential for mitophagy (Kissová, 2004), is not needed for the selective degradation of mitochondria (Kanki, 2009b; Okamoto, 2009). This fact was also confirmed in this study (data not shown). Nevertheless, the comparison of both studies lead to some discrepancies concerning the need of Atg13 or Atg21 for mitophagy (Kanki, 2009b; Okamoto, 2009).

In regard to the discrepancies, the initiation of different mitophagy processes can not be excluded, meaning recognition and determination of superfluous, aged or highly damaged mitochondria (by external or internal stress factors, e.g. reactive oxygen species). Therefore, different conditions to induce mitophagy were tested and established in this study. After growth for up to 72 hours in medium containing 2 % lactate, mitochondria are aged and might be severely damaged. The mitophagic degradation was monitored by western blot analysis and a time-dependent increase of free GFP in wild type cells was shown. In the *atg18*Δ control cells, deficient for autophagy (Barth, 2001), and *atg32*Δ, deficient for mitophagy (Kanki, 2009b; Okamoto, 2009), no signal for free GFP was detected (Figure 32, chapter 4.4.4). These observations were consistent with published results (Okamoto, 2009).

Superfluous mitochondria, which generate reactive oxygen species (ROS) as a consequence of metabolic processes, might present a specific cargo for autophagy, to ensure cellular survival. In the literature, degradation of mitochondria was further initiated by the shift to SD-N medium containing glucose (Kanki and Klionsky, 2008), the common method to induce autophagy (Takeshige, 1992). As the switch from medium containing 2 % lactate to SD-N medium did not result in measurable mitophagic degradation in this study (data not shown), 0.2 µg/ml rapamycin was added to the cells of interest. The addition of rapamycin leads to the initiation of autophagy, by inhibition of the TOR kinase (Noda and Ohsumi, 1998). Indeed, in contrast to *atg18*Δ and *atg32*Δ control cells, wild type cells showed an increased level of mitophagy after treatment with rapamycin (Figure 33, chapter 4.4.4).

A slight rate of unselective autophagy was already detectable in wild type and *atg32*Δ cells before treatment with rapamycin**.** This observation led to the conclusion that unselective autophagy is already induced after 14 - 16 hours of growth in preculture medium containing 2 % lactate.

As already mentioned, mitochondria are a major source of reactive oxygen species (ROS), therefore a qualitiy control of mitochondria is indispensable. Recent publications postulated an induction of autophagy by ROS (e.g. O_2^- or H_2O_2) (Kiffin, 2006; Chen, 2009), suggesting a function of mitochondrially generated H_2O_2 in regulating the lipidation of Atg8 via the Atg4-activity (Scherz-Shouval and Elazar, 2007). ROS are generated endogenously in cells by reduction of oxygen and can lead to the production of more ROS. They are highly damaging towards cellular constituents, e.g. DNA, proteins and lipids after an increase of concentration beyond the antioxidant buffering capacity. To protect the cellular constituents, yeast (and other organisms) has developed a ubiquitous enzymatic and non-enzymatic oxidant defence system. For example O_2^-, a product of incomplete one-electron reduction of oxygen which can be converted to H_2O_2 by two different superoxid dismutases (SOD). One is the cytoplasmical Cu/ZnSod/Sod1, encoded by *SOD1*, and the other is the mitochondrial MnSod/Sod2, encoded by *SOD2*. H_2O_2 is furthermore converted to O_2 and H_2O by the gluthathione peroxidase, which uses gluthathione as reductant, or by different catalases. E.g. H_2O_2, which is produced by fatty acid ß-oxidation, is converted by the peroxisomal catalase A (encoded by *CTA1*) (Jamieson, 1998; Chen, 2009).

In this thesis, H_2O_2 was tested as external stress factor to induce the selective degradation of dysfunctional mitochondria. Different concentrations of H_2O_2 were tested in wild type and *atg18*Δ cells expressing mito-GFP. In parallel the survivial rate was analysed, to exclude affects of dead cells. The treatment with 0.05 mM H_2O_2 for three hours led to a cell survival rate of 89 % and measurable signal for free GFP in wild type cells but not in *atg18*Δ cells, used as negative control (Figure 34 (A) and (B), chapter 4.4.4). An increase of the concentration of H_2O_2 from 0.1 to 1 mM led to a decrease in cell survival to 83 % to 63 %. As in former litertature this decrease in viability of wild type cells after exposure to 1.2 mM H_2O_2 appeared more drastically (about 30 %) (Collinson and Dawes, 1992; Palermo, 2007), 0.05 mM H_2O_2 was used in further experiments in this study (Figure 34 (C) and (D), chapter 4.4.4). In contrast to the control cells *atg18*Δ and *atg32*Δ, the treatment with H_2O_2 induced mitophagy in wild type cells. Initiated by growth in lactate medium during preculture, also in this experiment a slight rate of unselective autophagy was detected in wild type and *atg32*Δ cells before treatment with H_2O_2.

In further experiments, the ability of paraquat (N, N'-dimethyl-4,4'-bipyridinium dichloride) to induce mitophagy in yeast was tested. This pesticide has already been linked to Parkinson's disease by the damage of mitochondria (Cocheme and Murphy, 2008; Terzioglu and Galter, 2008; Narendra, 2010a). It impairs the mitochondrial function by the acception of electrons from one of the electron carriers, yielding to the production of O_2^- and H_2O_2.

Different concentrations of paraquat were tested in wild type and *atg18*Δ cells, used as negative control, expressing mito-GFP. Again, in parallel the survival rate was analysed. The addition of 5 to 15 mM paraquat to wild type cells led to a decrase in cell survivial to 80 to 75 %. The treatment with 2 mM paraquat for three hours led to a cell survival rate of 84 % and measurable mitophagy induction in wild type cells, but not in *atg18*Δ cells (Figure 35 (A) and (B), chapter 4.4.4). This observation was similar to results in literature, where the treatment of yeast cells with 2.5 mM paraquat has led to a decrease in cell viability to 88 % (Lee and Hassan, 1985).

Hence, 2 mM paraquat was used for further experiments (Figure 35 (C) and (D), chapter 4.4.4). In contrast to the *atg18*Δ and *atg32*Δ control cells, mitophagy was induced in wild type cells by the treatment with 2 mM paraquat. Initiated by the preculture conditions, also in this experiment a slight rate of unselective autophagy was detected in wild type and *atg32*Δ cells before treatment with paraquat.

The results indicated that mitochondria are severely damaged by the treatment with H_2O_2 and paraquat, which further leads to the production of more ROS far beyond the antioxidant buffering capacity of the cell. Damaged mitochondria, which are not immediately degraded, are a risk for the cell and cellular survival. At this point mitophagy supports the oxidant defence system (e.g. SOD and catalases). Recent publications have shown that the addition of paraquat, yielding to the production of O_2^- and H_2O_2, further induces the biosynthesis of the mitochondrial MnSOD/Sod2 (Hassan and Fridovich, 1979), indicating a role in protection of mitochondria from respiration-generated ROS.

To determine if these stressors selectively induce mitophagy, unselective bulk autophagy was monitored in parallel using Pgk1-GFP in all strains tested under the same conditions. A slight rate of unselective bulk autophagy was already induced after 14 – 16 hours of growth in preculture medium containing 2 % lactate. Initial observations indicated a difference between the amounts of free GFP produced by autophagy or mitophagy. But as the use of preculture medium containing 2 % lactate already induced unselective autophagy, it can only be speculated about an exclusive role of paraquat or H_2O_2 in the induction of mitophagy. Further investigations, using optimised growth conditions might avoid the induction of unselective

autophagy and probably prove that the treatment with paraquat specifically induces only mitophagy, but not unselective autophagy.

Studies in *H. polymorpha* have shown, that the shift of methanol-grown cells to glucose medium initiates macropexophagy, while in *P. pastoris* the same conditions initiate micropexophagy. Ethanol, however, induces macropexophagy in both yeasts (Veenhuis, 1983; Tuttle and Dunn, 1995; Sakai, 2006). Furthermore, in *S. cerevisiae*, after a shift from medium containing lactate to SD-N medium, a micromitophagic uptake of mitochondria by the vacuolar membrane has been observed by electron microscopy (Kissová, 2007). Together, these results lead to the assumption, that different conditions to induce mitophagy might alternatively cause micro- or macromitophagy.

The different methods to induce mitophagy used in this study, did not result in obvious differences between the tested deletion strains. To elucidate the mechanism of mitophagy in *S. cerevisiae*, further work especially electron microscopy will be needed.

In a screen for yeast deletion mutants defective in mitophagy, done with cells of post log phase in medium containing glycerol, Ccz1 has been identified (Okamoto, 2009). As Ccz1 is further known to be required for the fusion of autophagosomes with the vacuole (Meiling-Wesse, 2002),these findings might indicate that most of the mitochondria are degraded via a macroautophagic process. Notably, this speculation about a macroautophagic process in glycerol medium, is not contrary to the suggestion that microautophagic degradation of mitochondria is favored by lactate-grown cells (Kissová, 2007).

ATG13 deleted cells were also analysed in this study. Atg13 activates Atg1 in a TOR-dependent manner and is therefore an essential protein for autophagy, including PMN and the Cvt-pathway (Kamada, 2000; Krick, 2008b). The detection of mitophagy in *atg13*Δ cells expressing mito-GFP in this study (Figure 32 - 35, chapter 4.4.4), led to the idea that Atg1 can be activated in an Atg13-independent manner under respiratory growth conditions, what has already been observed and discussed in former literature (Okamoto, 2009). Remarkably, another group published an Atg13-dependent initiation of mitophagy (Kanki, 2009b). These discrepancies may be caused by the use of different marker proteins for the degradation assays. On the one hand, using a plasmid similar to the mito-GFP plasmid of this study, has resulted in a clear signal for free GFP in *atg13*Δ cells and, on the other hand, the chromosomal GFP-fusion of Om45 in *atg13*Δ cells showed no signal for free GFP under starvation. A similar observation was made for *atg21*Δ cells in these publications (Kanki, 2009b; Okamoto, 2009). In this study, *atg21*Δ cells grown for 72 hours in medium containing

lactate showed a normal rate of mitophagy (data not shown) confirming the results of Okamoto *et al.* (2009).

Perhaps, using the plasmid expressed mito-GFP as marker protein is the more sensitive method to measure mitophagy than using chromosomally expressed Om45-GFP, hence a direct comparison of these two marker proteins, using both conditions for the induction of mitophagy within one experiment should shed light on this question.

5.4.2 Mitophagy is increased in *yme1*Δ cells

Yme1 is a subunit of the mitochondrial inner membrane i-AAA protease complex and is responsible for the degradation of unfolded or misfolded mitochondrial proteins (Leonhard, 1996). A loss of the Yme1 function leads to more dysfunctional mitochondria, probably inducing an increased rate of mitophagy (Campbell and Thorsness, 1998).

YME1 deleted cells were tested in the mito-GFP degradation assay and showed a drastically increased amount of free GFP after growth for 72 hours in lactate medium resulting in a mitophagic rate of 122 % compared to wild type cells. Already after growth for 24 hours, *yme1*Δ cells showed a signal intensity for free GFP of 57 % compared to 13 % in wild type cells (Figure 36, chapter 4.4.5).

This significant 3.5 fold increase in mitophagy after 24 hours represents the selective degradation of damaged mitochondria, caused by unfolded or misfolded mitochondrial proteins in the absence of Yme1. Speculatively, these proteins could be specifically labelled to destignate the mitochondria for degradation.

Nevertheless, these results confirm the observations in former literature, where the, by approximately 3.5 fold, increased ALP acitivity of *yme1*Δ cells compared to wild type cells in medium containg glycerol and ethanol has been reflective of selective mitochondrial degradation and not of a general increase in unselective autophagy (Campbell and Thorsness, 1998).

5.4.3 Part of the ESCRT machinery is required for mitophagy

The Vps class E proteins Vps27 and Vps28 have been shown to be needed for the selective piecemeal microautophagy of the nucleus (PMN) (Bremer, 2009). But deletion of *VPS27* or *VPS28* does not effect the maturation of prApe1 under nutrient rich or starvation conditions (Reggiori, 2004b) or the autophagic degradation of GFP-Atg8 under starvation conditions (Bremer, 2009). This is in contrast to the mammalian system, where autophagic degradation is inhibited in cells depleted of several ESCRT proteins such as the homologue of Vps24 (Filimonenko, 2007).

To test the need of class E proteins for mitophagy, different deletion strains were monitored (Table 19). Deletions of *VPS27* (ESCRT-O) and *VPS23* (ESCRT-I) were used for mito-GFP and Pgk1-GFP degradation assays. The cells were grown for up to 72 hours in medium containing 2 % lactate as sole carbon source. Both pathways show a strong signal for free GFP in *vps27*Δ and also *vps23*Δ cells (Figure 37 (A), chapter 4.4.6). The quantification of signal intensity for GFP of both strains (Figure 37 (D)) led to the conclusion that neither Vps27 nor Vps23 influence the degradation of mitochondria or the unselective bulk autophagy of cytosolic material. In contrast, *vps28*Δ cells (ESCRT-I) showed a drastical decrease in mitophagy (38 %), but not in unselective autophagy (77 %) (Figure 37 (B) and (D)). The additionally tested strains *vps24*Δ (ESCRT-III), *vps25*Δ (ESCRT-II) and *vps32*Δ (ESCRT-III) also showed a drastical decrease of degraded mito-GFP compared to wild type cells (Figure 37 (C)). Quantification analysis supported these observations. In v*ps24*Δ cells a signal intensity of 21 % for mitophagy compared to wild type cells was detected. Also *vps25*Δ and *vps32*Δ cells showed a decrease in the mitophagic rate to 15 % and 13 % (Figure 37 (C)). As Vps23 is a member of ESCRT subunit 0 and Vps27 is the link between ESCRT-0 and ESCRT-I (Katzmann, 2003), the results of this study indicated, that proteins of ESCRT-I, -II and -III are needed for mitophagy, while ESCRT-0 is excluded. As the ESCRT subunit 0 and Vps27 are known to be responsible for the recognition of ubiquitinated cargo in MVB pathway (Katzmann, 2001; Bilodeau, 2003), such a role in mitophagy can be excluded.

Using the same conditions and a comparable plasmid for detection of mitophagy, another group has also identified *vps24*Δ and *vps32*Δ cells as „partially defective“ as well as *vps2*Δ cells, which also represent the ESCRT subunit III. In contrast to this study, *vps25*Δ and *vps28*Δ cells have not been defective in mitophagy (Okamoto, 2009).

Unselective autophagy was measured under the same growth conditions (72 hours in medium 2 % lactate) using Pgk1-GFP in parallel. These strains showed only a slight defect concerning

ESCRT -I, -II and -III (Table 19, chapter 4.4.6), indicating a special but not indispensable role in mitophagy of the tested ESCRT proteins.

So far, the role of the ESCRT machinery for mitophagy is unclear. Microautophagic degradation, including the selective degradation of mitochondria, has been suggested to be favored by cells grown on lactate medium (Kissová, 2007). As selective ESCRT subunits were required for mitophagy after growth on lactate medium, but not for unselective autophagy, this might point to a potential role of the ESCRT subunits in micromitophagy.
An inactivation of ESCRT subunits might cause a direct effect in a micromitophagy-dependent degradation of mitochondria, by preventing the closure of the membrane bud around mitochondrial structures. As the ESCRT machinery also affects vacuole biogenesis, an indirect effect caused by an impairment of the vacuolar membrane, can not be excluded.

5.4.4 Ubiquitination affects mitophagy in *S. cerevisiae*

A deletion of *Doa4* is known to deplete the cellular ubiquitin level (Swaminathan, 1999; Ren, 2008). In *S. cerevisiae*, unselective autophagy was not affected in *doa4*Δ cells (Krick, 2010). In mammalian cells, the E3-like ubiquitin ligase Parkin was shown to play an irreplaceable role in designating mitochondria for mitophagy by ubiquitination (Narendra, 2008). Ubiquitination was further shown to affect mitochondrial morphology and inheritance.
Mitochondria continuously grow, divide and fuse throughout cellular life and it is the frequency of fission events relative to fusion events that largely determines steady-state organelle morphology (Shaw and Nunnari, 2002). Damaged parts of mitochondria remain fragmented and thus are believed to be preferentially sequestered by autophagosomes (Twig, 2008). Mitofusins are ubiquitinated in a PINK1- and Parkin-dependent manner in mammalian cells and *Drosophila*, suggesting a proteasomal degradation, which furthermore leads to a block in mitochondrial fusion machinery and an autophagy-dependent degradation of mitochondrial fragments (Gegg, 2010; Ziviani, 2010). Moreover, the ubiquitination of mammalian Drp1 affects mitochondrial fission (Chang and Blackstone).

A role of ubiquitin in labelling dysfunctional mitochondria might also be conceivable in *S. cerevisiae.* Therefore, the need of Doa4 for mitophagy compared to unselective autophagy was tested. Figure 38 (A) (chapter 4.4.7) shows a significant reduction in the mitophagic rate, while unselective autophagy was not strongly affected. These observations were supported by quantification analysis, which showed a significant decrease of mitophagy to 37 % (SEM = 11) (Figure 38 (B)). The decrease of unselective autophagy to 65 % (SEM =

11) probably indicates a general effect on cellular health, caused by the depletion of the cellular ubiquitin level. The significant reduction in mitophagic degradation leads to speculations about a specific role of ubiquitin in mitophagy. Ubiquitin has seven lysines (lys), in which three are typically used for polyubiquitination. Notably, different ubiquitin chains have specific consequences for the tagged substrates and are linked to diverse cellular functions (Ikeda and Dikic, 2008). For instance, monoubiquitination or oligomeric Lys63-linked ubiquitin chains target the proteins to the vacuole, whereas polyubiquitination linked via Lys48 of ubiquitin targets the proteins to the proteasome. In mammalian cells, Parkin has been shown to mediate the formation of two distinct polyubiquitin chains on the substrates at depolarised mitochondria, linked through Lys27 and Lys63 (Geisler, 2010). Hence, it has to be tested whether mono- or polyubiquitin is required for mitophagy in yeast. This can be done by mito-GFP degradation assays in *doa4*Δ cells using furthermore plasmids expressing different ubiquitin mutants, containing substitutions of defined lysines to arginines (e.g. Lys63 – Arg63).

Ubp3 and its cofactor Bre5 are needed for the starvation induced selective autophagic degradation of the large 60S subunit of ribosomes (ribophagy), by removal of ubiquitin from a yet unknown substrate (Kraft, 2008). Nevertheless, experiments in this study showed that neither Ubp3 nor Bre5 impair the process of mitophagy (data not shown).

The need of Doa4 might give a hint for ubiquitination in labelling of dysfunctional mitochondria for degradation. As mitofusins are reported to be substrates for such a well-directed ubiquitination in mammalian cells (Gegg, 2010), also yeast's mitofusins might fulfill such a function.

The mitochondrial fusion machinery in *S. cerevisiae* is well understood. Fzo1, a mitochondrial outer membrane protein, is required for the fusion of mitochondria and therefore essential for the biogenesis of functional mitochondria. The depletion of this GTPase leads to a petite phenotype and fragmented mitochondrial morphology (Hermann, 1998; Rapaport, 1998). Another known dynamin-related GTPase is Mgm1 (Wong, 2000), which exists in two isoforms. The smaller isoform is generated by the cleaveage of Pcp1, a rhomboid-like serine protease. Even though the exact function of both isoforms is still not clear, the larger isoform was shown to be more important for mitochondrial fusion (Herlan, 2003). Furthermore Ugo1, a mitochondrial transmembrane protein located in the outer membrane, was shown to link Mgm1 to Fzo1 for mitochondrial fusion (Sesaki and Jensen, 2004).

The dynamin-related GTPase Dnm1 participates in mitochondrial fission and therefore fulfills an antagonistic activity to Fzo1. Deletion of *DNM1* leads to a block in membrane fission indicating a regulatory role (Bleazard, 1999), notably not resulting in a petite phenotype. Depending on the used conditions, *dnm1*Δ cells show slight to strong defects in mitophagy (Kanki, 2009b), indicating a role of the mitophagic fission machinery in mitophag. Alternatively, the autophagic core machinery could be recruited to damaged parts of the mitochondria and somehow promote fission to allow mitophagy.

Fzo1, Mgm1 and Ugo1, representing the mitochondrial fusion machinery, are good canditates for further investigations. As already mentioned, the deletion of *FZO1* or also *MGM1* lead to a petite phenotype, resulting in poor growth in medium containing lactate as the sole carbon source. The degradation assay of mito-GFP used in this study includes the preculturing in 2 % lactate medium and is therefore not suitable. Preculturing of yeast in medium containing 2 % glucose as carbon source leads to the so-called glucose repression, meaning the repression of genes required for metabolisms of alternative carbon sources, including respiratory enzymes (Strittmatter, 1957; Trumbly, 1992). Moreover, absence of mitochondrial structures was observed in yeast cells grown aerobically on glucose (Polakis, 1964). To avoid glucose repression, experiments were done using preculture medium containing 2 % galactose as sole carbon source. First measurements using mito-GFP resulted in an undetectable signal for free GFP in wild type cells (data not shown), confirming observations of other groups (Kanki, 2009c; Okamoto, 2009). However, an optimisation of growth conditions using galactose as sole carbon source may lead to interesting results, elucidating the role of the membrane fusion machinery in mitophagy. This might also provide substrates for a proposed ubiquitination.

This study gives new insights into the selective degradation of mitochondria via mitophagy. The supposed role of Doa4 and some ESCRT proteins offers possibilities for a number of speculations.

A Vps27- and ESCRT subunit I-mediated recruitment of the ESCRT machinery to ubiquitinated mitochondria can be excluded. Atg32, which was shown to be essential for mitophagy in all experiments, might not require ubiquitination, due to its ability to bind Atg8 directly or by an interaction via Atg11 (Kanki, 2009c; Okamoto, 2009). An additional ubiquitination of Atg32 is therefore questionable. The suggested ubiquitination might be a signal for the cell to differentiate between superfluous or damaged, and therefore dysfunctional, mitochondria and might also be a trigger to induce micro- or macromitophagy. The possibility to distinguish between micro- and macromitophagy by different deletions is essential and therefore a major focus of further investigations.

5.5 The nucleolus might represent a specific cargo for PMN

Since the discovery of PMN in 2003, this selective microautophagic degradation of parts of the nucleus, which requires a subset of autophagic proteins, became a focus of interest (Roberts, 2003; Krick, 2008b). Also Atg11, a protein required for cargo recruitment in the Cvt pathway or pexophagy (Kim, 2001), is required (Krick, 2008b). PMN is a unique microautophagic process at contact sites between the vacuole and the nucleus (NV junctions). These NV junctions are formed through specific interaction between Vac8 and the C-terminus of Nvj1, that is upregulated upon nutrient starvation. The deletion of Vac8 or Nvj1 blocks PMN. Nvj1 is furthermore believed to interact via its N-terminus with an unknown inner nuclear membrane protein (Kvam and Goldfarb, 2006). Tsc13, an ER-membrane protein, is sequestered into NV junctions from the ER by interacting with Nvj1 in a Vac8-independent manner. As a consequence, it is incorporated into PMN structures and targeted to the vacuole (Kvam, 2005). Osh1 is a member of the Osh family in yeast, and a homologue of the mammalian oxysterol-binding protein (OSBP) (Levine and Munro, 2001), which may function in nonvesicular lipid trafficking. Osh1 is targeted to NV junctions through interaction with Nvj1, proportional to the expression of Nvj1, also in the absence of Vac8 (Kvam and Goldfarb, 2004). However, Osh1 is not necessary for the formation of the NV junctions or efficient PMN, but the depletion of the whole Osh family of yeast leads to a block in PMN, indicating overlapping functions of this protein family (Kvam and Goldfarb, 2004). Due to the interaction with NV junctions, Osh1 exhibits a substrate for PMN by incorporation into PMN structures and is therefore used as common marker protein (Kvam and Goldfarb, 2004; Millen, 2009).

Up to now, a specific nuclear cargo for PMN is still missing and is a major focus of investigation.

A specific cargo-recognition, indicated by the need of Atg11, is indispensable to preserve the integrity of the nucleus. Indeed chromosomal DNA and nuclear pore complexes are excluded from NV junctions (Pan, 2000; Roberts, 2003). As the TOR kinase arrests pre-rRNA processing and stabilizes pre-rRNA precursors in the nucleolus under starvation (Powers and Walter, 1999), Roberts *et al.* (2003) have speculated that preribosomes, which are no longer needed in the cytoplasm under nutrient limitation, might be substrates of PMN.

Western blot analysis of nucleolar GFP fusion proteins did not result in the identification of a selective PMN cargo (Figure 39, chapter 4.5.1), however the microscopic

analysis of some nucleolus proteins under nutrient starvation after staining of the vacuolar membrane with FM4-64, resulted in interesting observations (Figure 40, chapter 4.5.2).
Nop8 is a nucleolar protein, required for 60S ribosomal subunit biogenesis (Zanchin and Goldfarb, 1999). Cells chromosomally expressing Nop8-GFP, showed a green fluorescent signal inside the vacuole, indicating the autophagy depending degradation of nucleolar material. Furthermore, cells expressing the nucleolar Cic1-GFP (Jager, 2001) seemed to have green vesicles inside the vacuole under nutrient starvation. In contrast Utp5-GFP and Utp10-GFP, two small subunit proteins of the processome, which is a ribosome assembly intermediate (Bernstein, 2004), did not exhibit green fluorescent signal outside of the nucleolus. Notably, under nutrient starvation, in cells chromosomally expressing Sik1-GFP, nucleolar structures with a striking colocalisation with the vacuolar membrane were observed (Figure 40). For subsequent microscopy experiments, cells expressing Nog1-GFP were used. Nog1, a nuclear GTP-binding protein, is tethered to the nucleolus upon nutrient starvation or rapamycin treatment (Honma, 2006). This might indicate a translocation of Nog1-GFP to the PMN active side. Indeed, in starved Nog1-GFP cells, PMN-like, Nog1-GFP containing structures pinching off from the vacuolar membrane into the vacuole were observed (Figure 41, chapter 4.5.2).
Furthermore, in microscopic analysis of starved cells chromosomally expressing Sik1-RFP and plasmid encoded Osh1-GFP, NV junctions were shown to localise directly next to the nucleolus in about 70 % of the cells (Figure 42 (A) and (B), chapter 4.5.3; SEM = 0.6). For further investigations Sik1-RFP cells expressing the PAS marker GFP-Atg8 were used for microscopic analysis. In these cells, 30 % of the observed PAS dots localised in close proximity to the nucleolus after starvation (Figure 43 (A) and (B), chapter 4.5.4). Notably, incubation of cells in SD-N medium does not selectively induce PMN.

Taken together, the experiments in this study point to a specific recognition of single nucleolar proteins. Especially the observation of GFP signal inside the vacuole of cells chromosomally expressing Nop8-GFP, might support the speculations of Roberts *et al.* (2003), suggesting preribosomes as a selective cargo for PMN by a TOR regulated pre-rRNA processing.
Nevertheless, a selective autophagic uptake of other nuclear proteins than the nucleolus components by PMN is not excluded.

Nevertheless, the detected GFP signals outside the nucleolus in the tested strains appeared weak and no clear free-floating autophagic bodies inside the vacuole were observed under PMSF treatment. Additionally, western blot analysis showed no degradation of the

nucleolar fusion proteins, maybe because of the slight amount that was degraded by PMN. Microscopic analysis of further nucleolar or nuclear proteins, also by time-lapse experiments, might identify a specific nucleolar or nuclear cargo for PMN.

6. Literature

Amerik, A.Y., Nowak, J., Swaminathan, S.und Hochstrasser, M. (2000). The Doa4 deubiquitinating enzyme is functionally linked to the vacuolar protein-sorting and endocytic pathways. Mol Biol Cell *11*, 3365-3380.

Baba, M., Osumi, M., Scott, S.V., Klionsky, D.J.und Ohsumi, Y. (1997). Two distinct pathways for targeting proteins from the cytoplasm to the vacuole/lysosome. The Journal of Cell Biology *139*, 1687-1695.

Baba, M., Takeshige, K., Baba, N.und Ohsumi, Y. (1994). Ultrastructural analysis of the autophagic process in yeast: detection of autophagosomes and their characterization. The Journal of Cell Biology *124*, 903-913.

Babst, M. (2005). A protein's final ESCRT. Traffic *6*, 2-9.

Babst, M., Katzmann, D.J., Estepa-Sabal, E.J., Meerloo, T.und Emr, S.D. (2002). Escrt-III: an endosome-associated heterooligomeric protein complex required for mvb sorting. Dev Cell *3*, 271-282.

Babst, M., Sato, T.K., Banta, L.M.und Emr, S.D. (1997). Endosomal transport function in yeast requires a novel AAA-type ATPase, Vps4p. EMBO J *16*, 1820-1831.

Barth, H., Meiling-Wesse, K., Epple, U.D.und Thumm, M. (2001). Autophagy and the cytoplasm to vacuole targeting pathway both require Aut10p. FEBS Letters *508*, 23-28.

Barth, H., Meiling-Wesse, K., Epple, U.D.und Thumm, M. (2002). Mai1p is essential for maturation of proaminopeptidase I but not for autophagy. FEBS Letters *512*, 173-179.

Baxter, B.K., Abeliovich, H., Zhang, X., Stirling, A.G., Burlingame, A.L.und Goldfarb, D.S. (2005). Atg19p ubiquitination and the cytoplasm to vacuole trafficking pathway in yeast. J Biol Chem *280*, 39067-39076.

Bernstein, K.A., Gallagher, J.E., Mitchell, B.M., Granneman, S.und Baserga, S.J. (2004). The small-subunit processome is a ribosome assembly intermediate. Eukaryot Cell *3*, 1619-1626.

Bilodeau, P.S., Winistorfer, S.C., Kearney, W.R., Robertson, A.D.und Piper, R.C. (2003). Vps27-Hse1 and ESCRT-I complexes cooperate to increase efficiency of sorting ubiquitinated proteins at the endosome. J Cell Biol *163*, 237-243.

Bleazard, W., McCaffery, J.M., King, E.J., Bale, S., Mozdy, A., Tieu, Q., Nunnari, J.und Shaw, J.M. (1999). The dynamin-related GTPase Dnm1 regulates mitochondrial fission in yeast. Nat Cell Biol *1*, 298-304.

Bogomolnaya, L.M., Pathak, R., Cham, R., Guo, J., Surovtseva, Y.V., Jaeckel, L.und Polymenis, M. (2004). A new enrichment approach identifies genes that alter cell cycle progression in Saccharomyces cerevisiae. Curr Genet *45*, 350-359.

Braun, R.und Zischka, H. (2008). Mechanisms of Cdc48/VCP-mediated cell death — from yeast apoptosis to human disease. Biochimica et Biophysica Acta (BBA) - Molecular Cell Research *1783*, 1418-1435.

Braun, S., Matuschewski, K., Rape, M., Thoms, S.und Jentsch, S. (2002). Role of the ubiquitin-selective CDC48(UFD1/NPL4)chaperone (segregase) in ERAD of OLE1 and other substrates. EMBO J *21*, 615-621.

Bremer, S. (2009). Molecular analysis of vesicle biogenesis during autophagy. Dissertation, Georg August Universität, Göttingen.

Brody, J.R.und Kern, S.E. (2004). History and principles of conductive media for standard DNA electrophoresis. Anal Biochem *333*, 1-13.

Bryant, N.J.und Stevens, T.H. (1998). Vacuole biogenesis in Saccharomyces cerevisiae: protein transport pathways to the yeast vacuole. Microbiol Mol Biol Rev *62*, 230-247.

Buchberger, A. (2010). Control of ubiquitin conjugation by cdc48 and its cofactors. Subcell Biochem *54*, 17-30.

Buchberger, A., Howard, M.J., Proctor, M.und Bycroft, M. (2001). The UBX domain: a widespread ubiquitin-like module. J Mol Biol *307*, 17-24.

Burd, C.G.und Emr, S.D. (1998). Phosphatidylinositol(3)-phosphate signaling mediated by specific binding to RING FYVE domains. Mol Cell *2*, 157-162.

Campbell, C.L.und Thorsness, P.E. (1998). Escape of mitochondrial DNA to the nucleus in yme1 yeast is mediated by vacuolar-dependent turnover of abnormal mitochondrial compartments. J Cell Sci *111 (Pt 16)*, 2455-2464.

Chang, C.R.und Blackstone, C. Dynamic regulation of mitochondrial fission through modification of the dynamin-related protein Drp1. Ann N Y Acad Sci *1201*, 34-39.

Chen, Y., Azad, M.B.und Gibson, S.B. (2009). Superoxide is the major reactive oxygen species regulating autophagy. Cell Death Differ *16*, 1040-1052.

Cocheme, H.M.und Murphy, M.P. (2008). Complex I is the major site of mitochondrial superoxide production by paraquat. J Biol Chem *283*, 1786-1798.

Collinson, L.P.und Dawes, I.W. (1992). Inducibility of the response of yeast cells to peroxide stress. J Gen Microbiol *138*, 329-335.

Conibear, E.und Stevens, T.H. (1998). Multiple sorting pathways between the late Golgi and the vacuole in yeast. Biochim Biophys Acta *1404*, 211-230.

Cuervo, A.M. (2010). Chaperone-mediated autophagy: selectivity pays off. Trends Endocrinol Metab *21*, 142-150.

Darsow, T., Rieder, S.E.und Emr, S.D. (1997). A multispecificity syntaxin homologue, Vam3p, essential for autophagic and biosynthetic protein transport to the vacuole. J Cell Biol *138*, 517-529.

Dove, S.K., Piper, R.C., McEwen, R.K., Yu, J.W., King, M.C., Hughes, D.C., Thuring, J., Holmes, A.B., Cooke, F.T., Michell, R.H., Parker, P.J.und Lemmon, M.A. (2004). Svp1p defines a family of phosphatidylinositol 3,5-bisphosphate effectors. EMBO J *23*, 1922-1933.

Dragon, F., Gallagher, J.E., Compagnone-Post, P.A., Mitchell, B.M., Porwancher, K.A., Wehner, K.A., Wormsley, S., Settlage, R.E., Shabanowitz, J., Osheim, Y., Beyer, A.L., Hunt, D.F.und Baserga, S.J. (2002). A large nucleolar U3 ribonucleoprotein required for 18S ribosomal RNA biogenesis. Nature *417*, 967-970.

Epple, U.D., Eskelinen, E.L.und Thumm, M. (2003). Intravacuolar membrane lysis in Saccharomyces cerevisiae. Does vacuolar targeting of Cvt17/Aut5p affect its function? J Biol Chem *278*, 7810-7821.

Epple, U.D., Suriapranata, I., Eskelinen, E.L.und Thumm, M. (2001). Aut5/Cvt17p, a putative lipase essential for disintegration of autophagic bodies inside the vacuole. J Bacteriol *183*, 5942-5955.

Eskelinen, E.L. (2005). Maturation of autophagic vacuoles in Mammalian cells. Autophagy *1*, 1-10.

Fader, C.M.und Colombo, M.I. (2009). Autophagy and multivesicular bodies: two closely related partners. Cell Death Differ *16*, 70-78.

Farre, J.C., Krick, R., Subramani, S.und Thumm, M. (2009). Turnover of organelles by autophagy in yeast. Curr Opin Cell Biol *21*, 522-530.

Farré, J.C., Manjithaya, R., Mathewson, R.D.und Subramani, S. (2008). PpAtg30 tags peroxisomes for turnover by selective autophagy. Dev Cell *14*, 365-376.

Filimonenko, M., Stuffers, S., Raiborg, C., Yamamoto, A., Malerod, L., Fisher, E.M., Isaacs, A., Brech, A., Stenmark, H.und Simonsen, A. (2007). Functional multivesicular bodies are required for autophagic clearance of protein aggregates associated with neurodegenerative disease. J Cell Biol *179*, 485-500.

Fischer von Mollard, G.und Stevens, T.H. (1999). The Saccharomyces cerevisiae v-SNARE Vti1p is required for multiple membrane transport pathways to the vacuole. Mol Biol Cell *10*, 1719-1732.

Gegg, M.E., Cooper, J.M., Chau, K.Y., Rojo, M., Schapira, A.H.und Taanman, J.W. (2010). Mitofusin 1 and mitofusin 2 are ubiquitinated in a PINK1/parkin-dependent manner upon induction of mitophagy. Hum Mol Genet *19*, 4861-4870.

Geisler, S., Holmstrom, K.M., Skujat, D., Fiesel, F.C., Rothfuss, O.C., Kahle, P.J.und Springer, W. (2010). PINK1/Parkin-mediated mitophagy is dependent on VDAC1 and p62/SQSTM1. Nat Cell Biol *12*, 119-131.

Goldman, S.J., Taylor, R., Zhang, Y.und Jin, S. (2010). Autophagy and the degradation of mitochondria. Mitochondrion *10*, 309-315.

Guan, J., Stromhaug, P.E., George, M.D., Habibzadegah-Tari, P., Bevan, A., Dunn, W.A.und Klionsky, D.J. (2001). Cvt18/Gsa12 is required for cytoplasm-to-vacuole transport, pexophagy, and autophagy in Saccharomyces cerevisiae and Pichia pastoris. Mol Biol Cell *12*, 3821-3838.

Hanahan, D. (1983). Studies on transformation of Escherichia coli with plasmids. J Mol Biol *166*, 557-580.

Hanahan, D., Jessee, J.und Bloom, F.R. (1991). Plasmid transformation of Escherichia coli and other bacteria. Methods Enzymol *204*, 63-113.

Harding, T.M., Hefner-Gravink, A., Thumm, M.und Klionsky, D.J. (1996). Genetic and phenotypic overlap between autophagy and the cytoplasm to vacuole protein targeting pathway. J Biol Chem *271*, 17621-17624.

Hartmann-Petersen, R., Wallace, M., Hofmann, K., Koch, G., Johnsen, A.H., Hendil, K.B.und Gordon, C. (2004). The Ubx2 and Ubx3 cofactors direct Cdc48 activity to proteolytic and nonproteolytic ubiquitin-dependent processes. Curr Biol *14*, 824-828.

Hassan, H.M.und Fridovich, I. (1979). Intracellular production of superoxide radical and of hydrogen peroxide by redox active compounds. Arch Biochem Biophys *196*, 385-395.

He, C., Song, H., Yorimitsu, T., Monastyrska, I., Yen, W.L., Legakis, J.E.und Klionsky, D.J. (2006). Recruitment of Atg9 to the preautophagosomal structure by Atg11 is essential for selective autophagy in budding yeast. The Journal of Cell Biology *175*, 925-935.

Herlan, M., Vogel, F., Bornhovd, C., Neupert, W.und Reichert, A.S. (2003). Processing of Mgm1 by the rhomboid-type protease Pcp1 is required for maintenance of mitochondrial morphology and of mitochondrial DNA. J Biol Chem *278*, 27781-27788.

Hermann, G.J., Thatcher, J.W., Mills, J.P., Hales, K.G., Fuller, M.T., Nunnari, J.und Shaw, J.M. (1998). Mitochondrial fusion in yeast requires the transmembrane GTPase Fzo1p. J Cell Biol *143*, 359-373.

Herskowitz, I. (1988). Life cycle of the budding yeast Saccharomyces cerevisiae. Microbiol Rev *52*, 536-553.

Hoffmann, W. (1985). Molecular characterization of the CAN1 locus in Saccharomyces cerevisiae. A transmembrane protein without N-terminal hydrophobic signal sequence. J Biol Chem *260*, 11831-11837.

Honma, Y., Kitamura, A., Shioda, R., Maruyama, H., Ozaki, K., Oda, Y., Mini, T., Jeno, P., Maki, Y., Yonezawa, K., Hurt, E., Ueno, M., Uritani, M., Hall, M.N.und Ushimaru, T. (2006). TOR regulates late steps of ribosome maturation in the nucleoplasm via Nog1 in response to nutrients. EMBO J *25*, 3832-3842.

Horvath, A.und Riezman, H. (1994). Rapid protein extraction from Saccharomyces cerevisiae. Yeast *10*, 1305-1310.

Huh, W.K., Falvo, J.V., Gerke, L.C., Carroll, A.S., Howson, R.W., Weissman, J.S.und O'Shea, E.K. (2003). Global analysis of protein localization in budding yeast. Nature *425*, 686-691.

Hurley, J.H.und Emr, S.D. (2006). The ESCRT complexes: structure and mechanism of a membrane-trafficking network. Annual review of biophysics and biomolecular structure *35*, 277-298.

Hurley, J.H.und Hanson, P.I. (2010). Membrane budding and scission by the ESCRT machinery: it's all in the neck. Nat Rev Mol Cell Biol *11*, 556-566.

Hutchins, M.U., Veenhuis, M.und Klionsky, D.J. (1999). Peroxisome degradation in Saccharomyces cerevisiae is dependent on machinery of macroautophagy and the Cvt pathway. J Cell Sci *112 (Pt 22)*, 4079-4087.

Ichimura, Y., Kirisako, T., Takao, T., Satomi, Y., Shimonishi, Y., Ishihara, N., Mizushima, N., Tanida, I., Kominami, E., Ohsumi, M., Noda, T.und Ohsumi, Y. (2000). A ubiquitin-like system mediates protein lipidation. Nature *408*, 488-492.

Ikeda, F.und Dikic, I. (2008). Atypical ubiquitin chains: new molecular signals. 'Protein Modifications: Beyond the Usual Suspects' review series. EMBO Rep *9*, 536-542.

Inoue, Y.und Klionsky, D.J. (2010). Regulation of macroautophagy in Saccharomyces cerevisiae. Semin Cell Dev Biol *21*, 664-670.

Ishihara, N., Hamasaki, M., Yokota, S., Suzuki, K., Kamada, Y., Kihara, A., Yoshimori, T., Noda, T.und Ohsumi, Y. (2001). Autophagosome requires specific early Sec proteins for its formation and NSF/SNARE for vacuolar fusion. Mol Biol Cell *12*, 3690-3702.

Jaeger, P.A.und Wyss-Coray, T. (2010). Beclin 1 complex in autophagy and Alzheimer disease. Arch Neurol *67*, 1181-1184.

Jager, S., Strayle, J., Heinemeyer, W.und Wolf, D.H. (2001). Cic1, an adaptor protein specifically linking the 26S proteasome to its substrate, the SCF component Cdc4. EMBO J *20*, 4423-4431.

Jamieson, D.J. (1998). Oxidative stress responses of the yeast Saccharomyces cerevisiae. Yeast *14*, 1511-1527.

Janke, C., Magiera, M.M., Rathfelder, N., Taxis, C., Reber, S., Maekawa, H., Moreno-Borchart, A., Doenges, G., Schwob, E., Schiebel, E.und Knop, M. (2004). A versatile toolbox for PCR-based tagging of yeast genes: new fluorescent proteins, more markers and promoter substitution cassettes. Yeast *21*, 947-962.

Jarosch, E., Taxis, C., Volkwein, C., Bordallo, J., Finley, D., Wolf, D.H.und Sommer, T. (2002). Protein dislocation from the ER requires polyubiquitination and the AAA-ATPase Cdc48. Nat Cell Biol *4*, 134-139.

Kabeya, Y., Kamada, Y., Baba, M., Takikawa, H., Sasaki, M.und Ohsumi, Y. (2005). Atg17 functions in cooperation with Atg1 and Atg13 in yeast autophagy. Mol Biol Cell *16*, 2544-2553.

Kamada, Y., Funakoshi, T., Shintani, T., Nagano, K., Ohsumi, M.und Ohsumi, Y. (2000). Tor-mediated induction of autophagy via an Apg1 protein kinase complex. The Journal of Cell Biology *150*, 1507-1513.

Kanki, T., Kang, D.und Klionsky, D.J. (2009a). Monitoring mitophagy in yeast: the Om45-GFP processing assay. Autophagy *5*, 1186-1189.

Kanki, T.und Klionsky, D.J. (2008). Mitophagy in yeast occurs through a selective mechanism. J Biol Chem *283*, 32386-32393.

Kanki, T.und Klionsky, D.J. (2009). Atg32 is a tag for mitochondria degradation in yeast. Autophagy *5*, 1201-1202.

Kanki, T., Wang, K., Baba, M., Bartholomew, C.R., Lynch-Day, M.A., Du, Z., Geng, J., Mao, K., Yang, Z., Yen, W.L.und Klionsky, D.J. (2009b). A genomic screen for yeast mutants defective in selective mitochondria autophagy. Mol Biol Cell *20*, 4730-4738.

Kanki, T., Wang, K., Cao, Y., Baba, M.und Klionsky, D.J. (2009c). Atg32 is a mitochondrial protein that confers selectivity during mitophagy. Dev Cell *17*, 98-109.

Katzmann, D.J., Babst, M.und Emr, S.D. (2001). Ubiquitin-dependent sorting into the multivesicular body pathway requires the function of a conserved endosomal protein sorting complex, ESCRT-I. Cell *106*, 145-155.

Katzmann, D.J., Stefan, C.J., Babst, M.und Emr, S.D. (2003). Vps27 recruits ESCRT machinery to endosomes during MVB sorting. J Cell Biol *162*, 413-423.

Kawamata, T., Kamada, Y., Kabeya, Y., Sekito, T.und Ohsumi, Y. (2008). Organization of the pre-autophagosomal structure responsible for autophagosome formation. Mol Biol Cell *19*, 2039-2050.

Keeble, J.A.und Gilmore, A.P. (2007). Apoptosis commitment--translating survival signals into decisions on mitochondria. Cell Res *17*, 976-984.

Kiffin, R., Bandyopadhyay, U.und Cuervo, A.M. (2006). Oxidative stress and autophagy. Antioxid Redox Signal *8*, 152-162.

Kihara, A., Noda, T., Ishihara, N.und Ohsumi, Y. (2001). Two distinct Vps34 phosphatidylinositol 3-kinase complexes function in autophagy and carboxypeptidase Y sorting in Saccharomyces cerevisiae. The Journal of Cell Biology *152*, 519-530.

Kim, J., Huang, W.P., Stromhaug, P.E.und Klionsky, D.J. (2002). Convergence of multiple autophagy and cytoplasm to vacuole targeting components to a perivacuolar membrane compartment prior to de novo vesicle formation. J Biol Chem *277*, 763-773.

Kim, J., Kamada, Y., Stromhaug, P.E., Guan, J., Hefner-Gravink, A., Baba, M., Scott, S.V., Ohsumi, Y., Dunn, W.A., Jr.und Klionsky, D.J. (2001). Cvt9/Gsa9 functions in sequestering selective cytosolic cargo destined for the vacuole. J Cell Biol *153*, 381-396.

Kirisako, T., Baba, M., Ishihara, N., Miyazawa, K., Ohsumi, M., Yoshimori, T., Noda, T.und Ohsumi, Y. (1999). Formation process of autophagosome is traced with Apg8/Aut7p in yeast. The Journal of Cell Biology *147*, 435-446.

Kirisako, T., Ichimura, Y., Okada, H., Kabeya, Y., Mizushima, N., Yoshimori, T., Ohsumi, M., Takao, T., Noda, T.und Ohsumi, Y. (2000). The reversible modification regulates the membrane-binding state of Apg8/Aut7 essential for autophagy and the cytoplasm to vacuole targeting pathway. The Journal of Cell Biology *151*, 263-276.

Kissová, I., Deffieu, M., Manon, S.und Camougrand, N. (2004). Uth1p is involved in the autophagic degradation of mitochondria. J Biol Chem *279*, 39068-39074.

Kissová, I., Salin, B., Schaeffer, J., Bhatia, S., Manon, S.und Camougrand, N. (2007). Selective and non-selective autophagic degradation of mitochondria in yeast. Autophagy *3*, 329-336.

Klionsky, D.J. (2005). Autophagy. Curr Biol *15*, R282-283.

Klionsky, D.J., Cregg, J.M., Dunn, W.A., Emr, S.D., Sakai, Y., Sandoval, I.V., Sibirny, A., Subramani, S., Thumm, M., Veenhuis, M.und Ohsumi, Y. (2003). A unified nomenclature for yeast autophagy-related genes. Dev Cell *5*, 539-545.

Klionsky, D.J., Cuervo, A.M.und Seglen, P.O. (2007). Methods for monitoring autophagy from yeast to human. Autophagy *3*, 181-206.

Klionsky, D.J., Cueva, R.und Yaver, D.S. (1992). Aminopeptidase I of Saccharomyces cerevisiae is localized to the vacuole independent of the secretory pathway. J Cell Biol *119*, 287-299.

Kraft, C., Deplazes, A., Sohrmann, M.und Peter, M. (2008). Mature ribosomes are selectively degraded upon starvation by an autophagy pathway requiring the Ubp3p/Bre5p ubiquitin protease. Nat Cell Biol *10*, 602-610.

Krick, R., Bremer, S., Welter, E., Schlotterhose, P., Muehe, Y., Eskelinen, E.L.und Thumm, M. (2010). Cdc48/p97 and Shp1/p47 regulate autophagosome biogenesis in concert with ubiquitin-like Atg8. J Cell Biol *190*, 965-973.

Krick, R., Henke, S., Tolstrup, J.und Thumm, M. (2008a). Dissecting the localization and function of Atg18, Atg21 and Ygr223c. Autophagy *4*, 896-910.

Krick, R., Muehe, Y., Prick, T., Bremer, S., Schlotterhose, P., Eskelinen, E.L., Millen, J., Goldfarb, D.S.und Thumm, M. (2008b). Piecemeal microautophagy of the nucleus requires the core macroautophagy genes. Mol Biol Cell *19*, 4492-4505.

Krick, R., Mühe, Y., Prick, T., Bredschneider, M., Bremer, S., Wenzel, D., Eskelinen, E.L.und Thumm, M. (2009). Piecemeal microautophagy of the nucleus: Genetic and morphological traits. Autophagy *5*.

Krick, R., Tolstrup, J., Appelles, A., Henke, S.und Thumm, M. (2006). The relevance of the phosphatidylinositolphosphat-binding motif FRRGT of Atg18 and Atg21 for the Cvt pathway and autophagy. FEBS Letters *580*, 4632-4638.

Kroemer, G., Galluzzi, L.und Brenner, C. (2007). Mitochondrial membrane permeabilization in cell death. Physiol Rev *87*, 99-163.

Kvam, E., Gable, K., Dunn, T.M.und Goldfarb, D. (2005). Targeting of Tsc13p to nucleus-vacuole junctions: a role for very-long-chain fatty acids in the biogenesis of microautophagic vesicles. Mol Biol Cell *16*, 3987-3998.

Kvam, E.und Goldfarb, D. (2004). Nvj1p is the outer-nuclear-membrane receptor for oxysterol-binding protein homolog Osh1p in Saccharomyces cerevisiae. Journal of Cell Science *117*, 4959-4968.

Kvam, E.und Goldfarb, D. (2006). Structure and function of nucleus-vacuole junctions: outer-nuclear-membrane targeting of Nvj1p and a role in tryptophan uptake. Journal of Cell Science *119*, 3622-3633.

Laemmli, U.K. (1970). Cleavage of structural proteins during the assembly of the head of bacteriophage T4. Nature *227*, 680-685.

Latterich, M., Fröhlich, K.U.und Schekman, R. (1995). Membrane fusion and the cell cycle: Cdc48p participates in the fusion of ER membranes. Cell *82*, 885-893.

Lee, F.J.und Hassan, H.M. (1985). Biosynthesis of superoxide dismutase in Saccharomyces cerevisiae: effects of paraquat and copper. J Free Radic Biol Med *1*, 319-325.

Leonhard, K., Herrmann, J.M., Stuart, R.A., Mannhaupt, G., Neupert, W.und Langer, T. (1996). AAA proteases with catalytic sites on opposite membrane surfaces comprise a proteolytic system for the ATP-dependent degradation of inner membrane proteins in mitochondria. EMBO J *15*, 4218-4229.

Levine, T.P.und Munro, S. (2001). Dual targeting of Osh1p, a yeast homologue of oxysterol-binding protein, to both the Golgi and the nucleus-vacuole junction. Mol Biol Cell *12*, 1633-1644.

Loewen, C.J., Roy, A.und Levine, T.P. (2003). A conserved ER targeting motif in three families of lipid binding proteins and in Opi1p binds VAP. EMBO J *22*, 2025-2035.

Longatti, A.und Tooze, S.A. (2009). Vesicular trafficking and autophagosome formation. Cell Death Differ *16*, 956-965.

Longtine, M.S., McKenzie, A., Demarini, D.J., Shah, N.G., Wach, A., Brachat, A., Philippsen, P.und Pringle, J.R. (1998). Additional modules for versatile and economical PCR-based gene deletion and modification in Saccharomyces cerevisiae. Yeast *14*, 953-961.

Mari, M., Griffith, J., Rieter, E., Krishnappa, L., Klionsky, D.J.und Reggiori, F. (2010). An Atg9-containing compartment that functions in the early steps of autophagosome biogenesis. J Cell Biol *190*, 1005-1022.

Matsuda, N., Sato, S., Shiba, K., Okatsu, K., Saisho, K., Gautier, C.A., Sou, Y.S., Saiki, S., Kawajiri, S., Sato, F., Kimura, M., Komatsu, M., Hattori, N.und Tanaka, K. (2010). PINK1

stabilized by mitochondrial depolarization recruits Parkin to damaged mitochondria and activates latent Parkin for mitophagy. J Cell Biol *189*, 211-221.

Meiling-Wesse, K., Barth, H.und Thumm, M. (2002). Ccz1p/Aut11p/Cvt16p is essential for autophagy and the cvt pathway. FEBS Lett *526*, 71-76.

Meiling-Wesse, K., Barth, H., Voss, C., Eskelinen, E.L., Epple, U.D.und Thumm, M. (2004). Atg21 is required for effective recruitment of Atg8 to the preautophagosomal structure during the Cvt pathway. J Biol Chem *279*, 37741-37750.

Mewes, H.W., Albermann, K., Bahr, M., Frishman, D., Gleissner, A., Hani, J., Heumann, K., Kleine, K., Maierl, A., Oliver, S.G., Pfeiffer, F.und Zollner, A. (1997). Overview of the yeast genome. Nature *387*, 7-65.

Meyer, H.H. (2005). Golgi reassembly after mitosis:
The AAA family meets the ubiquitin family. Biochimica et Biophysica Acta (BBA) - Molecular Cell Research *1744*, 465-517.

Meyer, H.H., Kondo, H.und Warren, G. (1998). The p47 co-factor regulates the ATPase activity of the membrane fusion protein, p97. FEBS Lett *437*, 255-257.

Meyer, H.H., Shorter, J.G., Seemann, J., Pappin, D.und Warren, G. (2000). A complex of mammalian ufd1 and npl4 links the AAA-ATPase, p97, to ubiquitin and nuclear transport pathways. EMBO J *19*, 2181-2192.

Meyer, H.H., Wang, Y.und Warren, G. (2002). Direct binding of ubiquitin conjugates by the mammalian p97 adaptor complexes, p47 and Ufd1-Npl4. EMBO J *21*, 5645-5652.

Millen, J., Krick, R., Prick, T., Thumm, M.und Goldfarb, D. (2009). Measuring piecemeal microautophagy of the nucleus in Saccharomyces cerevisiae. Autophagy *5*, 75-81.

Misra, S.und Hurley, J.H. (1999). Crystal structure of a phosphatidylinositol 3-phosphate-specific membrane-targeting motif, the FYVE domain of Vps27p. Cell *97*, 657-666.

Mizuno, Y., Ohta, S., Tanaka, M., Takamiya, S., Suzuki, K., Sato, T., Oya, H., Ozawa, T.und Kagawa, Y. (1989). Deficiencies in complex I subunits of the respiratory chain in Parkinson's disease. Biochem Biophys Res Commun *163*, 1450-1455.

Nakatogawa, H., Ichimura, Y.und Ohsumi, Y. (2007). Atg8, a ubiquitin-like protein required for autophagosome formation, mediates membrane tethering and hemifusion. Cell *130*, 165-178.

Nakatogawa, H., Suzuki, K., Kamada, Y.und Ohsumi, Y. (2009). Dynamics and diversity in autophagy mechanisms: lessons from yeast. Nat Rev Mol Cell Biol *10*, 458-467.

Narendra, D., Tanaka, A., Suen, D.F.und Youle, R.J. (2008). Parkin is recruited selectively to impaired mitochondria and promotes their autophagy. J Cell Biol *183*, 795-803.

Narendra, D.P., Jin, S.M., Tanaka, A., Suen, D.F., Gautier, C.A., Shen, J., Cookson, M.R.und Youle, R.J. (2010a). PINK1 is selectively stabilized on impaired mitochondria to activate Parkin. PLoS Biol *8*, e1000298.

Narendra, D.P., Kane, L.A., Hauser, D.N., Fearnley, I.M.und Youle, R.J. (2010b). p62/SQSTM1 is required for Parkin-induced mitochondrial clustering but not mitophagy; VDAC1 is dispensable for both. Autophagy *6*.

Nieminen, A.L. (2003). Apoptosis and necrosis in health and disease: role of mitochondria. Int Rev Cytol *224*, 29-55.

Nixon, R.A. (2007). Autophagy, amyloidogenesis and Alzheimer disease. J Cell Sci *120*, 4081-4091.

Noda, T., Matsuura, A., Wada, Y.und Ohsumi, Y. (1995). Novel system for monitoring autophagy in the yeast Saccharomyces cerevisiae. Biochem Biophys Res Commun *210*, 126-132.

Noda, T.und Ohsumi, Y. (1998). Tor, a phosphatidylinositol kinase homologue, controls autophagy in yeast. J Biol Chem *273*, 3963-3966.

Ohsumi, Y.und Mizushima, N. (2004). Two ubiquitin-like conjugation systems essential for autophagy. Semin Cell Dev Biol *15*, 231-236.

Okamoto, K., Kondo-Okamoto, N.und Ohsumi, Y. (2009). Mitochondria-anchored receptor Atg32 mediates degradation of mitochondria via selective autophagy. Dev Cell *17*, 87-97.

Palermo, V., Falcone, C.und Mazzoni, C. (2007). Apoptosis and aging in mitochondrial morphology mutants of S. cerevisiae. Folia Microbiol (Praha) *52*, 479-483.

Pan, X., Roberts, P., Chen, Y., Kvam, E., Shulga, N., Huang, K., Lemmon, S.und Goldfarb, D.S. (2000). Nucleus-vacuole junctions in Saccharomyces cerevisiae are formed through the direct interaction of Vac8p with Nvj1p. Mol Biol Cell *11*, 2445-2457.

Pankiv, S., Clausen, T.H., Lamark, T., Brech, A., Bruun, J.A., Outzen, H., Overvatn, A., Bjorkoy, G.und Johansen, T. (2007). p62/SQSTM1 binds directly to Atg8/LC3 to facilitate degradation of ubiquitinated protein aggregates by autophagy. J Biol Chem *282*, 24131-24145.

Peterson, M.R., Burd, C.G.und Emr, S.D. (1999). Vac1p coordinates Rab and phosphatidylinositol 3-kinase signaling in Vps45p-dependent vesicle docking/fusion at the endosome. Curr Biol *9*, 159-162.

Piper, R.C., Cooper, A.A., Yang, H.und Stevens, T.H. (1995). VPS27 controls vacuolar and endocytic traffic through a prevacuolar compartment in Saccharomyces cerevisiae. The Journal of Cell Biology *131*, 603-617.

Polakis, E.S., Bartley, W.und Meek, G.A. (1964). Changes in the structure and enzyme activity of Saccharomyces cerevisiae in response to changes in the environment. Biochem J *90*, 369-374.

Powers, T.und Walter, P. (1999). Regulation of ribosome biogenesis by the rapamycin-sensitive TOR-signaling pathway in Saccharomyces cerevisiae. Mol Biol Cell *10*, 987-1000.

Prick, T.und Thumm, M. (2008). Measuring macroautophagy in S. cerevisiae: autophagic body accumulation and total protein turnover. Methods Enzymol *451*, 57-66.

Raiborg, C.und Stenmark, H. (2009). The ESCRT machinery in endosomal sorting of ubiquitylated membrane proteins. Nature *458*, 445-452.

Rapaport, D., Brunner, M., Neupert, W.und Westermann, B. (1998). Fzo1p is a mitochondrial outer membrane protein essential for the biogenesis of functional mitochondria in Saccharomyces cerevisiae. J Biol Chem *273*, 20150-20155.

Reggiori, F.und Klionsky, D.J. (2002). Autophagy in the eukaryotic cell. Eukaryot Cell *1*, 11-21.

Reggiori, F., Shintani, T., Nair, U.und Klionsky, D.J. (2005). Atg9 cycles between mitochondria and the pre-autophagosomal structure in yeasts. Autophagy *1*, 101-109.

Reggiori, F., Tucker, K.A., Stromhaug, P.E.und Klionsky, D.J. (2004a). The Atg1-Atg13 complex regulates Atg9 and Atg23 retrieval transport from the pre-autophagosomal structure. Dev Cell *6*, 79-90.

Reggiori, F., Wang, C.W., Nair, U., Shintani, T., Abeliovich, H.und Klionsky, D.J. (2004b). Early stages of the secretory pathway, but not endosomes, are required for Cvt vesicle and autophagosome assembly in Saccharomyces cerevisiae. Mol Biol Cell *15*, 2189-2204.

Ren, J., Pashkova, N., Winistorfer, S.und Piper, R. (2008). DOA1/UFD3 Plays a Role in Sorting Ubiquitinated Membrane Proteins into Multivesicular Bodies. Journal of Biological Chemistry *283*, 21599-21611.

Renart, J., Reiser, J.und Stark, G.R. (1979). Transfer of proteins from gels to diazobenzyloxymethyl-paper and detection with antisera: a method for studying antibody specificity and antigen structure. Proc Natl Acad Sci U S A *76*, 3116-3120.

Rieder, S.E., Banta, L.M., Kohrer, K., McCaffery, J.M.und Emr, S.D. (1996). Multilamellar endosome-like compartment accumulates in the yeast vps28 vacuolar protein sorting mutant. Mol Biol Cell *7*, 985-999.

Roberts, P., Moshitch-Moshkovitz, S., Kvam, E., O'Toole, E., Winey, M.und Goldfarb, D. (2003). Piecemeal microautophagy of nucleus in Saccharomyces cerevisiae. Mol Biol Cell *14*, 129-141.

Rusten, T.E.und Stenmark, H. (2009). How do ESCRT proteins control autophagy? J Cell Sci *122*, 2179-2183.

Saiki, R.K., Gelfand, D.H., Stoffel, S., Scharf, S.J., Higuchi, R., Horn, G.T., Mullis, K.B.und Erlich, H.A. (1988). Primer-directed enzymatic amplification of DNA with a thermostable DNA polymerase. Science *239*, 487-491.

Sakai, Y., Oku, M., van der Klei, I.J.und Kiel, J.A. (2006). Pexophagy: autophagic degradation of peroxisomes. Biochim Biophys Acta *1763*, 1767-1775.

Sato, T.K., Darsow, T.und Emr, S.D. (1998). Vam7p, a SNAP-25-like molecule, and Vam3p, a syntaxin homolog, function together in yeast vacuolar protein trafficking. Mol Cell Biol *18*, 5308-5319.

Scherz-Shouval, R.und Elazar, Z. (2007). ROS, mitochondria and the regulation of autophagy. Trends Cell Biol *17*, 422-427.

Schuberth, C.und Buchberger, A. (2008). UBX domain proteins: major regulators of the AAA ATPase Cdc48/p97. Cell. Mol. Life Sci. *65*, 2360-2371.

Schuberth, C., Richly, H., Rumpf, S.und Buchberger, A. (2004). Shp1 and Ubx2 are adaptors of Cdc48 involved in ubiquitin-dependent protein degradation. EMBO Rep *5*, 818-824.

Scott, S.V., Baba, M., Ohsumi, Y.und Klionsky, D.J. (1997). Aminopeptidase I is targeted to the vacuole by a nonclassical vesicular mechanism. The Journal of Cell Biology *138*, 37-44.

Scott, S.V., Nice, D.C., 3rd, Nau, J.J., Weisman, L.S., Kamada, Y., Keizer-Gunnink, I., Funakoshi, T., Veenhuis, M., Ohsumi, Y.und Klionsky, D.J. (2000). Apg13p and Vac8p are part of a complex of phosphoproteins that are required for cytoplasm to vacuole targeting. J Biol Chem *275*, 25840-25849.

Sesaki, H.und Jensen, R.E. (2004). Ugo1p links the Fzo1p and Mgm1p GTPases for mitochondrial fusion. J Biol Chem *279*, 28298-28303.

Shaw, J.M.und Nunnari, J. (2002). Mitochondrial dynamics and division in budding yeast. Trends Cell Biol *12*, 178-184.

Sheng, Y., Mancino, V.und Birren, B. (1995). Transformation of Escherichia coli with large DNA molecules by electroporation. Nucleic Acids Res *23*, 1990-1996.

Shibata, M., Lu, T., Furuya, T., Degterev, A., Mizushima, N., Yoshimori, T., MacDonald, M., Yankner, B.und Yuan, J. (2006). Regulation of intracellular accumulation of mutant Huntingtin by Beclin 1. J Biol Chem *281*, 14474-14485.

Shintani, T., Huang, W.P., Stromhaug, P.E.und Klionsky, D.J. (2002). Mechanism of cargo selection in the cytoplasm to vacuole targeting pathway. Dev Cell *3*, 825-837.

Sikorski, R.S.und Hieter, P. (1989). A system of shuttle vectors and yeast host strains designed for efficient manipulation of DNA in Saccharomyces cerevisiae. Genetics *122*, 19-27.

Smith, D.B.und Johnson, K.S. (1988). Single-step purification of polypeptides expressed in Escherichia coli as fusions with glutathione S-transferase. Gene *67*, 31-40.

Strittmatter, C.F. (1957). Adaptive variation in the level of oxidative activity in Saccharomyces cerevisiae. J Gen Microbiol *16*, 169-183.

Strømhaug, P.E., Reggiori, F., Guan, J., Wang, C.W.und Klionsky, D.J. (2004). Atg21 is a phosphoinositide binding protein required for efficient lipidation and localization of Atg8 during uptake of aminopeptidase I by selective autophagy. Mol Biol Cell *15*, 3553-3566.

Suzuki, K., Kirisako, T., Kamada, Y., Mizushima, N., Noda, T.und Ohsumi, Y. (2001). The pre-autophagosomal structure organized by concerted functions of APG genes is essential for autophagosome formation. EMBO J *20*, 5971-5981.

Suzuki, K., Kondo, C., Morimoto, M.und Ohsumi, Y. Selective transport of alpha-mannosidase by autophagic pathways: identification of a novel receptor, Atg34p. J Biol Chem *285*, 30019-30025.

Suzuki, K., Kubota, Y., Sekito, T.und Ohsumi, Y. (2007). Hierarchy of Atg proteins in pre-autophagosomal structure organization. Genes Cells *12*, 209-218.

Swaminathan, S., Amerik, A.Y.und Hochstrasser, M. (1999). The Doa4 deubiquitinating enzyme is required for ubiquitin homeostasis in yeast. Mol Biol Cell *10*, 2583-2594.

Sychrova, H.und Chevallier, M.R. (1993). Cloning and sequencing of the Saccharomyces cerevisiae gene LYP1 coding for a lysine-specific permease. Yeast *9*, 771-782.

Takeshige, K., Baba, M., Tsuboi, S., Noda, T.und Ohsumi, Y. (1992). Autophagy in yeast demonstrated with proteinase-deficient mutants and conditions for its induction. The Journal of Cell Biology *119*, 301-311.

Tal, R., Winter, G., Ecker, N., Klionsky, D.J.und Abeliovich, H. (2007). Aup1p, a yeast mitochondrial protein phosphatase homolog, is required for efficient stationary phase mitophagy and cell survival. J Biol Chem *282*, 5617-5624.

Tatsuta, T.und Langer, T. (2008). Quality control of mitochondria: protection against neurodegeneration and ageing. EMBO J *27*, 306-314.

Terzioglu, M.und Galter, D. (2008). Parkinson's disease: genetic versus toxin-induced rodent models. FEBS J *275*, 1384-1391.

Tong, A.H.und Boone, C. (2006). Synthetic genetic array analysis in Saccharomyces cerevisiae. Methods Mol Biol *313*, 171-192.

Tong, A.H., Evangelista, M., Parsons, A.B., Xu, H., Bader, G.D., Page, N., Robinson, M., Raghibizadeh, S., Hogue, C.W., Bussey, H., Andrews, B., Tyers, M.und Boone, C. (2001). Systematic genetic analysis with ordered arrays of yeast deletion mutants. Science *294*, 2364-2368.

Towbin, H., Staehelin, T.und Gordon, J. (1979). Electrophoretic transfer of proteins from polyacrylamide gels to nitrocellulose sheets: procedure and some applications. Proc Natl Acad Sci U S A *76*, 4350-4354.

Trumbly, R.J. (1992). Glucose repression in the yeast Saccharomyces cerevisiae. Mol Microbiol *6*, 15-21.

Tucker, K.A., Reggiori, F., Dunn, W.A., Jr.und Klionsky, D.J. (2003). Atg23 is essential for the cytoplasm to vacuole targeting pathway and efficient autophagy but not pexophagy. J Biol Chem *278*, 48445-48452.

Tuttle, D.L.und Dunn, W.A., Jr. (1995). Divergent modes of autophagy in the methylotrophic yeast Pichia pastoris. J Cell Sci *108 (Pt 1)*, 25-35.

Twig, G., Hyde, B.und Shirihai, O.S. (2008). Mitochondrial fusion, fission and autophagy as a quality control axis: the bioenergetic view. Biochim Biophys Acta *1777*, 1092-1097.

Veenhuis, M., Douma, A., Harder, W.und Osumi, M. (1983). Degradation and turnover of peroxisomes in the yeast Hansenula polymorpha induced by selective inactivation of peroxisomal enzymes. Arch Microbiol *134*, 193-203.

Wallace, D.C. (2005). A mitochondrial paradigm of metabolic and degenerative diseases, aging, and cancer: a dawn for evolutionary medicine. Annu Rev Genet *39*, 359-407.

Wang, C.W., Kim, J., Huang, W.P., Abeliovich, H., Stromhaug, P.E., Dunn, W.A., Jr.und Klionsky, D.J. (2001). Apg2 is a novel protein required for the cytoplasm to vacuole targeting, autophagy, and pexophagy pathways. J Biol Chem *276*, 30442-30451.

Wang, C.W., Stromhaug, P.E., Kauffman, E.J., Weisman, L.S.und Klionsky, D.J. (2003). Yeast homotypic vacuole fusion requires the Ccz1-Mon1 complex during the tethering/docking stage. J Cell Biol *163*, 973-985.

Weber, T.A.und Reichert, A.S. (2010). Impaired quality control of mitochondria: aging from a new perspective. Exp Gerontol *45*, 503-511.

Welter, E., Thumm, M.und Krick, R. (2010). Quantification of nonselective bulk autophagy in S. cerevisiae using Pgk1-GFP. Autophagy *6*, 794-797.

Wong, E.D., Wagner, J.A., Gorsich, S.W., McCaffery, J.M., Shaw, J.M.und Nunnari, J. (2000). The dynamin-related GTPase, Mgm1p, is an intermembrane space protein required for maintenance of fusion competent mitochondria. J Cell Biol *151*, 341-352.

Wu, K.K. (2006). Analysis of protein-DNA binding by streptavidin-agarose pulldown. Methods Mol Biol *338*, 281-290.

Wurmser, A.E.und Emr, S.D. (2002). Novel PtdIns(3)P-binding protein Etf1 functions as an effector of the Vps34 PtdIns 3-kinase in autophagy. The Journal of Cell Biology *158*, 761-772.

Xie, Z., Nair, U.und Klionsky, D.J. (2008a). Atg8 controls phagophore expansion during autophagosome formation. Mol Biol Cell *19*, 3290-3298.

Xie, Z., Nair, U.und Klionsky, D.J. (2008b). Dissecting autophagosome formation: the missing pieces. Autophagy *4*, 920-922.

Xilouri, M., Vogiatzi, T., Vekrellis, K.und Stefanis, L. (2008). alpha-synuclein degradation by autophagic pathways: a potential key to Parkinson's disease pathogenesis. Autophagy *4*, 917-919.

Yang, Q., She, H., Gearing, M., Colla, E., Lee, M., Shacka, J.J.und Mao, Z. (2009). Regulation of neuronal survival factor MEF2D by chaperone-mediated autophagy. Science *323*, 124-127.

Ye, Y., Meyer, H.H.und Rapoport, T.A. (2001). The AAA ATPase Cdc48/p97 and its partners transport proteins from the ER into the cytosol. Nature *414*, 652-656.

Yen, W.L., Legakis, J.E., Nair, U.und Klionsky, D.J. (2007). Atg27 is required for autophagy-dependent cycling of Atg9. Mol Biol Cell *18*, 581-593.

Yorimitsu, T.und Klionsky, D.J. (2005). Autophagy: molecular machinery for self-eating. Cell Death Differ *12 Suppl 2*, 1542-1552.

Zanchin, N.I.und Goldfarb, D.S. (1999). Nip7p interacts with Nop8p, an essential nucleolar protein required for 60S ribosome biogenesis, and the exosome subunit Rrp43p. Mol Cell Biol *19*, 1518-1525.

Ziviani, E., Tao, R.N.und Whitworth, A.J. (2010). Drosophila parkin requires PINK1 for mitochondrial translocation and ubiquitinates mitofusin. Proc Natl Acad Sci U S A *107*, 5018-5023.

DANKSAGUNG

Hiermit möchte ich ganz besonders Herrn Prof. Thumm für die Bereitstellung dieses sehr interessanten Themas und für die gute Betreuung danken.
Bei Herrn Prof. Braus möchte ich mich für die Tätigkeit als Co-Referent bedanken.

Weiterhin möchte ich mich allen Mitgliedern meines Thesis Komitees: Herrn Prof. Thumm, Herrn Prof. Braus und Herrn Prof. Ficner für alle Ratschläge und Anregugnen bedanken.

Vielen Dank an Herrn Prof. Rehling für wissenschaftliche Ratschläge, besonders auf dem Gebiet der Mitophagy.

Mein besonderer Dank gilt Rosi, die mir im Laufe der Jahre immer wieder mit Rat und Tat zur Seite stand. Ganz besonders in den letzten Monaten des Schreibens war sie mir mit ihrer Geduld und wissenschaftlicher Expertise eine sehr große Hilfe.

Der gesamten Arbeitsgruppe Thumm: Petra, Lisa, Rosi und Peter möchte ich danken, für das angenehme Arbeitsklima, die wissenschaftlichen Diskussionen und vor allem für das freundschaftliche Miteinander während und außerhalb der Arbeitszeiten. Auch meine ehemaligen Kollegen Sebastian und Jörn sind an dieser Stelle natürlich nicht vergessen. Vielen Dank auch für das Korrekturlesen der Arbeit.

Allen anderen Mitgliedern der Biochemie II und I möchte ich ebenfalls für viele wissenschaftlich-hilfreiche Tipps und die vielen netten Gespräche privater Natur danken.

Ein großer Dank geht an meine Freunde. Vor allem Conny, Anja, Antje und Janine möchte ich hier besonders hervorheben. Vielen Dank für die vielen Telefonate und das offene Ohr, das ihr immer für mich hattet.

Ganz herzlich möchte ich meiner Mutter danken, für die finanzielle und vor allem mentale und emotionale Unterstützung während meines Studium und meiner Arbeit hier in Göttingen. Ein großer Dank geht an meine Oma, meine Omi, meine Schwester, meinen Neffen und mein Nichte. Vielen Dank auch an meinen Opa, der mir immer ein großes Vorbild war und sicherlich sehr stolz auf mich wäre.

DANKE!

CURRICULUM VITAE

Personal Data

Name	Evelyn Cornelia Welter
Born	15.04.1982 in Ottweiler/Germany

Education

10.2007- present	**Dissertation at the Georg-August-Universtiy of Göttingen** Department of Biochemistry II, Center for Biochemistry and Molecular Cell Biology, Prof. Dr. Michael Thumm
11.2001- 07.2007	**Studies in Biology at the University of Rostock** Major subject: Biochemistry Minor subjects: Molecular biology and Microbiology **Diploma thesis at the University of Rostock** Charakterisierung der Linaloolsynthase aus *Nicotiana alata* Department: Biochemie der Pflanze, Prof. Dr. Birgit Piechulla
1994- 2001	**Gymnasium Ottweiler**
1988- 1994	**Grundschule Lebesch, Ottweiler**

Publications

Welter, E., Thumm, M. und Krick R. (2010). Quantification of nonselective bulk autophagy in S. cerevisiae using Pgk1-GFP. Autophagy *6*, 794-797.

Krick, R., Bremer, S., **Welter, E.**, Schlotterhose, P., Muehe, Y., Eskelinen, E.L.und Thumm, M. (2010). Cdc48/p97 and Shp1/p47 regulate autophagosome biogenesis in concert with ubiquitin-like Atg8. J Cell Biol *190*, 965-973.

Krick, R., Bremer, S., **Welter, E.**, Eskelinen, E.L.und Thumm, M. (2011). Cheating on ubiquitin with Atg8. Autophagy *7*.